CONSTRUCTION AND ANALYSIS OF A LONG WAVELENGTH INTEGRATING SPHERE REFLECTOMETER

By

Roger Allen Williams

Bachelor of Science
Texas A. and M. University
College Station, Texas
1961

Master of Science
Oklahoma State University
Stillwater, Oklahoma
1963

Submitted to the faculty of the Graduate College
of the Oklahoma State University
in partial fulfillment of the requirements
for the degree of
DOCTOR OF PHILOSOPHY
May, 1967

CONSTRUCTION AND ANALYSIS OF A LONG

WAVELENGTH INTEGRATING SPHERE

REFLECTOMETER

Thesis Approved:

J. A. Mitchell
Thesis Adviser

J. K. Fenton

A. M. Rowe

N. N. Durham
Dean of the Graduate College

ACKNOWLEDGMENTS

The author would like to express his sincere appreciation and extend his gratitude to the following individuals who have had a part, in one way or another, in aiding me during my graduate program:

Dr. J. A. Wiebelt, who served as committee chairman and thesis adviser, for his assistance and guidance, and especially for his encouragement and patience;

Mr. Dupree Maples, for his encouragement, assistance, and technical discussions during much of this study;

Mrs. Jenifer Walford, for invaluable assistance and advice in preparation of the manuscript;

Mr. Faye McQuiston and the staff of the Mechanical Engineering Laboratory for assistance in preparing the instrument which was the object of this study;

My wife, Betty, for her encouragement, sacrifice, and kind understanding during the years of graduate study.

TABLE OF CONTENTS

LIST OF FIGURES

LIST OF TABLES

CHAPTER I

INTRODUCTION

This dissertation concerns the construction of an instrument which is capable of determining the reflectance of a surface when that surface is irradiated with infrared radiation, and the determination of the type and magnitude of the errors involved in the measured characteristic. The instrument chosen to achieve this purpose was a sulfur-coated, integrating sphere reflectometer. The determination of the quantity and quality of the errors involved was achieved through a combination of theoretical and experimental considerations.

The practical, as opposed to academic, need for infrared reflectance information was greatly enhanced by the advent of the space age, an event which produced many new engineering problems and requirements. Many of the problems were known to exist before the launching of the first satellite, but had been ignored completely, or were considered to be negligible. In a space environment, many of these problems assumed a degree of importance which precluded their neglect.

One such problem which increased greatly in importance when considered against an "outer space" background was that of heat transfer by radiation. In an atmospheric environment, where heat

transfer by conduction and convection can occur, the heat transfer by radiation by all systems but those at high temperatures was negligible. Certainly the radiative transfer by an object having a satellite temperature in an atmospheric environment could, in many instances, be considered to be negligible when compared to the conduction or convective transfer. In a space environment, however, heat transfer by radiation must be considered, since conduction and convection phenomena do not occur.

In order to successfully predict the heat transfer by radiation to or from a body in a space environment, the thermal radiation properties of the body must be known. For an opaque body, the monochromatic reflectance plus the monochromatic absorptance equals unity. If the approximation is made that the monochromatic emittance of the body equals the monochromatic absorptance, any one of the three quantities is sufficient to define the radiative properties of the body.

In determining any one of the quantities for a specific surface, much greater accuracy is attained when the quantity is measured rather than calculated. This is due to the fact that theoretical predictions are, for the most part, based on a theoretically perfect surface and do not account for the characteristics of real surfaces. Some work on theoretical roughness is available, but to date no widespread application of this work has been made.

A large amount of experimental data has been published giving either the reflectance or emittance of certain materials, but the great majority of this information has been restricted to the

visible and near infrared region of the electromagnetic spectrum, and very little long wavelength information is available.

The need for properties in the long wavelength region of the spectrum arises from the fact that a satellite absorbs energy from the earth and the atmosphere and emits energy at its own temperature. The wavelength range of radiant energy emitted by the earth is approximately 3 to 30 microns, and by the atmosphere is approximately 3.5 to 35 microns. An average spacecraft temperature of 500°R might be expected. This temperature corresponds to a wavelength range of 3 to 30 microns. In order to calculate a meaningful energy balance on the satellite, the thermal radiation properties of the satellite surface in this wavelength range are required.

In many respects, the reflectance of a surface is the least difficult of the three properties to measure. In most reflectance measurements, the effects of conduction and convection can be ignored, but this is not the case in most emittance and absorptance measurements. Therefore, the logical method for determining the thermal radiation properties in the long wavelength region of the electromagnetic spectrum appears to be the measurement of the reflectance of a surface.

There are three different types of instruments generally utilized in determining the reflectance of a surface. There are advantages and disadvantages associated with each of the three types and the relative merits are debatable.

One type of instrument is the hohlraum, or heated cavity,

reflectometer. The walls of a cavity are maintained at a uniform temperature and a cooled sample, which may form part of the wall, is irradiated uniformly because the monochromatic irradiation in a hohlraum is constant. Thus, the energy reflected through a small solid angle can be compared to the energy emitted by a section of the wall, which is a measure of the energy uniformly incident on the sample over a hemisphere. This gives the fraction of incident energy that is reflected into the directions of measurement. Then, through the principle of reciprocity, the fraction of energy which is reflected into the hemisphere above the sample can be determined when the irradiating energy is incident through some small angle in the directions of measurement.

The principle of reciprocity, first formulated by Helmholz (1), is generally accepted to mean that, when monochromatic energy is incident upon a surface through a small solid angle and is reflected through a small solid angle, the direction of the reflected and incident energy may be reversed, without additional losses in energy.

The main problems associated with the operation of the heated cavity reflectometer lie in maintaining the cavity walls at a uniform temperature, since any variation from a true black-body cavity may result in large errors. Of course the viewing aperture introduces an error, but it will be found that all three basic reflectometers are subject to hole losses and hole errors.

Gier, Dunkle, and Bevans (2) constructed a heated cavity reflectometer capable of making reflectance measurements to a wave-

length of 15 microns, this limit being imposed by the NaCl prism in the monochromator. It would appear that the wavelength range is limited not by any characteristic of the cavity itself but by the attendant optics and instrumentation, and the energy available for detection at long wavelengths.

Another basic type of reflectometer is the hemispherical reflectometer. The application of this instrument is based on the concept of conjugate focal points about the center of curvature of the hemisphere. That is, if a sample and a detector are placed at the conjugate focal points of a hemisphere, the energy reflected by the sample will be directed to the detector. The image of the sample reflected by the hemisphere to the detector will be subject to spherical aberration, and a large error may be involved due to the aberration. Dunn (3) has, to a great extent, eliminated this type of error by utilizing an ellipsoid instead of a hemisphere and placing the sample and the detector at conjugate focal points along the major axis. His instrument is included in the hemispherical class, even though no hemisphere is involved, because it is based on the same concept of conjugate focal points as the hemispherical reflectometer. Another instrument in this class is the double parabaloid reflectometer.

Janssen and Torburg (4) constructed a hemispherical reflectometer capable of measurements extending to 30 microns by using a cesium iodide prism. Since the hemisphere utilizes a highly polished inner surface, the small amount of energy available for detection in the long wavelength regions is not a critical problem, and, as in

the case of the heated cavity reflectometer, the wavelength range of the instrument is limited by the supporting optics.

The third type of reflectometer is the integrating sphere reflectometer. The operation of this instrument is based on the fact that, if the walls are diffuse, the configuration factor between any pair of points within a sphere is the same as any other pair of points. The integrating sphere reflectometer is not subject to any inherent possibility of error, nor are there critical variables to be controlled if the walls are diffuse. Of course hole losses are present, as mentioned previously, but the errors involved in the operation of the integrating sphere reflectometer are of a constant nature and can, therefore, be estimated accurately before the instrument is operated.

The integrating sphere reflectometer has long been utilized in determining the spectral and total reflectance of surfaces in the wavelength region of 2.5 microns and less. The upper limit of 2.5 microns has been imposed by the reflectance of the magnesium oxide coating commonly used, which is seen in Figure (1) to decrease sharply at approximately 2.5 microns (5).

Examination of the blackbody radiation curves shown in Figure (2) reveals the fact that, as the wavelength increases, the amount of energy available for detection within a given wavelength interval decreases greatly. In order to adapt the traditional integrating sphere reflectometer to long wavelength measurements, the efficiency of the sphere in utilizing the available energy must be increased and/or the sensitivity of the detector must be increased.

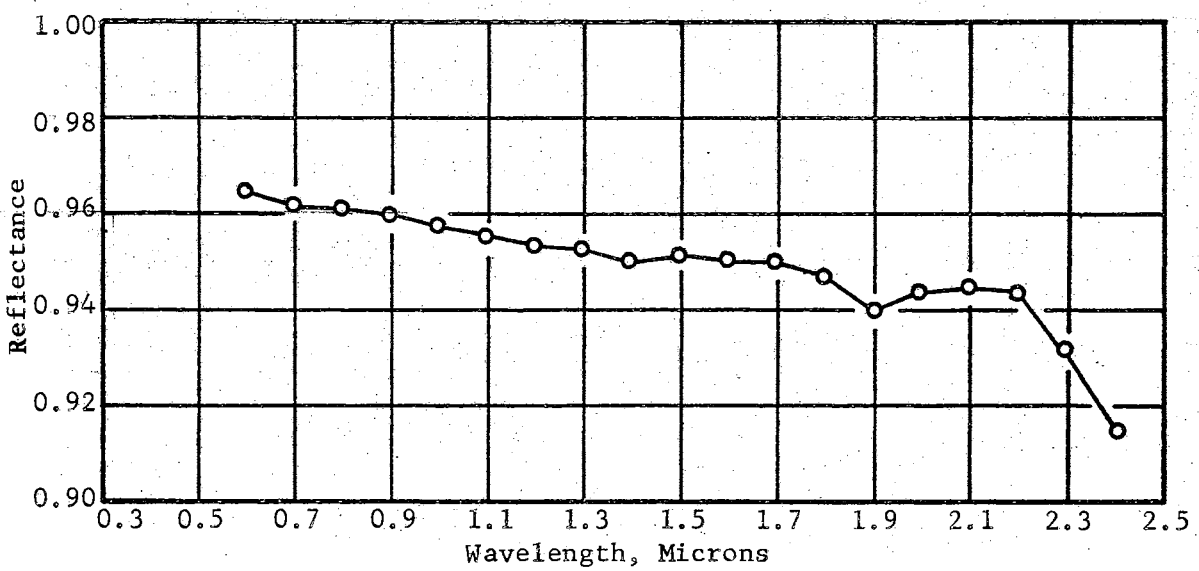

Figure 1. Spectral Reflectance of Magnesium Oxide, Average of Three Curves (Ref. 5)

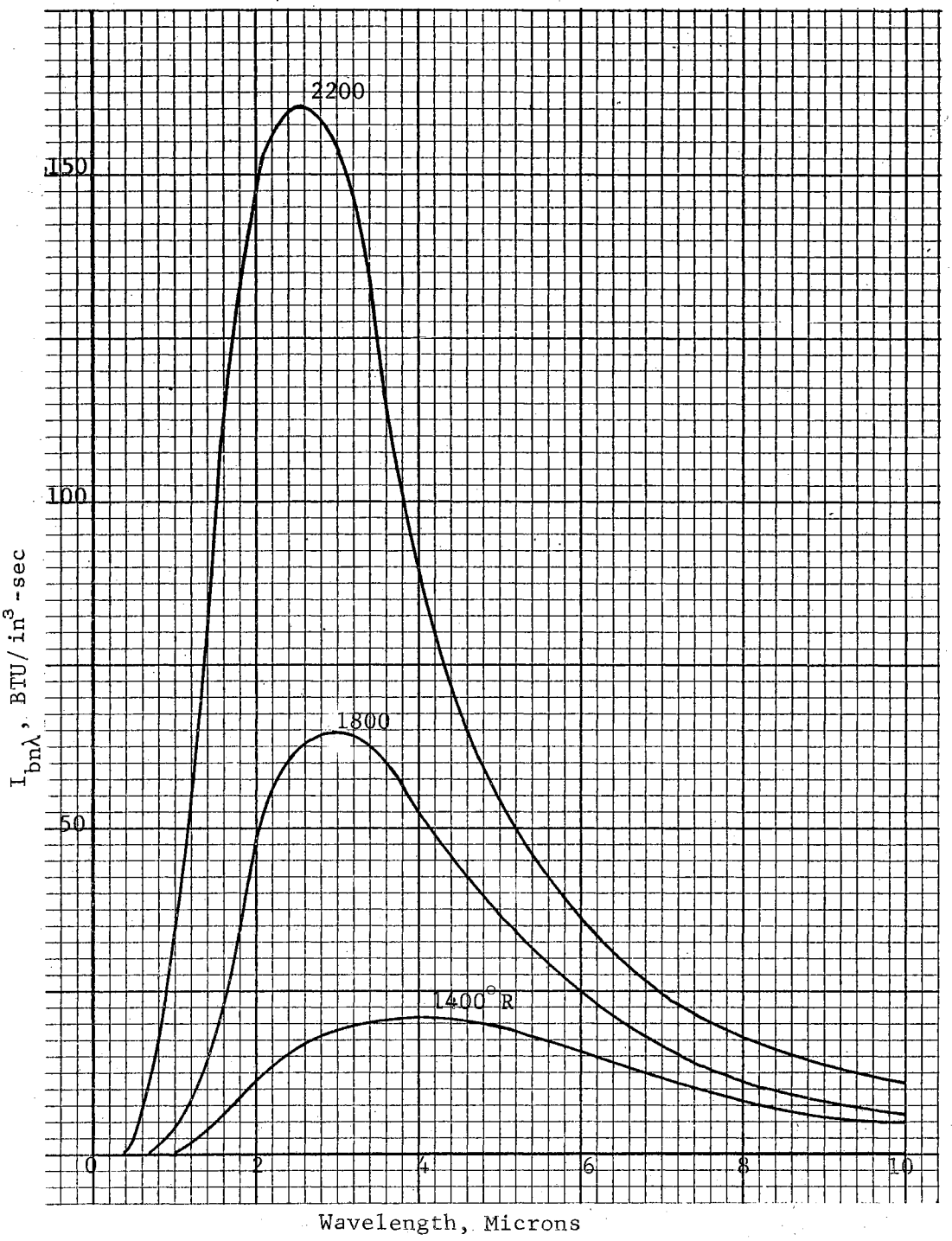

Figure 2. Spectral Blackbody Intensity Distribution

Since any substantial increase in the sensitivity of the detector would involve a costly and extensive experimental program, it appeared logical to attempt to extend the useful range of the integrating sphere reflectometer by increasing its efficiency. As shown later, the efficiency of a sphere is a function of its coating reflectance and its radius. The successful extension of the range of the integrating sphere depends, then, upon selecting a coating with high reflectance at wavelengths greater than the customary 2.5 microns, and a radius small enough to produce high sphere efficiency yet large enough to preclude unacceptable errors.

It has been shown (6) that certain forms of sulfur have a high reflectance at wavelengths up to approximately 15 microns. Birkebak, et al. (7) reported on an integrating sphere with a 7 inch diameter, utilizing flowers of sulfur as a coating, used to measure the reflectance of a surface when the surface was diffusely irradiated. No mention was made of the reliability of the measurements obtained using this instrument.

The purpose of this investigation, then, was the critical analysis of the performance of an integrating sphere of small radius, utilizing a mu-type sulfur as a coating. The integrating sphere under consideration measures the reflectance of a surface when irradiated through some small solid angle.

CHAPTER II

HISTORY OF THE INTEGRATING SPHERE

As stated previously, the theory of the integrating sphere is based on the fact that, if the walls are diffuse, the configuration factor between any pair of points within the sphere is identical to that between any other pair of points. This fact was first recognized by Sumpner (8) in 1893. He developed an expression for the average illumination at a point within a diffuse sphere as a function of direct and reflected illumination. Apparently he did not recognize the utility of his findings because he did not use a sphere in his succeeding works. In fact, Sumpner later used a hollow cylinder in an attempt to determine the spatial intensity of a light source.

Ulbricht (9) was the first to utilize the characteristics of a diffuse sphere. In 1900, without knowledge of Sumpner's work, Ulbricht developed the same type of expressions, and constructed a spherical instrument to determine the "mean spherical candlepower" of an incandescent lamp. Ulbricht's use of a magnesium oxide coated sphere as a "globe photometer" gave rise to the term "Ulbricht sphere", of which most subsequent sphere reflectometers are modifications.

W. F. Little (10), in 1916, reported on a reflectance method which consisted of projecting a beam of light through a small hole in the wall of a sphere onto a test surface which was placed near the

center of the sphere. The brightness of an observation window was compared to the brightness when a standard surface was placed in the sphere, the ratio of the two brightness signals being accepted as the ratio of the reflection factors of the two surfaces, where reflection factor is defined as the ratio of reflected to incident energy.

Also in 1916, Rosa and Taylor (11) described a method of measuring the reflection factor of the surface of an integrating sphere. The method consisted of determining the ratio of the average illumination received by the sphere surface to the total illumination of the sphere by both direct and reflected light, the ratio being the absorption factor of the sphere surface. While Rosa and Taylor considered their sphere method of determining the reflection factor of a sphere surface very precise, they recognized the fact that, because the method could only be applied to materials which could be formed into a sphere, its application was severly limited.

Luckiesh (12) described, in 1918, a reflectometer which utilized an opal glass sphere. No integrating action was required of the sphere. It was used, instead, to provide diffuse illumination for the sample which was mounted in a cut-off section of the sphere. The initial energy was provided by a series of lamps placed below the sample and outside the sphere, the lamps and the sphere both having been placed inside a white box. The combination supposedly provided diffuse irradiation of the sample, the reflectance of which was measured by a photometer which viewed the sample from the opposite side of the sphere.

In 1920, Benford (13) postulated that the brightness of the

interior of a spherical integrator depended upon three factors: the quantity of light received from the light source; the coefficient of reflection; and the solid angle of the spherical surface, if the integrator was an incomplete sphere. His absolute method for determining the coefficient of diffuse reflection was based on the last named factor. That is, he proposed to arrive at two separate equations relating brightness to flux, reflection coefficient, and solid angle by removing from the sphere wall two different areas. Then, in his words,

> . . . in the solution of these two equations all factors except the two readings of comparative brightness, the solid angles corresponding to the two brightness readings, and the unknown coefficient of reflection are eliminated . . .

The test equipment proposed by Benford consisted of a sphere that had one or more removable sections, leaving sections of known solid angle, and whose interior surface was coated with the material to be tested. He did recognize the fact that interreflections would occur, and developed his two equations as two infinite series.

The test upon which Benford reported was the determination of the coefficient of reflection of magnesium carbonate. He constructed a part-sphere of magnesium carbonate by machining concave surfaces in five blocks of the material and arranging them in such a way that they formed five-sixths of a sphere. He analyzed his procedure for errors with respect to photometry and the size of the areas removed and reached the conclusion that the method "may properly be called a precision method".

Also in 1920, Taylor (14) presented the design for an absolute reflectometer, and developed a theory based on his design. The reflectometer is shown schematically in Figure (3). In Taylor's

experimental instrument, c', the portion of the sphere which was cut off, was 10 per cent of the total sphere area. The hole was left open while the sphere wall was irradiated. Then the sample to be tested, in the form of a plane surface, was placed over the hole, and irradiated by the lamp. Then, by combining the brightness measurements in the two cases with a knowledge of the sphere geometry, the reflection factor of the test surface could supposedly be determined. All errors in the measurements taken with the instrument were described as experimental errors.

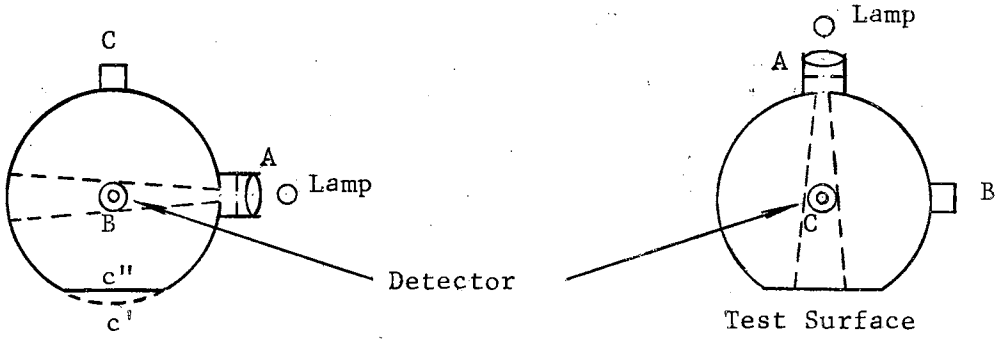

Figure 3. Schematic of Taylor Reflectometer

In the same year, Taylor (15) also described a portable instrument for the measurement of absolute reflection and transmission factors. It consisted of a 5 inch diameter spun copper ball, coated with a diffusely reflecting white paint and having three openings. Into one opening was fitted the surface to be tested. A Macbeth illuminometer, or photometer, was fitted into another opening 90° around the sphere from the test surface, the photometer opening being shielded from the test surface by an opaque screen. The third opening was fitted with a lighting tube, which was a cylinder containing a flashlight bulb and a series of lenses. The lighting

tube was used to introduce a narrow beam of light into the sphere, the light falling first on the test surface and then on a location on the wall which was not screened from the photometer. The ratio of the photometer signal when the beam fell on the test surface to that when the beam fell on the sphere wall was, according to Taylor, the reflection factor.

Results obtained using the portable instrument were given for several types of surfaces and compared with what Taylor called a point-by-point method. While the results of the two methods were not exactly the same, Taylor considered them to be in perfect agreement and dismissed the differences as being due to "experimental errors".

Taylor (16) later utilized a 4 inch diameter sphere with a magnesium oxide coating in determining the reflection of ultraviolet energy from surfaces. He incorporated a quartz monochromator into his apparatus, and pointed out that the same principals of the integrating sphere which apply to total reflectance also apply to monochromatic reflectance.

Karrer (17) published a paper in 1921 in which he reviewed the methods and instruments used in measuring the reflection factor of surfaces, discussed the use and theory of the Ulbricht sphere, and described a reflectometer which consisted of a photometric sphere and a Martens polarization photometer. Except for the fact that the three openings in the sphere were located differently with respect to each other and a different type of photometer was used, Karrer's reflectometer was very similar to Taylor's portable instrument. In fact, Karrer himself stated:

> The novelty in this suggestion lies not in the use of this particular photometer in the study of the transmission and reflection by bodies nor in the use of the sphere in this connection, but in the use of the sphere in a way that is in accord with the simple theory of the sphere, and that, in conjunction with a photometer such as the Martens, allows an absolute determination of either the transmission or reflection factor in one observation.

The utility of Karrer's reflectometer was not in the sphere itself but in the polarization photometer. This enabled the operator to compare the brightness of the test surface to that of the sphere surface nearby with one observation and hence eliminated the need for rotating the photometer in order to view the test surface and the sphere surface separately.

In 1928, McNicholas (18) published a comprehensive paper concerning absolute methods in reflectometry. He recognized the utility of Helmholtz' reciprocal relations as applied to reflectance measurements, and presented expressions for the relationship between hemispherical reflectance under unidirectional irradiation and unidirect reflectance under hemispherical irradiation.

McNicholas constructed and analyzed a sphere reflectometer, shown schematically in Figure (4). It was designed to utilize three sources, either separately or in combinations. The sample formed a part of the sphere wall. The directly irradiated portions of the sphere wall were shielded from the sample by means of screens placed inside the sphere. The reference location was adjacent to the sample, and the reflectance of the sample was determined by viewing the sample and the reference location in turn. A disadvantage of the instrument was the inability to measure reflectance at more than one angle. The values yielded by McNicholas' sphere reflectometer

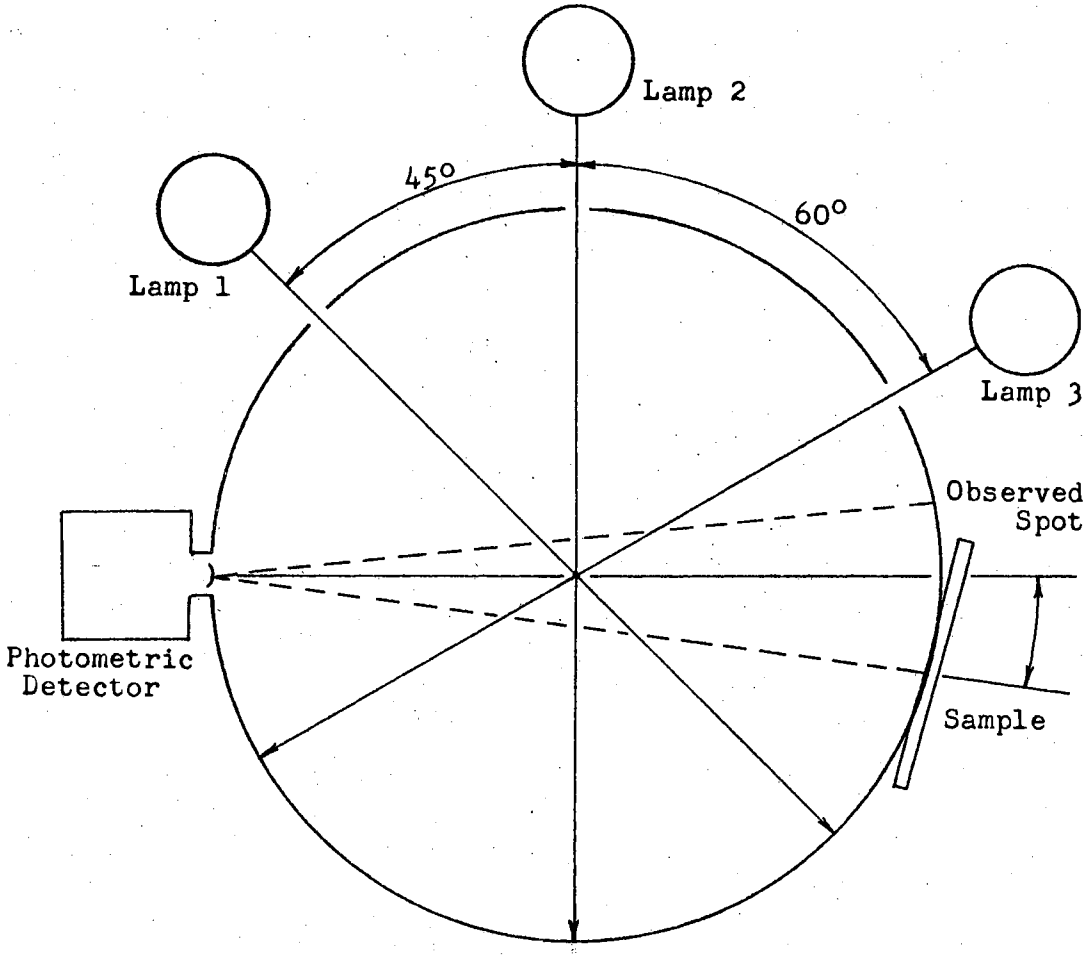

Figure 4. Schematic of McNicholas' Sphere Reflectometer

differed by six per cent from those determined by a hemispherical reflectometer. He attributed the difference in values to the departure of the sphere wall from a perfect diffuser and to the variation of the reflectance over different parts of the sphere.

Despite the fact that McNicholas designed, constructed, and analyzed a sphere reflectometer, he obviously placed more faith in the results obtained from a hemispherical reflectometer. In comparing the measurements of the two types of reflectometers, he blamed the six per cent variation on incorrect conditions existing in the sphere. In fact, he seemed to favor the sphere more as a source of diffuse irradiation than as an integrating device, and described an absolute reflectometer in the following manner:

> An arrangement providing completely diffused illumination of known amount, with means for observing the brightness of the sample at any desired angle from the normal in one azimuth is, then, an absolute reflectometer of a most general type, depending on no theory whatever of the action of an integrating device.

Hardy and Pineo (19), in 1931, investigated the errors in reflection factors obtained from an integrating sphere due to the finite sizes of the holes and the sample. They analyzed the cases in which the sample and the standard alternately occupied the same opening (substitution method) and in which both the sample and the standard were present at all times (simultaneous method). They reported that, while the error involved in the simultaneous method was of the order of 1 per cent, that of the substitution method could be as high as 25 per cent.

In 1934, Benford (20) reported on an improved version of his earlier part-sphere reflectometer. He claimed that his earlier model

was the only absolute reflectometer which had been introduced prior to 1934, and contended that his improved version was the first reflectometer applicable to surfaces which were not completely diffuse. His newer model consisted of two blocks of magnesium carbonate into which had been bored hemispherical cavities. The tops of the two blocks had then been cut off to create apertures to accomodate the sample and admit the irradiating energy. An etched glass window was placed over the sample aperture which separated the sample from the interior of the part-sphere. The purpose of the etched glass was to insure that all of the reflected energy, including any specular component, was reflected diffusely. It was in this manner that the reflectometer was made applicable to samples with both diffuse and specular reflectance components.

Benford, et al, (21) applied the part-sphere technique to the determination of the spectral reflectance of magnesium carbonate and magnesium oxide in 1947. Their results seemed fairly accurate, but they reported great difficulty in forming the test materials into spherical parts.

Finklestein (22), in 1950, designed and built an integrating sphere for ultraviolet reflectance measurements. His integrating sphere was not unique, but he did analyze the sphere and determined a sphere efficiency. He defined the efficiency as the ratio of the light flux absorbed by the photomultiplier detector to the light flux reflected by the sample. Using magnesium oxide as a sphere coating, with Benford's value of magnesium oxide reflectance, and magnesium oxide as the sample, he calculated the efficiency of a

five inch sphere to be 4 per cent in the ultraviolet region. His prediction that sphere efficiency decreases with increasing sphere radius was substantiated by later investigators.

Middleton and Sanders (23) performed what has come to be accepted as the most accurate measurements of the spectral reflectance of magnesium oxide using an integrating sphere reflectometer. They used a 10 centimeter diameter sphere composed of two silver-plated brass castings with an auto lamp for a source. They analyzed the sphere performance and determined an expression for the error involved in the measurements. As a result of their analysis, Middleton and Sanders estimated the reflectance values obtained to be accurate to $\pm$ 0.002.

Jacquez and Kuppenheim (24) made an important contribution to the study of integrating spheres in 1954. They presented the theory of the integrating sphere based on the solution, using the Hilbert-Schmidt theory, of the integral equation for multiple reflections in a cavity. They developed relations for the efficiency and the error of an integrating sphere as functions of sphere openings, sphere radius, and average wall reflectance. They were able to show conclusively that the efficiency and the error increase as the sphere radius decreases.

Tingwaldt (25) constructed a sphere reflectometer which departed radically from prior sphere reflectometers in that he utilized white zinc as a wall coating and he placed the source inside the sphere. The sphere reflectometer is shown schematically in Figure (5). The sample was prevented from receiving direct irradiation

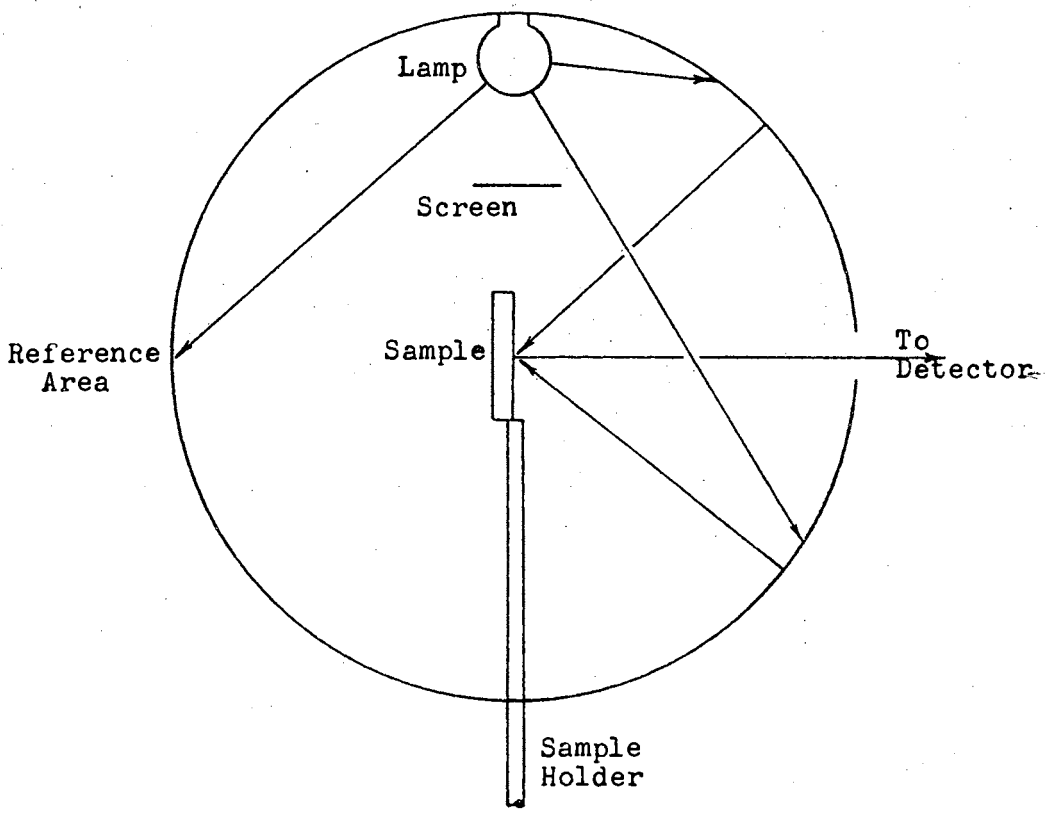

Figure 5. Schematic of Tingwaldt's Directional Reflectometer

from the source by placing it parallel to the longitudinal axis of the source, and by shielding it with a screen. He utilized an optical pyrometer with calibrated filters as a detector and, by the proper choice of filters, could determine monochromatic characteristics. The sample could be rotated to provide angular distribution measurements. Because the source was inside the sphere, the walls were not uniformily irradiated. This would seem to be an inherent source of error.

In 1955, Tellex and Waldron (26) reported on a sphere reflectometer used to determine the reflectance of magnesium oxide. The sphere was made of glass, and, since the reflectance of the magnesium oxide was determined as a function of its thickness, the sample was the wall coating.

Toporets (27) modified the integrating sphere to provide diffuse reflectance measurements from surfaces which were diffusely irradiated. He mounted the sample parallel to the direction of incident energy, as shown schematically in Figure (6), and placed a milk glass window over the entrance opening. The milk glass window supposedly caused the interior of the sphere to be diffusely irradiated and it, in turn, reflected the incident energy in a diffuse manner. Since the sample surface was parallel to the incident beam, it was impossible for the surface to receive energy directly from the milk glass window. The sphere, which was coated with barium sulfate, was constructed to allow the sample to be withdrawn from the "line of sight" of the detector so that the wall could be viewed to provide a measure of the incident energy. The sphere was rotated

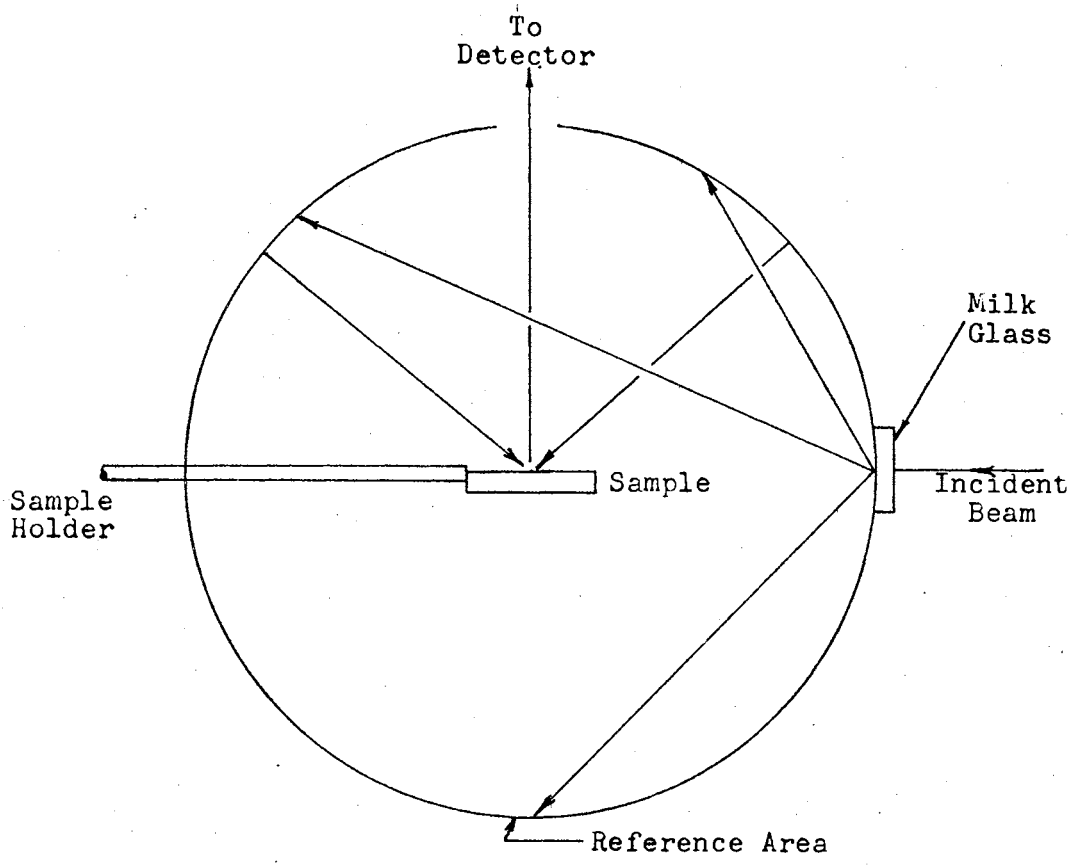

Figure 6. Schematic of Toporet's Reflectometer

about the horizontal sample to measure the angular distribution of the reflected energy.

Edwards, et al, (28) constructed and analyzed an integrating sphere reflectometer to measure the reflectance of imperfectly diffuse samples. Their instrument, which utilized a centered sample and a 16 inch diameter magnesium oxide coated aluminum sphere, gave results which had a reported accuracy of $\pm$ 0.015 for both absolute and relative measurements.

Fussell, et al, (29) designed and constructed a portable integrating sphere reflectometer. The instrument consisted of a 6 inch aluminum sphere with a coating of barium sulfate powder and a photomultiplier detector. The barium sulfate powder was chosen in preference to magnesium oxide because of its greater durability. The maximum absolute error in their measurements was estimated to be 7.2 per cent.

Brandenberg (30) used a magnesium oxide coated sphere as a hemispherical source of uniform brightness as well as a reference in determining the reflectivity of solids when irradiated at grazing angles of incidence. His experimental values differed from theoretical values for various samples by 5 per cent.

In 1966, Zerlaut and Krupnick (31) reported on an integrating sphere reflectometer for the determination of the absolute hemispherical spectral reflectance of a surface. Their instrument, which utilized a magnesium oxide coated sphere, was not unique in its design, but rather in its operation. By applying a mathematical procedure described in the report, the absolute reflectance of the

sphere wall itself could be determined. This was a point which had in the past been ignored, the wall reflectance being accepted as that value assigned to the coating material by other measurements. Also, a procedure was described whereby the absolute reflectance of a standard could be determined. This knowledge, along with the knowledge of the wall reflectance and sphere geometry, supposedly made it possible to determine with great accuracy the magnitude of the error in both absolute and relative measurements.

CHAPTER III

THEORY OF THE INTEGRATING SPHERE

Basis for Integrating Sphere Theory

As stated previously, the theory of the integrating sphere is based upon the fact that, within a diffuse sphere, the configuration factor, between any pair of points on the sphere wall is the same as any other pair. This fact can be proved quite easily using geometry and the definition of configuration factor.

Consider Figure (7), which is a two-dimensional representation of a sphere having diffuse walls. It is desired to determine the configuration factor between the elemental area dA_1 and any arbitrary elemental area dA_2.

The total energy leaving dA_1 in all directions is

$$\pi I_1 dA_1 \qquad (1)$$

The energy which leaves dA_1 and is incident on dA_2 is

$$I_1 \cos\theta_1 \cos\theta_2 dA_2 dA_1 / R_{12}^2 \qquad (2)$$

where I_1 is the intensity of the energy leaving dA_1, R_{12} is the line joining dA_1 and dA_2, and θ_1 and θ_2 are the angles between R_{12} and the normals to dA_1 and dA_2, respectively.

The configuration factor between two surfaces 1 and 2 is defined as the fraction of the total energy leaving a diffuse surface

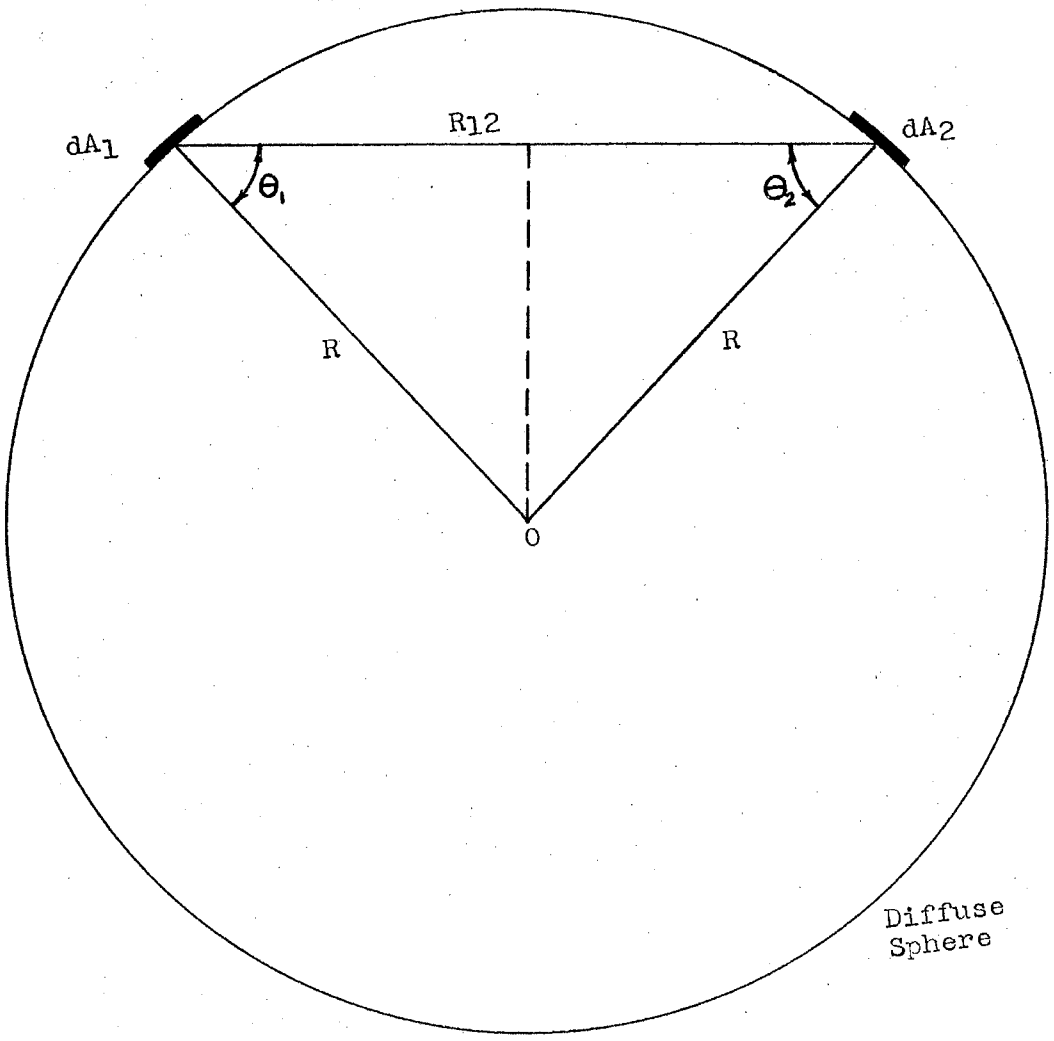

Figure 7. Integrating Sphere Geometry

1 which is directly incident on surface 2. Elemental area dA_1 is a diffuse surface by the original assumption that the walls of the sphere were diffuse. From Equations (1) and (2), the fraction of energy leaving dA_1 which reaches dA_2 directly can be determined.

$$F_{dA_1-dA_2} = \frac{I_1 \cos\theta_1 \cos\theta_2 \, dA_2 \, dA_1}{\pi I_1 \, dA_1 \, R_{12}^2} \qquad (3)$$

$$F_{dA_1-dA_2} = \frac{\cos\theta_1 \cos\theta_2 \, dA_2}{\pi R_{12}^2} \qquad (4)$$

But, from the geometry of the sphere, it is seen that θ_1 and θ_2 are equal. Therefore,

$$F_{dA_1-dA_2} = \frac{\cos^2\theta \, dA_2}{\pi R_{12}^2} \qquad (5)$$

If a perpendicular is erected at the midpoint of R_{12}, it will intersect the center of the sphere, forming two right triangles, as shown in Figure (7). Using one of the right triangles, the following relationship can be derived:

$$\cos\theta = \frac{R_{12}}{2}\left(\frac{1}{R}\right) \qquad (6)$$

$$\frac{\cos\theta}{R_{12}} = \frac{1}{2R} \qquad (7)$$

$$\frac{\cos^2\theta}{R_{12}^2} = \frac{1}{4R^2} \qquad (8)$$

Hence,

$$F_{dA_1-dA_2} = \frac{1}{4\pi R^2} dA_2 \qquad (9)$$

Since the areas dA_1 and dA_2 were arbitrarily chosen, the configuration factor F between them will be the same as that between

any other locations whose areas equal dA_1 and dA_2.

Simplified Theory of the Integrating Sphere

Figures (8) and (9) show schematically the two operations involved in determining the absolute reflectance of a sample. In Figure (8), a collimated monochromatic beam of energy is directed onto the sphere wall. The incident energy is reflected from the sphere wall, a part of it being reflected directly to the detector, and the remainder being reflected to the rest of the sphere. In the simplified theory, the assumptions are made that the sphere walls are completely diffuse, interior parts do not effect the interreflections within the sphere, and that no energy is lost through the entrance port. At each reflection from the wall, a fraction of the energy will reach the detector directly and the remainder will be reflected to other portions of the sphere walls where further interreflections will occur. As a result of the energy being reflected to the detector, the detector will produce a signal which will be proportional to the integral, over that portion of the wall which the detector views, of the energy which, in turn, will be a measure of the energy associated with the incident beam.

Figure (9) shows schematically the same arrangement as Figure (8), with the exception that the sample is in place. In this case, the monochromatic beam strikes the sample rather than the sphere wall. A portion of the incident energy is absorbed and the remainder is reflected onto the sphere wall. Here again the assumption is made that the sphere functions as a perfect reflecto-

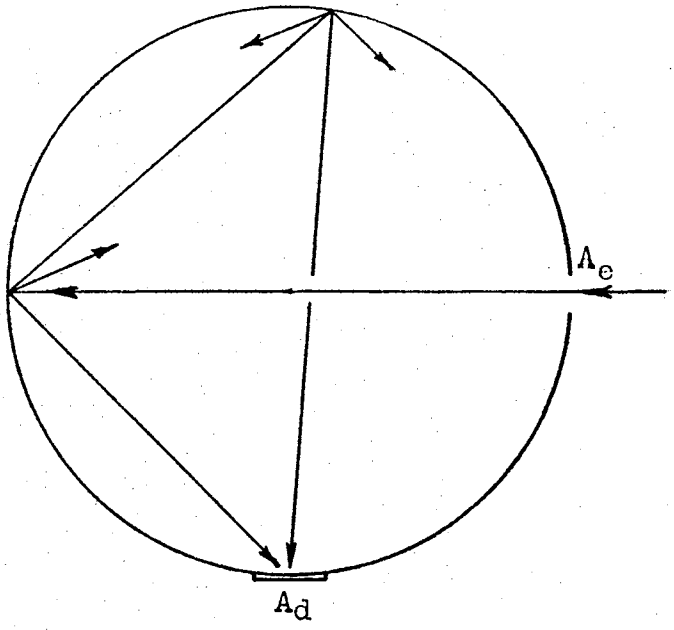

Figure 8. Interreflections Within Integrating Sphere (Sample Not Present)

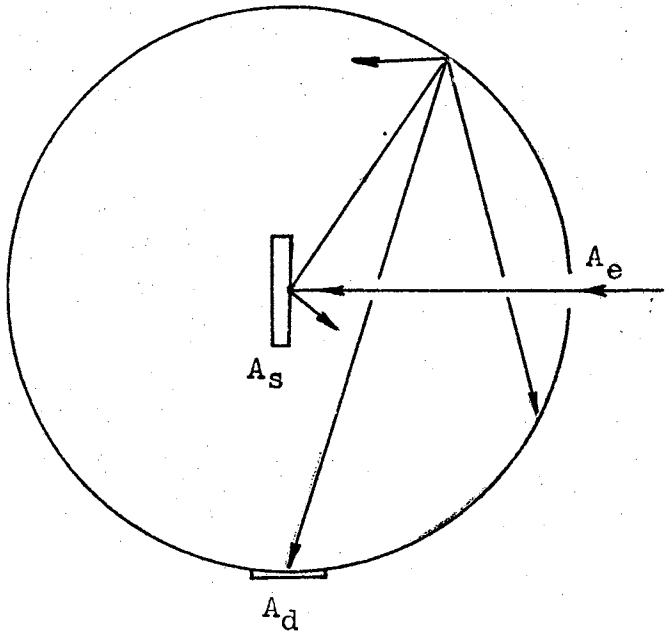

Figure 9. Interreflections Within Integrating Sphere (Sample Present)

meter; i. e., no phenomena occur which will result in an erroneous detector signal. In reality, several error-producing phenomena occur, but these will be covered later in an error analysis.

Of the energy reflected by the sample to the wall, part is reflected from the wall to the detector and the remainder is reflected to other portions of the wall where further interreflections occur. Again, the detector will yield an integrated signal which will be some fraction of the first signal, the fraction being equal to the reflectance of the sample.

The operations may be expressed by the mathematical relationships given below. When the monochromatic beam is incident on the sphere wall, the detector will yield a signal S_1.

$$S_1 = \int_{A_W}\int_{A_d} K(\phi_d,\theta_d) I_W(\phi_W,\theta_W) \frac{\cos\theta_d \cos\theta_W}{R_{wd}^2} dA_d\, dA_W \qquad (10)$$

where $K(\varphi_d,\theta_d)$ is the sensitivity of the detector, θ_d is the polar angle between the detector area dA_d normal and R_{wd}, R_{wd} is the line of sight between dA_d and dA_w, θ_w is the polar angle between the source area dA_w normal and R_{wd}, and $I_w(\varphi_w,\theta_w)$ is the intensity of the source area.

If the detector is not angularly sensitive, and the wall is diffuse, K can be removed from the integral, and $I_w(\varphi_w,\theta_w)$ can be written as I_w. As shown previously, $\cos\theta_d\cos\theta_w/R_{wd}^2 = 1/4R^2$. Then,

$$S_1 = \frac{K}{4R^2}\int_{A_W}\int_{A_d} I_W\, dA_d\, dA_W \qquad (11)$$

If A_d is sufficiently small so that I_w is effected only negligibly by interreflections from A_d,

$$S_1 = \frac{KA_d}{4R^2} \int_{A_W} I_W \, dA_W \tag{12}$$

But, for a diffuse surface,

$$I_W = \frac{J_W}{\pi} \tag{13}$$

where J_W is the radiosity of the wall. Hence,

$$S_1 = \frac{KA_d}{4\pi R^2} \int_{A_W} J_W \, dA_W \tag{14}$$

If the incident beam has associated with it a power of P watts, the radiosity of the wall is related to this power by the following relationship.

$$\int_{A_W} J_W \, dA_W = P\rho + P\rho\bar{\rho} + P\rho\bar{\rho}^2 + \cdots \tag{15}$$

where ρ is the reflectance of the wall to direct irradiation, and $\bar{\rho}$ is the average reflectance of the entire sphere.

The first term on the right-hand side of Equation (15) represents the energy associated with the first reflection from the wall. Because the wall is diffuse, the initially-reflected energy irradiates uniformily every other part of the sphere wall. The second term in the equation represents reflection of the initially-reflected energy, and the third term represents reflection of the twice-reflected energy. The process of interreflection is repeated an infinite number of times, the amount of energy reflected each time being equal to $\bar{\rho}$ times the amount reflected on the previous reflection. This is illustrated by the infinite series in Equation

(15).

After factoring out P_ρ from the right-hand side of Equation (15), the power series remaining can be written as

$$(1 + \bar{\rho} + \bar{\rho}^2 + \bar{\rho}^3 + \cdots) = \frac{1}{1-\bar{\rho}}, \quad |\bar{\rho}| < 1.0 \tag{16}$$

Equation (15) can then be written as

$$\int_{A_W} J_W \, dA_W = \frac{P\rho}{1-\bar{\rho}} \tag{17}$$

It follows, then, that Equation (14) can be written as

$$S_1 = \frac{KA_d P}{4\pi R^2}\left(\frac{\rho}{1-\bar{\rho}}\right) \tag{18}$$

For the case in which the sample is in place and is irradiated by the same monochromatic beam with power P, the radiosity of the wall is due entirely to the energy reflected from the sample. That is,

$$\int_{A_W} J_W \, dA_W = P\rho\rho_s + P\rho\rho_s\bar{\rho} + P\rho\rho_s\bar{\rho}^2 + \cdots \tag{19}$$

Hence,

$$\int_{A_W} J_W \, dA_W = P\rho_s\left(\frac{\rho}{1-\bar{\rho}}\right) \tag{20}$$

where ρ_s is the spectral reflectance of the sample and Equation (18) becomes

$$S_2 = \frac{KA_d P\rho_s}{4\pi R^2}\left(\frac{\rho}{1-\bar{\rho}}\right) \tag{21}$$

The ratio of the two signals, S_1 and S_2, gives

$$\frac{S_2}{S_1} = \left[\frac{KA_d P}{4\pi R^2}\rho_s\left(\frac{\rho}{1-\bar{\rho}}\right)\right]\left[\frac{4\pi R^2}{KA_d P}\left(\frac{1-\bar{\rho}}{\rho}\right)\right] \tag{22}$$

or,

$$\rho_s = \frac{S_2}{S_1} \tag{23}$$

If a comparative, or relative, spectral reflectance measurement is desired, a standard of known spectral reflectance can be installed in place of the sample, in which case Equation (18) becomes

$$S_3 = \frac{K A_d P}{4\pi R^2} \rho_{st} \left(\frac{\rho}{1-\rho}\right) \tag{24}$$

and a ratio of S_2 to S_3 yields

$$\rho_s = \rho_{st} \left(\frac{S_2}{S_1}\right) \tag{25}$$

where ρ_{st} represents the spectral reflectance of the standard.

Theory of Efficiency and Error

The efficiency of a sphere may be defined as the ability of a real sphere to collect and measure incident energy when compared to an ideal sphere. The geometry and coating of an integrating sphere have been shown to have a definite effect upon both the efficiency and the error involved in the measurements. Jacquez and Kuppenheim (24) have formulated the general theory of the integrating sphere as an integral equation, solved the equation for a few cases, and determined a relationship between efficiency, error, and sphere geometry and coating. Although their solutions were for an integrating sphere in which the sample formed part of the sphere wall, and a standard was used to provide relative measurements, the principles involved are applicable to an integrating sphere utilizing a centered

sample.

Assuming that the sphere walls and sample reflect diffusely and that the incident beam is controlled such that it falls only upon the sample, Jacquez and Kuppenheim calculated that the measurement obtained would be, with the sample in place,

$$B_s = P\rho_s \frac{b/S}{1-(\rho d/S)-(\rho_s c/S)} \tag{26}$$

and, with the sample replaced by the standard,

$$B_{st} = P\rho_{st} \frac{b/S}{1-(\rho d/S)-(\rho_{st} c/S)} \tag{27}$$

where B_s and B_{st} represent responses of the measuring device, P is the incident flux, ρ_s and ρ_{st} are respectively the reflectances of the sample and the standard, a is the spherical area of the entrance port, ρ is the reflectance of the sphere wall, b is the spherical area of the detector port, S is the area of the sphere, and $d = S - a - b - c$.

The ratio of the two measurements is

$$\frac{B_s}{B_{st}} = \frac{\rho_s}{\rho_{st}}\left[1 - \frac{(\rho_{st}-\rho_s)c/S}{1-(\rho d/S)-(\rho_s c/S)}\right] \tag{28}$$

In Equation (26), the term $P\rho_s$ is the flux initially reflected from the sample, and the term $(b/S)/[1-(\rho d/S)-(\rho_s c/S)]$ may be considered the efficiency of the sphere since the energy measured is less by this factor than the energy reflected from the sample.

In Equation (28), the factor

$$\frac{(\rho_{st}-\rho_s)c/S}{1-(\rho d/S)-(\rho_s c/S)} = \epsilon, \tag{29}$$

where ϵ is the error involved in measuring ρ_s/ρ_{st}.

Substituting in the expression for the efficiency the value of d yields

$$\eta = \frac{b/S}{1-\rho\left(\frac{S-a-b-c}{S}\right)-\rho_s c/S} \tag{30}$$

$$\eta = \frac{b/S}{1-\rho+\rho(a/S)+\rho(b/S)+(\rho-\rho_s)c/S} \tag{31}$$

The dependence of the sphere efficiency on the entrance port area, detector port area, sphere radius, and wall reflectance may be determined by taking partial derivatives of the efficiency with respect to each, while holding the other quantities constant.

$$\partial\eta/\partial(a/S) = \frac{-\rho(b/S)}{\left[1-\rho+\rho(a/S)+\rho(b/S)+(\rho-\rho_s)c/S\right]^2} \tag{32}$$

$$\partial\eta/\partial(a/S) < 0 \tag{33}$$

$$\partial\eta/\partial(b/S) = \frac{1-\rho+\rho(a/S)+(\rho-\rho_s)c/S}{\left[1-\rho+\rho(a/S)+\rho(b/S)+(\rho-\rho_s)c/S\right]^2} \tag{34}$$

$$\partial\eta/\partial(b/S) > 0 \tag{35}$$

$$\partial\eta/\partial S = \frac{-b(1-\rho)}{\left[1-\rho+\rho(a/S)+\rho(b/S)+(\rho-\rho_s)c/S\right]^2} \tag{36}$$

$$\partial\eta/\partial S < 0 \tag{37}$$

$$\partial\eta/\partial\rho = \frac{b/S\left(\frac{S-a-b-c}{S}\right)}{\left[1-\rho\left(\frac{S-a-b-c}{S}\right)-\rho_s c/S\right]^2} \tag{38}$$

$$\partial\eta/\partial\rho > 0 \tag{39}$$

From the sign of the partial derivatives of the efficiency with respect to the four quantities, it is evident that the efficiency of the sphere increases as the detector area and reflectance increase and the entrance area and sphere radius decrease.

From Equation (29)

$$|\epsilon| = \left|\frac{(\rho_{st}-\rho_s)c}{S(1-\rho)+\rho(a+b)+c(\rho-\rho_s)}\right| \tag{40}$$

The effect of the sphere radius on the error may be determined by taking the partial derivative of the error with respect to the sphere area.

$$\partial\epsilon/\partial S = \frac{-c(\rho_{st}-\rho_s)(1-\rho)}{[S(1-\rho)+\rho(a+b)+c(\rho-\rho_s)]^2} \tag{41}$$

$$\partial\epsilon/\partial S < 0 \tag{42}$$

From Equations (41) and (42), it is seen that the error associated with the sphere decreases as the sphere radius increases. Since it was previously shown that the efficiency of the sphere decreases as the radius increases, any sphere radius chosen must represent a compromise between efficiency and error for the given

sphere. This compromise is especially critical when the reflectometer is designed for long wavelength measurements due to the small amount of energy available for detection in this region. Optimization of the radius will be dictated by the amount of energy available for detection. That is, the optimum sphere radius is the largest radius which permits the sphere to collect and measure the available energy. This radius will result in the smallest error for the spectral region of interest.

Type of Reflectance to be Measured

Reflectance is generally accepted as being equal to the ratio of the energy reflected from a unit area of a surface to the energy incident upon the same unit area of surface. Such a broad concept, however, precludes the communication of useful information concerning the characteristics of the surface. To provide useful information, the reflectance of the surface should be given in terms of the manner in which the energy is incident upon the surface, the manner in which the energy is reflected from the surface, the spectral distribution of both, and the properties of the surface itself.

A great deal of discussion has taken place concerning the proper use of the terms "reflectance" and "reflectivity". Worthing (32) has suggested that the term reflectance be reserved for a property of a system while reflectivity be applied to a clean, optically smooth surface of a system. Wiebelt (33) used the term reflectance to indicate a characteristic of a real surface and, as such, it was a function of the surface roughness, presence or absence

of foreign materials, and other characteristics of a real surface. Harrison (34), by way of further explanations, advised the use of reflectivity for a material and reflectance for a specimen. Since the integrating sphere reflectometer measures the reflecting characteristics of a specimen, the term reflectance will be used henceforth in this dissertation.

In attempting to satisfy the desire and the need for useful information, several different types of reflectances have been defined, differing by the manner in which the surface is irradiated and the manner in which the reflected energy is collected and measured. Dunn (3) has defined seven different types of reflectance. McNicholas (18) described the reflected energy in terms of "apparent reflectances" which were defined as the ratio of reflected energy to the energy incident from a source whose intensity was replaced by a uniform intensity extending over the entire hemisphere. He defined different types depending upon whether the incident energy was unidirectional, diffuse, or originated from a large extended source, which would be neither unidirectional nor diffuse irradiation.

The type of reflectance for which the integrating sphere reflectometer presently under investigation is best suited is defined by Wiebelt (33) as the directional monochromatic reflectance $\rho_\lambda(\varphi,\theta)$ which is described as the ratio of the energy reflected in any direction from the surface to the energy incident on the surface in the direction (φ,θ). Mathematically, $\rho_\lambda(\varphi,\theta)$ is expressed as

$$\rho_\lambda(\phi,\theta) \equiv \frac{\int_H I'_\lambda(\phi',\theta')\cos\phi' d\omega'}{\int_{\Delta\omega} I_\lambda(\phi,\theta)\cos\phi\, d\omega} \qquad (43)$$

where (φ',θ') and (φ,θ) are the directions of the reflected and the incident energy, respectively, I'_λ and I_λ are the functional distribution of monochromatic intensity of reflected and incident energy, respectively, and $d\omega'$ and $d\omega$ are solid angles associated with the reflected and incident energy, respectively. If the incident solid angle is small, Equation (43) becomes

$$\rho_\lambda(\phi,\theta) = \frac{\int_H I_\lambda(\phi',\theta')\cos\phi'\,d\omega'}{I_\lambda(\phi,\theta)\cos\phi\,\Delta\omega} \tag{44}$$

McNicholas applied Helmholz's reciprocity relations to arrive at a relationship between the case of irradiation at angle (θ,φ) and hemispherical reflection, and the case of hemispherical irradiation and reflection at an angle (θ,φ). He applied Helmholz's relation to Figure (10), and showed that the elementary beams are reversible with regard to both direction and angular flux density, where the angular flux density in a specified direction from a small emitting surface of intensity I is equal to I multiplied by the projected area of the surface in the direction considered. If I' is the intensity of the reflected energy,

$$I'_{\theta\phi}(\theta',\phi')\cos\theta' = I'_{\theta'\phi'}(\theta,\phi)\cos\theta \tag{45}$$

where the subscripts indicate the direction of irradiation. Multiplying both sides of Equation (45) by $\pi/Id\omega$,

$$\frac{\pi I'_{\theta\phi}(\theta',\phi')}{I\cos\theta\,d\omega} = \frac{\pi I'_{\theta'\phi'}(\theta,\phi)}{I\cos\theta'\,d\omega} \tag{46}$$

The denominators on each side of this equation express the irradiation of the sample in the direct and reciprocal cases, respec-

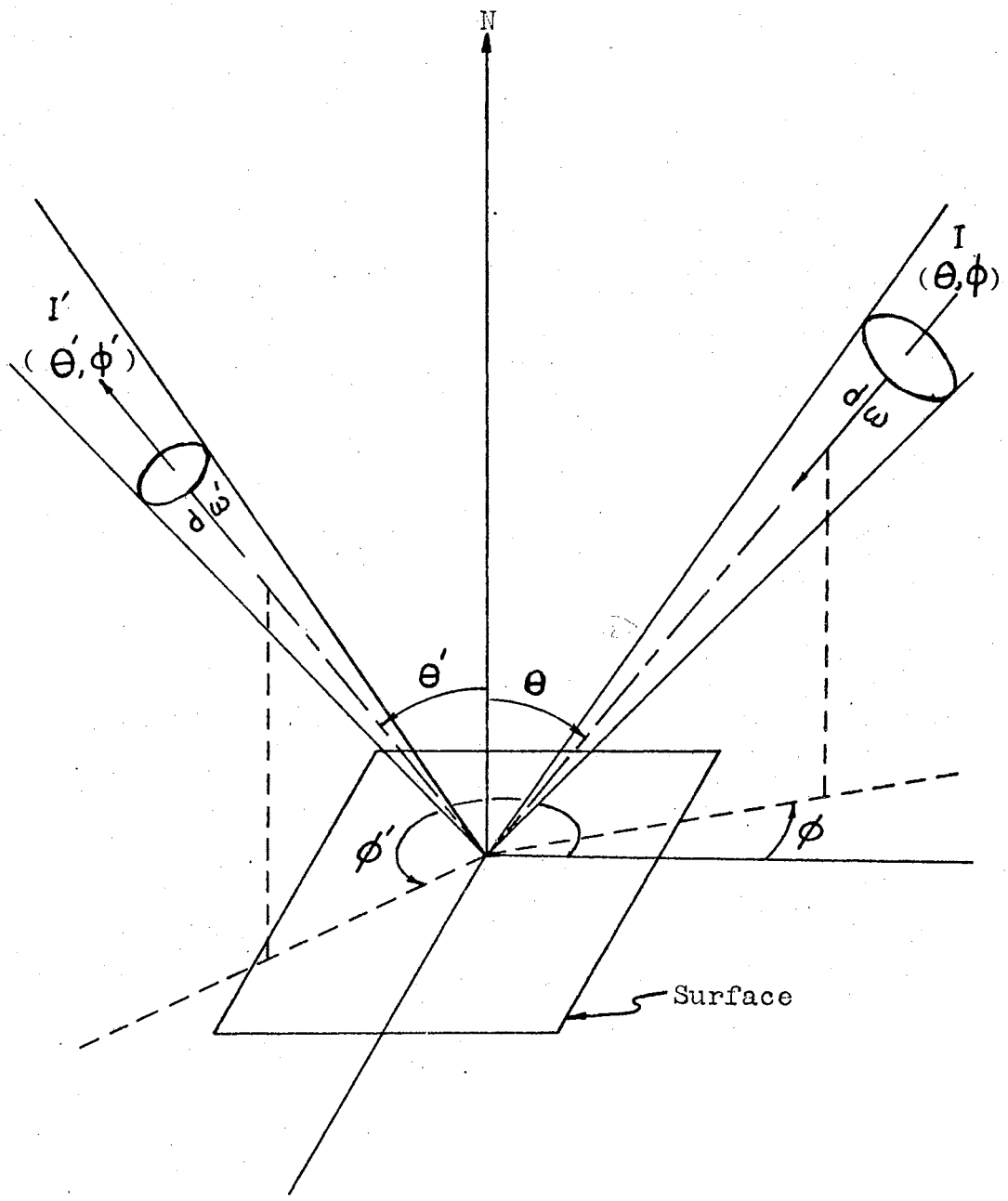

Figure 10. Irradiation and Reflection Through Elementary Beam dω and dω'

tively. McNicholas defined an equivalent-hemisphere intensity I_o by the relationship

$$I_o \equiv \frac{I \cos\theta \, d\omega}{\pi} \tag{47}$$

and an apparent reflectance as

$$A(\theta',\phi') \equiv \frac{I'(\theta',\phi')}{I_o} \tag{48}$$

The apparent reflectance is the reflectance that the sample would have if it was a perfect diffuser.

Applying these relationships to Equation (46) yields

$$\frac{I'_{\theta\phi}(\theta',\phi')}{I_o} = \frac{I'_{\theta'\phi'}(\theta,\phi)}{I_o} \tag{49}$$

and hence

$$A_u(\theta,\phi;\theta',\phi') = A_u(\theta',\phi';\theta,\phi) \tag{50}$$

where the subscript u denotes unidirectional irradiation, the first pair of angles indicates the direction of incidence, and the second pair denotes the direction of observation. Thus, the apparent reflectance in the direction (θ',φ') for unidirectional irradiation in the direction (θ,φ) equals the apparent reflectance in the direction (θ,φ) for unidirectional irradiation in the direction (θ',φ'). By integrating over the proper pairs of angles, it was shown that

$$\frac{\int A_u(\theta,\phi;\theta',\phi')\cos\theta \, d\omega}{\int \cos\theta \, d\omega} = \frac{\int A_u(\theta,\phi;\theta',\phi')\cos\theta' \, d\omega'}{\int \cos\theta' \, d\omega'} \tag{51}$$

or

$$R_u(\theta,\phi) = A_D(\theta',\phi') \tag{52}$$

where the subscript D indicates completely diffused irradiation, and where the quantity on the left side of the equal sign is the reflectance for unidirectional irradiation. That is, the apparent reflectance for diffuse irradiation is equal to the reflectance for unidirectional irradiation when the direction of observation for the apparent reflectance measurement equals the direction of incidence for the reflectance measurement. This relationship is illustrated in Figure (11).

The utility of the relationship with regard to the reflectometer under consideration lies in the fact that one measurement can determine two reflectance characteristics of a surface. That is, a sample can be irradiated at some angle (θ,φ) by a known amount of energy, and the amount of energy reflected in all directions can be determined. The ratio of these two quantities is $R_D(\theta,\varphi)$. But because of the laws of reciprocity, by knowing $R_D(\theta,\varphi)$, the reflectance of the surface, if it was a diffuse reflector, would be known for diffuse irradiation.

A slight modification of the reflectometer would permit the diffuse directional monochromatic reflectance to be measured where $\rho_{H\lambda}$ is defined as

$$\rho_{H\lambda}(\phi',\theta') \equiv \frac{\int_{\Delta\omega} I'_\lambda(\phi',\theta')\cos\phi' \, d\omega'}{\pi I_{\lambda o}} \tag{53}$$

and $\pi I_{\lambda o}$ indicates diffuse irradiation. Simply stated, $\rho_{H\lambda}(\varphi',\theta')$

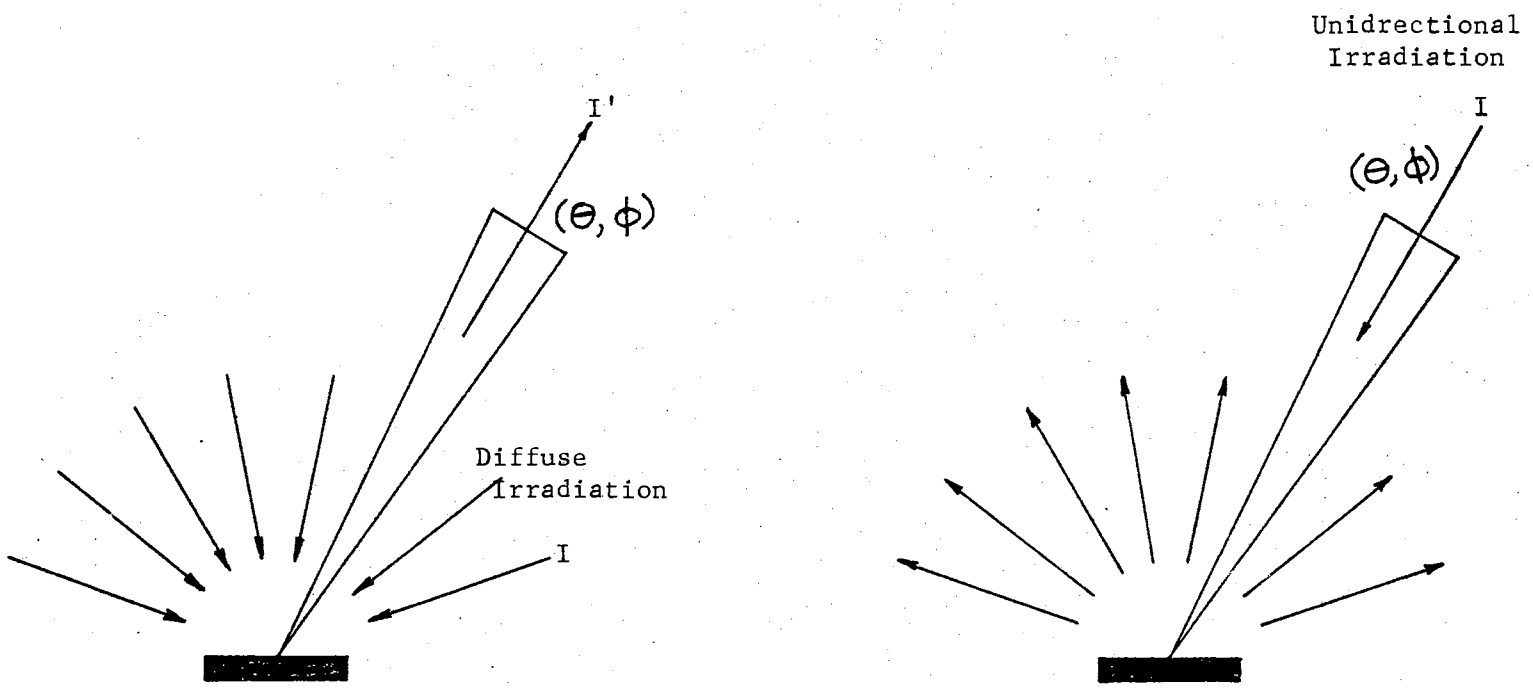

Figure 11. Representation of Apparent Reflectance for Diffuse Irradiation And Reflectance for Unidirectional Irradiation

is the ratio of the energy reflected in the wavelength band between λ and $\lambda + d\lambda$ over the solid angle ω in the direction (φ', θ') to the diffuse incident energy.

The sample could be diffusely irradiated by directing the incident beam upon the sphere wall. If the detector was placed so that it viewed only the sample when the sample was in place, the ratio of the signal produced when the sample was in place to the signal produced when the sample was not in place would be the diffuse directional monochromatic reflectance. As previously related, integrating sphere reflectometers have been so utilized many times. It is evident that, for a perfectly diffuse sample, the apparent reflectance for diffuse irradiation and the diffuse directional reflectance are identical.

Since surfaces are neither completely specular nor completely diffuse, the reflectance of every surface is a combination of diffuse and specular components, and a knowledge of the relative magnitudes of the two components is often useful. This is particularly true when a surface approximates either a specular or a diffuse surface, since the other component gives an indication of the magnitude of the error which might be involved in assuming the surface to be completely of one type.

For surfaces which do not exhibit off-specular peaks, the total reflectance of a sample is the sum of the diffuse component and the specular component. The reflectometer being considered is capable of determining both of these components by measuring the total reflectance and one of the components. That is, by measuring the

total monochromatic directional reflectance of a surface and the diffuse component of this reflectance, the specular component can be determined simply by subtracting the two. The diffuse component is determined by making the polar and azimuthal angles of incidence to the sample equal to zero. The energy which is specularly reflected from the sample then passes back out the entrance port, leaving only the diffuse component of reflected energy to be measured.

The diffuse component, as used in the previous paragraph, should be recognized as a very general term refering to all reflected energy with the exception of that which is reflected in a specular manner. The monochromatic specular directional reflectance $\rho_\lambda(\varphi,\theta)$ specular may be defined as

$$\rho_\lambda(\phi,\theta)_{SPECULAR} \equiv \frac{\int_{\Delta\omega'} I'_\lambda(\phi,\theta+180°)\cos\phi\, d\omega'}{\int_{\Delta\omega} I_\lambda(\phi,\theta)\cos\phi\, d\omega} \tag{54}$$

where $\Delta\omega = \Delta\omega'$. The diffuse component may be defined by

$$\rho_\lambda(\phi,\theta)_{DIFFUSE} \equiv \frac{\int_H I_\lambda(\phi',\theta')\cos\phi' d\omega'}{\int_{\Delta\omega} I_\lambda(\phi,\theta)\cos\phi\, d\omega} - \rho_\lambda(\phi,\theta)_{SPECULAR} \tag{55}$$

The specular and diffuse components of the monochromatic directional reflectance are shown in Figure (12).

Thus it is evident that the integrating sphere reflectometer investigated in this dissertation is able to measure, except as noted previously, the total monochromatic directional reflectance, and the diffuse and specular components of the monochromatic directional reflectance. By the reciprocity relations, the apparent reflectance may be determined, and, by modifying the reflectometer slightly, the diffuse directional monochromatic reflectance can

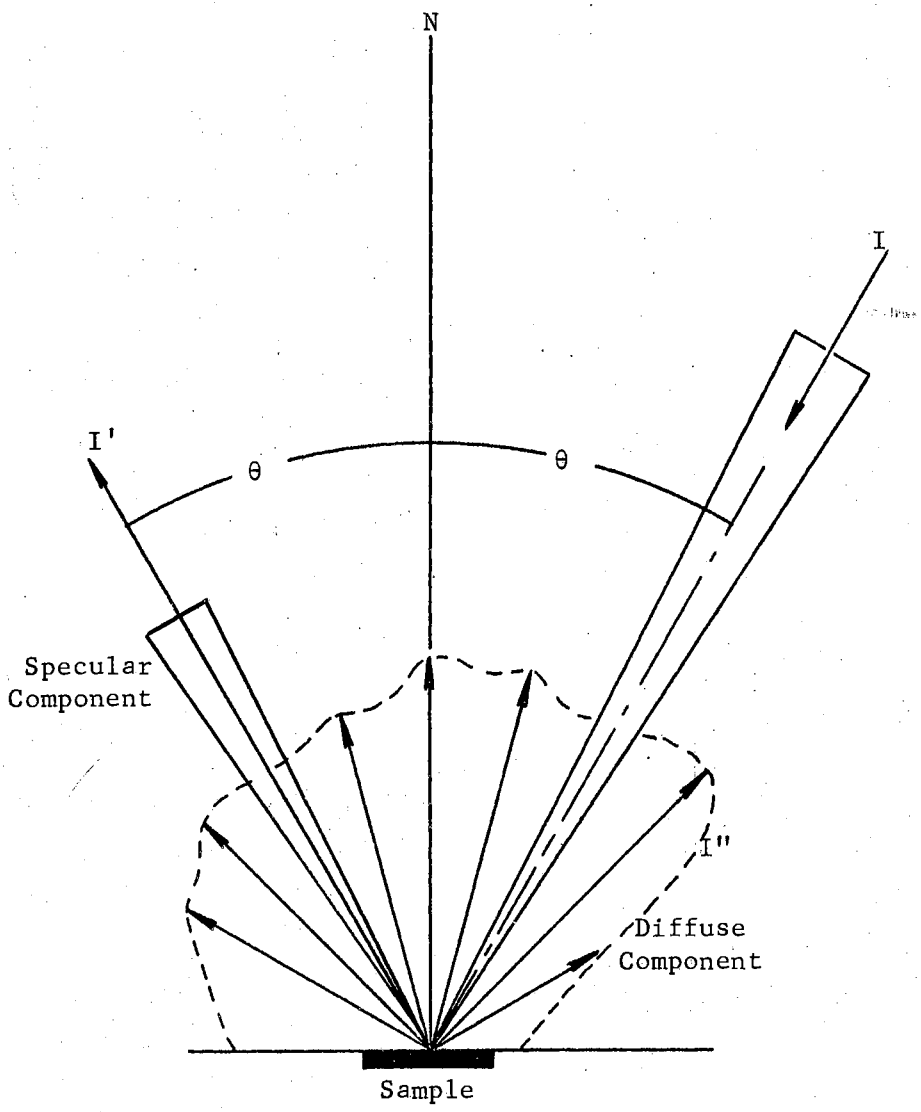

Figure 12. Specular and Diffuse Components of Monochromatic Directional Reflectance

be measured.

For those surfaces which exhibit off-specular peaks, only the total reflectance can be measured by the reflectometer under consideration. That is, the integrating sphere reflectometer is incapable of distinguishing components if the maximum energy is not reflected at the specular angle. Since few surfaces, however, exhibit peaks at near-normal angles, the total reflectance can be determined for most surfaces.

CHAPTER IV

CONSTRUCTION OF SPHERE REFLECTOMETER

The integrating sphere reflectometer may be considered to consist of three components: the sphere, the detection system, and the energy source. This chapter describes these components and the operations involved in constructing, preparing, and/or assembling them.

The Basic Sphere

The basic sphere chosen for the integrating sphere reflectometer was in the form of two aluminum hemispheres, which were manufactured by the Weber Brass Company, Cleveland, Ohio. A metal spinning process was used to produce the hemispherical form. The variation of the form from a perfect hemisphere was measured and found to be not more than 0.063 inches at any point, and less than a measurable amount at most points. The greatest variation from a true sphere occured at the lip, and was probably caused by turning up a portion of the lip to form a 1/2 inch flange around the hemisphere. The nominal radius of the hemispheres was 2 inches, and the thickness was 0.04 inches.

Three openings were made in one of the hemispheres while the other remained intact. The first opening was the entrance opening. It was a slit 3/4 inch long and 3/16 inch wide, located in the

center of the hemisphere. It was similar in shape to the slit in the globar water-cooled jacket, and 1/16 inch less in width than the image formed by the mirror system used for focusing the energy leaving the monochromator.

The second opening was a circular hole, having a diameter of 1/2 inch, whose purpose was to accomodate the Reeder end-on thermocouple. It was located 76° around the hemisphere from the entrance port and 35.4° up from a horizontal plane through the center of the sphere. With this configuration, the face of the thermocouple window was parallel to the incident beam and normal to the plane of the test sample.

The third opening was a slit similar to the entrance opening with the exception that the width was 6 per cent greater than the entrance slit. This auxillary entrance opening was located 76° around the sphere from the entrance opening, in the same horizontal plane. This opening was formed to permit the testing of a specular-diffuse sphere, which will be discussed in a later section.

A plug was constructed for covering either of the slits. It had a raised face which was 3/4 inch long, 3/16 inch wide, and 1/16 inch thick. It was curved to fit the inner surface of the sphere. Thus, when the plug was inserted into either slit, the curvature of the inner sphere surface was, for all practical purposes, uninterrupted.

A notch 1/2 inch wide was cut in the hemisphere flanges, and a hole 1/16 inch in diameter was drilled in the edge of the hemisphere. This permitted the spindle for the sample holder to pass into the sphere.

The sample holder consisted of two slotted aluminum side pieces which were held together by two strips of brass shim stock. One strip was placed across the bottom of the slotted side pieces and the other was attached to the back of the slotted pieces at the opposite end from the bottom piece. The sample holder spindle was attached to the top brass strip. The pieces thus formed a slotted frame 1/2 inch wide and 1 inch long into which the sample could be inserted. This arrangement permited the sample signal and the reference signal to be obtained without removing the sample holder from the sphere, since the incident beam passed undisturbed through the holder when the sample was not present.

The sphere wall coating is a highly critical component of the sphere reflectometer. Because the energy introduced into the sphere is reduced at each interreflection from the sphere wall due to absorption by the wall coating, it is desirable, from the standpoint of having maximum energy available for detection, that the wall coating have a high reflectance and low absorptance. This is especially true if only a small amount of energy is associated with the incident beam. Also, because of the nature of the integrating sphere reflectometer, it is essential that the coating reflect in a diffuse manner.

Agnew and McQuisten (6) were the first to recognize the ability of sulfur to meet the requirements of high and diffuse reflectance at long wavelengths. In attempting to determine a diffuse reflectance standard for comparative measurements, they investigated several materials and discovered the favorable characteristics of finely divided sulfur.

Kronstein, et al. (35) extended the study of sulfur as a standard of reflectance, investigating four forms of sulfur. Since Agnew had determined that finely divided sulfur reflects in an approximately diffuse manner at wavelengths up to 15 microns, Kronstein concentrated on determining the reflectance of different forms of sulfur in the wavelength region from 0.4 microns to 15 microns. After studying the characteristics of natural grown crystal of mineral sulfur, colloidal sulfur, sulfur flowers, and a high mu-content quenched sulfur, he determined that crystal and colloidal sulfur was not useful as reflectance standards, and that quenched sulfur had a reflectance of 90 per cent or greater at all wavelengths out to approximately 13.4 microns except for a region from 11 microns to 12.4 microns. The reflectance of sulfur flowers did not differ greatly from quenched sulfur, as shown in Figure (13). Because the two types of sulfur exhibited similar reflectances in Kronstein's work, it was decided that both should be tested for possible sphere coatings.

Several different methods of applying the coatings to the sphere walls were considered. Because quenched sulfur is insoluble, methods of application of sulfur flowers were possible which could not be utilized in applying the quenched sulfur. All methods subsequently utilized in applying both the sulfur flowers and quenched sulfur involved preliminary cleaning of the sphere with acetone to remove dirt and oxides.

Two different methods were used to apply the sulfur flowers to the aluminum hemispheres. One method consisted of heating the hemisphere to a temperature well above the vaporization temperature of

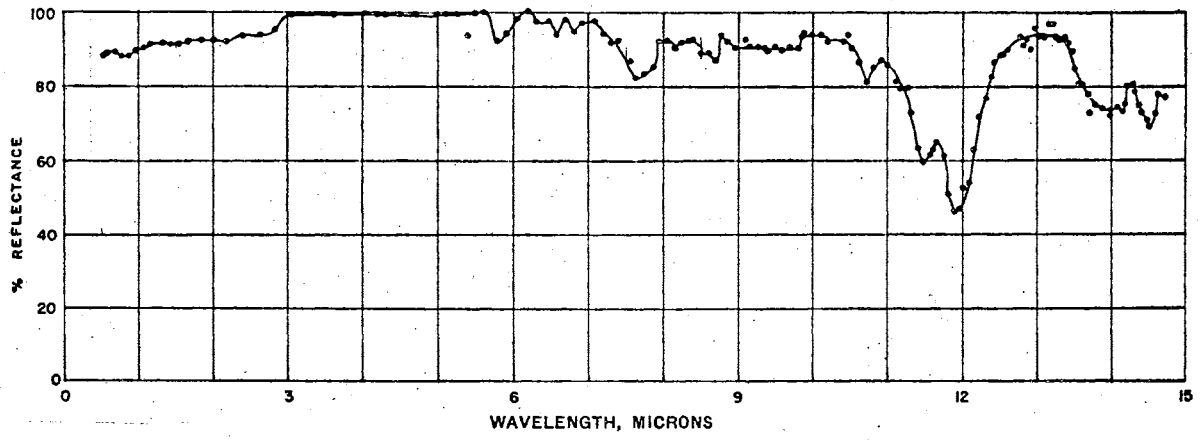

Sulfur sublimed m.f. (sulfur flowers), average of four curves (corrected reflectance curve).

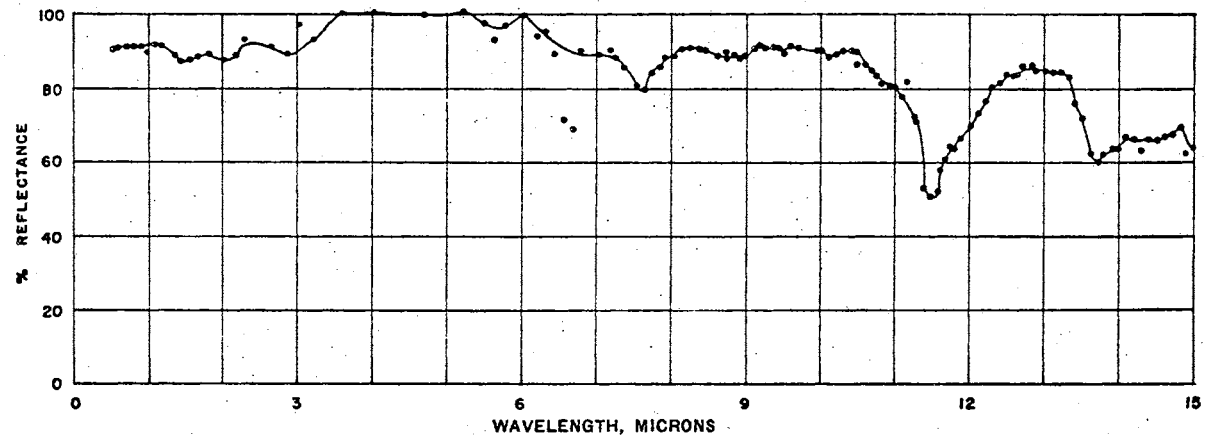

Sulfur vaporized and quenched (corrected reflectance curve).

Figure 13. Spectral Reflectance of Sulfur Forms (Ref. 35)

carbon disulfide, and spraying a supersaturated solution of sulfur flowers and carbon dissulfide onto the heated hemisphere. The carbon dissulfide evaporated upon contacting the hemisphere, leaving a very uniform coating of sulfur flowers. Much care had to be exercised in controlling the rate of application. If the solution was applied too rapidly, the hemisphere cooled to such an extent that the carbon dissulfide did not evaporate upon contact, but instead formed large drops which in turn led to large beads of sulfur. If the solution was applied too slowly, the sulfur already applied would melt in places due to non-uniform heating of the hemisphere. The procedure finally adopted was a 5 second application period followed by a 15 second delay to enable the hemisphere to return to its original temperature. This procedure yielded a surface which appeared quite uniform and which was very durable.

The second method consisted of applying alternate layers of white shellac and loose sulfur flowers. After a layer of shellac had been painted onto the walls of the hemisphere, a small quantity of sulfur flowers was introduced into the hemisphere. The hemisphere was then rotated and tilted, causing the loose flowers of sulfur to tumble about, covering the wet shellac. The coating resulting from three layers of sulfur and shellac appeared very uniform.

The term "quenched" sulfur arises from the fact that this particular form of sulfur is produced by a quenching process whereby sulfur vapors are dissolved in carbon disulfide, a process which results in a large fraction of the sulfur being present in the mu

form. The particular material selected for application was a "pure grade quenched sulfur" having a mu-content of 85 to 93 per cent, produced by Stauffer Chemical Company under the brand name "Crystex".

Three methods of quenched sulfur coating application were investigated. All three methods involved, as a first step, the application of two layers of contact cement, the second layer being applied after the first had dried.

The first method attempted was the application of a benzene and sulfur slurry using an air-operated sprayer while the hemispheres were irradiated by two 250 watt incandescent lamps. Several applications were required, and the resulting sulfur surface was severly pitted, the size of indentions being large compared to the thickness of the coating. Excellent bonding between the sphere walls and the sulfur coating occurred, but it was decided that the pitting prevented the coating from being as uniform as desired. It was felt that a satisfactory surface could be obtained if the benzene-sulfur slurry could be applied to the sphere walls with less force.

The second method attempted involved submerging the hemispheres, with the open side downward, in a benzene-sulfur slurry. The sulfur in the slurry was sufficient to cover completely the hemispheres after the benzene and sulfur had separated. It was thought that the sulfur would adhere to the cement-coated portion of the hemispheres and, upon evaporation of the benzene, would result in a uniform coating. However, in the presence of the large amount of benzene, the contact cement dissolved, and the sulfur would

not adhere to the bare metal of the hemispheres.

The third method attempted, and the one finally adopted, followed the procedure suggested by Dunn (3). After the contact cement had been applied and allowed to dry for an hour, the hemispheres were heated for ten minutes by placing them under the two incandescent lamps. The lamps were placed approximately 12 inches from the hemispheres. Heating the hemispheres for a short time softened the contact cement and made it more amenable to bonding with the sulfur. After the heating operation, a sulfur-benzene slurry was applied to the hemispheres by means of a BVI electric sprayer. The sprayer utilized was a Model VS-800, manufactured by Burgess Vibro-Crafters, Inc. The sulfur used in the slurry had previously been sifted through a 65 mesh screen. Application of the heat lamps was continued while the spraying was in process. This caused the slurry to dry rapidly upon the surface of the hemispheres and allowed almost continous application. Many applications were required, but this was due to the fact that the volume of slurry delivered by the sprayer was very small.

When the coating had reached a thickness of approximately 1/16 inch, it appeared to be of acceptable uniformity and it was decided that no further purpose could be served by the application of additional sulfur.

Kneissel (36) found in his work with sodium chloride coatings that the reflectance of the coating decreased as the roughness of the coating increased. In order to determine if the same phenomenon was true for sulfur, three hemispheres were coated with Crystex and tested for the gross effect of roughness.

For the sake of clarity, the hemispheres were identified as A, B, and C. Hemisphere A had entrance and detector openings, while hemispheres B and C had no openings. A and B were coated simultaneously. The slurry was applied in the form of a very fine mist and resulted in a uniform though rough coating. C had a uniform but somewhat smoother coating than did A and B. This was due to the fact that the slurry was applied to C in the form of large droplets which caused the Crystex to flow slightly before the benzene dried completely.

The Reeder thermocouple was inserted into A and signals were compared, under identical conditions, when A was mated with B and with C. The larger signal was obtained when C was mated with A, indicating a higher reflectance of the smoother hemisphere than that of the rough hemisphere. Thus the indication was that the reflectance of the Crystex was a function of roughness.

Loose Crystex was then introduced into hemisphere B. The hemisphere was then rotated, causing the loose Crystex to tumble about the inner surface of the hemisphere. This procedure, resulted in leveling the peaks and filling the valleys, yielded a coating in B which appeared much more smooth than that in C. Further tests revealed that the largest signal was obtained when the newly smoothed hemisphere B was mated with A, thus strengthening the postulate that the reflectance of the Crystex coating was a function of roughness. Hemisphere A was then smoothed in the same manner as B and still higher signals from all combinations were obtained.

The test to determine, qualitively, the reflectance of the different types of coatings relative to each other, involved mating

each test-coated hemisphere with the same quenched sulfur-coated hemisphere A, which was equipped with an entrance and detector opening. Each sphere combination was irradiated with the same amount of energy, using the same monochromator slit width and amplifier gain setting at each wavelength tested. The sphere was rotated such that the entering energy beam was initially incident on the common detector half of the sphere. Under this arrangement, the detector signal should be indicative of the relative reflectance of the coating material being tested. That is, the greater the reflectance of the material being tested, the greater will be the average reflectance of the sphere coating and, hence, the greater will be the detector signal.

The detector signals were recorded at the same wavelength for each test material. The white shellac, sulfur flowers coating exhibited very low reflectance and was not considered in the final results. The evaporated flowers of sulfur coating was smoothed in the same manner as the quenched sulfur coating before the test was conducted.

The results, shown in Figure (14), were normalized with the signal produced by the smoothed quenched sulfur-smoothed quenched sulfur combination. On the basis of this test, smoothed quenched sulfur was chosen as the sphere coating.

After determining that the smoothed quenched sulfur coating exhibited the highest relative reflectance among the coatings tested, the coating was tested for uniformity and diffuseness. The uniformity test involved placing the sphere on a rotary table, rotating the

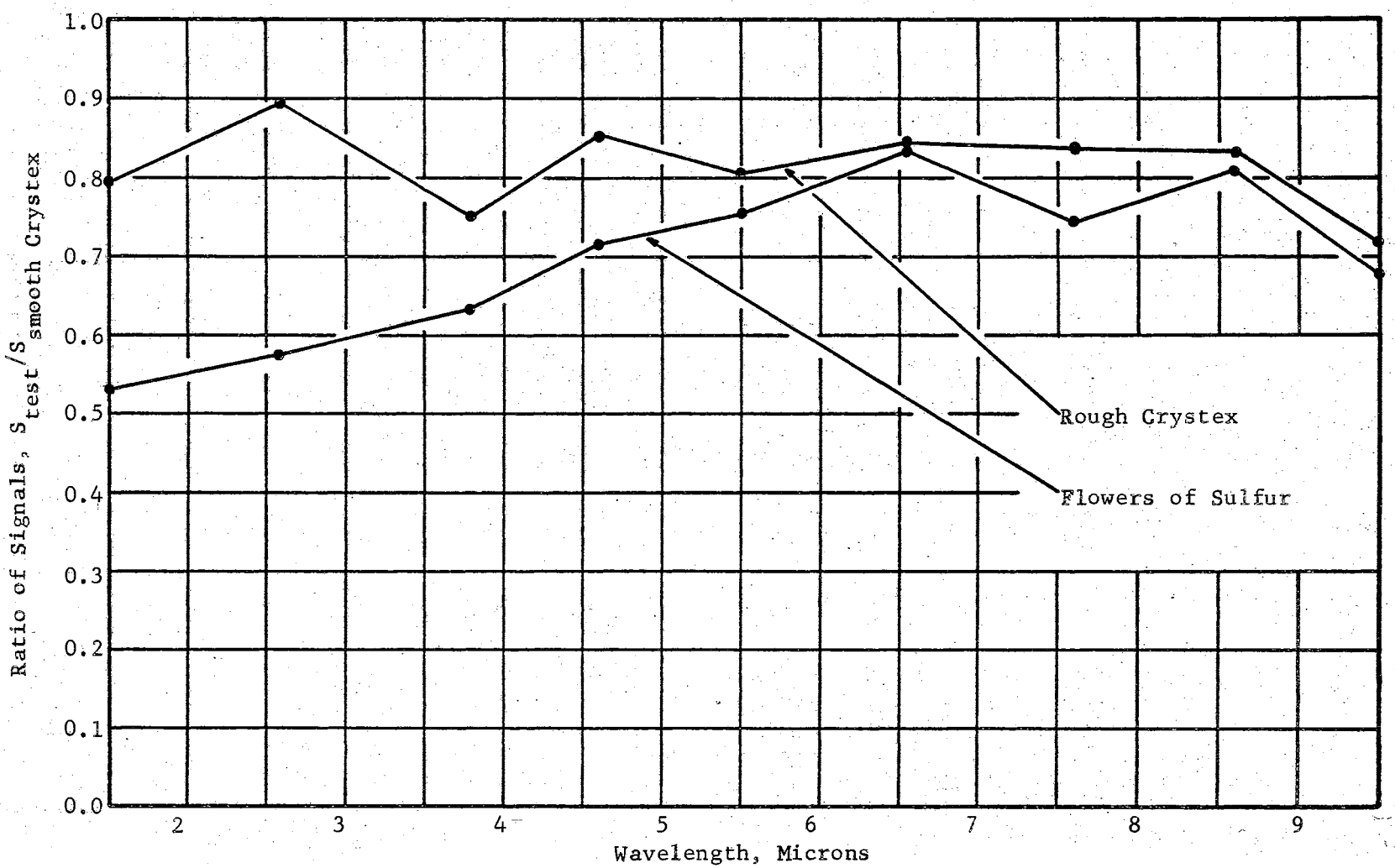

Figure 14. Comparison of Detector Signals for Different Coating Materials

sphere about an imaginary vertical line passing through the center of the entrance opening plane, and determining if the decrease in detector signal corresponded to the decrease in projected entrance area presented to the irradiating beam. The sphere was rotated through an included angle of 70°. The coating was tested at wavelengths of 0.58, 5.3, and 9.0 microns. The detector signals at each angle considered were adjusted to allow for the effect of sphere rotation.

Two correction factors were used to relate the detector signal at each angle θ to the signal produced when θ was zero. The first of these, C_1, was the cosine of the angle of rotation. That is, for a uniform coating, the signal produced when $\theta = \theta'$ should equal the product of the signal produced when $\theta = 0$ and the cosine of θ'. This corresponds to the case in which the sphere wall thickness is infinitely small.

The real sphere wall, of course, has a finite thickness. As seen in Figure (15), the sphere wall reduces the area through which the energy may enter the sphere. That is, the projected entrance area is less on the inner surface of the sphere than on the outer surface.

Correction factor C_2 was derived as follows, where the depth of the opening was assumed to be unity and the symbols are defined in Figure (15):

$$Z' = Z\cos\theta' \qquad P = t\sin\theta'$$

$$Z'' = Z' - P \qquad Z'' = Z\cos\theta' - t\sin\theta'$$

$$\frac{Z''}{Z} = \cos\theta' - \frac{t\sin\theta'}{Z}$$

For a linear system, where S_1 is the detector signal when $\theta = 0$ and S_2 is the signal when $\theta = \theta'$,

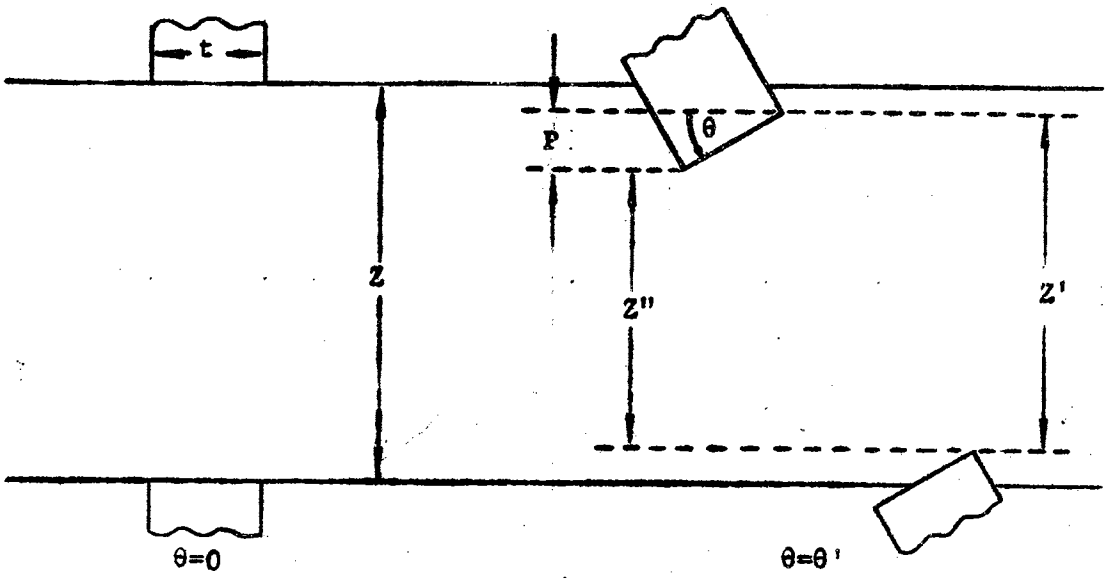

Figure 15. Entrance Opening Geometry

$$\frac{S_2}{S_1} = \frac{Z''}{Z}$$

or,

$$S_2 = S_1 (\cos\theta' - \frac{t\sin\theta'}{Z})$$

For Z = 3/16 inch and t = 1/16 inch,

$$S_2 = S_1 (\cos\theta' - \frac{\sin\theta'}{3})$$

C_2 is, then, equal to $(\cos\theta' - \frac{\sin\theta'}{3})$

Application of C_2 alone assumes that all of the energy which strikes the rotated edge of the entrance opening is reflected back out the entrance opening. Application of C_1 alone assumes that all of the energy striking the rotated edge is reflected into the sphere with none of the energy being absorbed by the edge. The actual case lies somewhere between these two extremes. For this reason, the corrected detector signal which was finally accepted as most

nearly approximating the actual case was the average of the values obtained when the two correction factors were applied individually. The results of the test at a wavelength of 9 microns are shown in Figure (16). The values of the detector signal were normalized when θ was 0. The variation over 70° is seen to be less than 4 per cent.

In the test for diffuseness, the entrance opening was plugged and the sphere rotated such that the auxillary opening, through which the energy was admitted, was horizontal. This placed the detector in the same horizontal plane as the auxillary opening. Because the opening presented to the incident beam was much wider than the beam, the sphere could be rotated through a large included angle without having to account for the reduction in entrance area. Under this arrangement, the angle at which specularly reflected energy would fall on the detector was 17.7°.

The sphere was rotated such that the angle of incidence on the sphere wall was varied from -20° to 40°. Under this procedure, any coating specularity was presented two opportunities to be manifested. That is, if the coating had an appreciable specular component, the detector signal would have been smaller than normal when the angle of incidence was zero and greater than normal when the angle of incidence equalled the specular angle.

The test was conducted at wavelengths of 3.5 and 6.5 microns. The sphere was rotated continously at 3.5 microns. At 6.5 microns, because the high amplifier gain necessitated slow response time, the sphere was rotated through 1° increments. No discernible change was noted in the detector signal at any angle for either

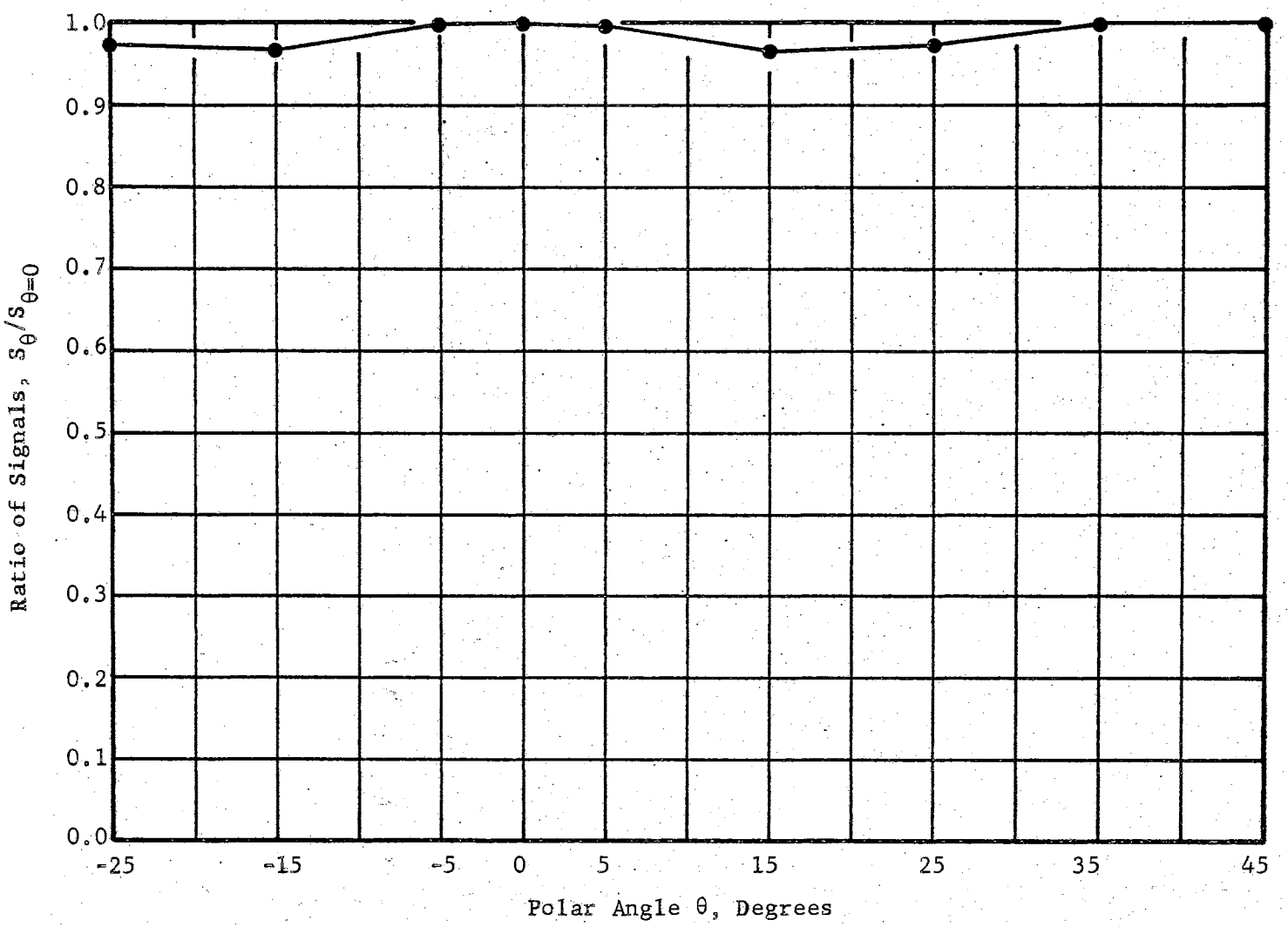

Figure 16. Results of Test for Non-Uniform Sphere Coating Reflectance

wavelength. Since no specular component was exhibited at 6.5 microns, it was believed that very little if any specularity would be exhibited at wavelengths as great as 10 microns. It was concluded, therefore, that the sphere coating was of acceptable diffuseness and uniformity.

The test for diffuseness also offered further evidence of the uniformity of the sphere coating. However, the diffuseness test did not extend over as wide a wavelength range as did the uniformity test due to the reduced entrance area presented by the horizontal slit.

As a result of these operations, the "sphere" portion of the integrating sphere reflectometer evolved as a 4 inch diameter sphere with a mu-type sulfur coating, a 3/16 by 3/4 inch entrance opening, and a 1/2 inch thermocouple opening. Through the use of a graduated scale attached to the top of the sphere and a pointer attached to the sample holder spindle, the polar angle of incidence could be varied over 90°, as desired. Thus, the directional reflectance as a function of polar angle of incidence could be determined.

The Detection System

Due to the known low efficiency of the sphere, and the small amount of energy available for detection in the long wavelength region, one of the criteria for choosing a detector was that it could be fitted, as nearly as possible, into the sphere wall. By such a placement, the effective area of the detector would be maximized and, hence, the signal from the detector would be as large as possible. The effective area of a detector may be defined

as the area of an imaginary detector forming part of the sphere wall which receives the same amount of energy as the actual detector.

Two types of detectors were available which met this criterion. One type was a bolometer. Due to the construction of the bolometer housing, the detecting element itself could be placed no nearer than 1/16 inch from the outer surface of the sphere, or approximately 5/32 inch from the inner surface of the sphere. Since the window in front of the sensing element was only 1/4 inch in diameter, the effective area of the detector was approximately two-thirds as great as it would have been if it had been mounted flush with the inner surface of the sphere. This assumes that the detector element area was large as the window, which it was not. Tests were conducted which verified the fact that the reduction in effective area reduced the sensitivity of the bolometer to a non-usable level.

The second detector available was a Reeder end-on designed thermocouple. It was equipped with a 7/16 inch diameter window, approximately 1/16 inch thick. With this construction, it was possible to insert the window into the sphere so that the face of the window was flush with the inner wall of the sphere coating and the thermocouple itself was approximately flush with the outer wall of the sphere. The thermocouple element was approximately 4 millimeters by 5 millimeters and was mounted in the center of the window. This configuration resulted in effective thermocouple dimensions of approximately 3.52 millimeters by 4.44 millimeters, or an effective area of approximately 78 per cent of the actual detector area. The blackened thermocouple had a resistance of 32 ohms and the window material was potassium bromide.

The Reeder thermocouple was tested for directional sensitivity by mounting it on a rotary table and rotating it through 180° while irradiating it with a monochromatic, parallel beam of energy. The thermocouple was tested at a wavelength of 10 microns, and the response was recorded as a function of the polar angle θ. The results are shown in Figure (17). The dashed line represents the response a perfect detector having no directional sensitivity would have shown under similar conditions.

For convenience, the detection system is considered to include the supporting instrumentation and the necessary optical components. A Perkin and Elmer Model 99 single beam, double pass monochromator was used to provide the monochromatic test beam. The beam was mechanically chopped by the monochromator at a rate of 13 cycles per second. The Reeder thermocouple was adapted for use with the Perkin and Elmer preamplifier and amplifier. The signal produced by the thermocouple was recorded by a Leeds and Northrup strip recorder.

The optical components necessary for transferring the energy from the source to the monochromator and from the monochromator to the sphere are shown schematically in Figure (18). All mirrors shown were prepared by vacuum depositing aluminum upon the front surfaces of glass blanks.

The components are: (a) spherical mirror with 9 inch radius and 18 inch focal length, used to collect a portion of the energy emitted by the source and focus it upon the monochromator entrance slit; (b) another spherical mirror having a 9 inch radius and 18 inch

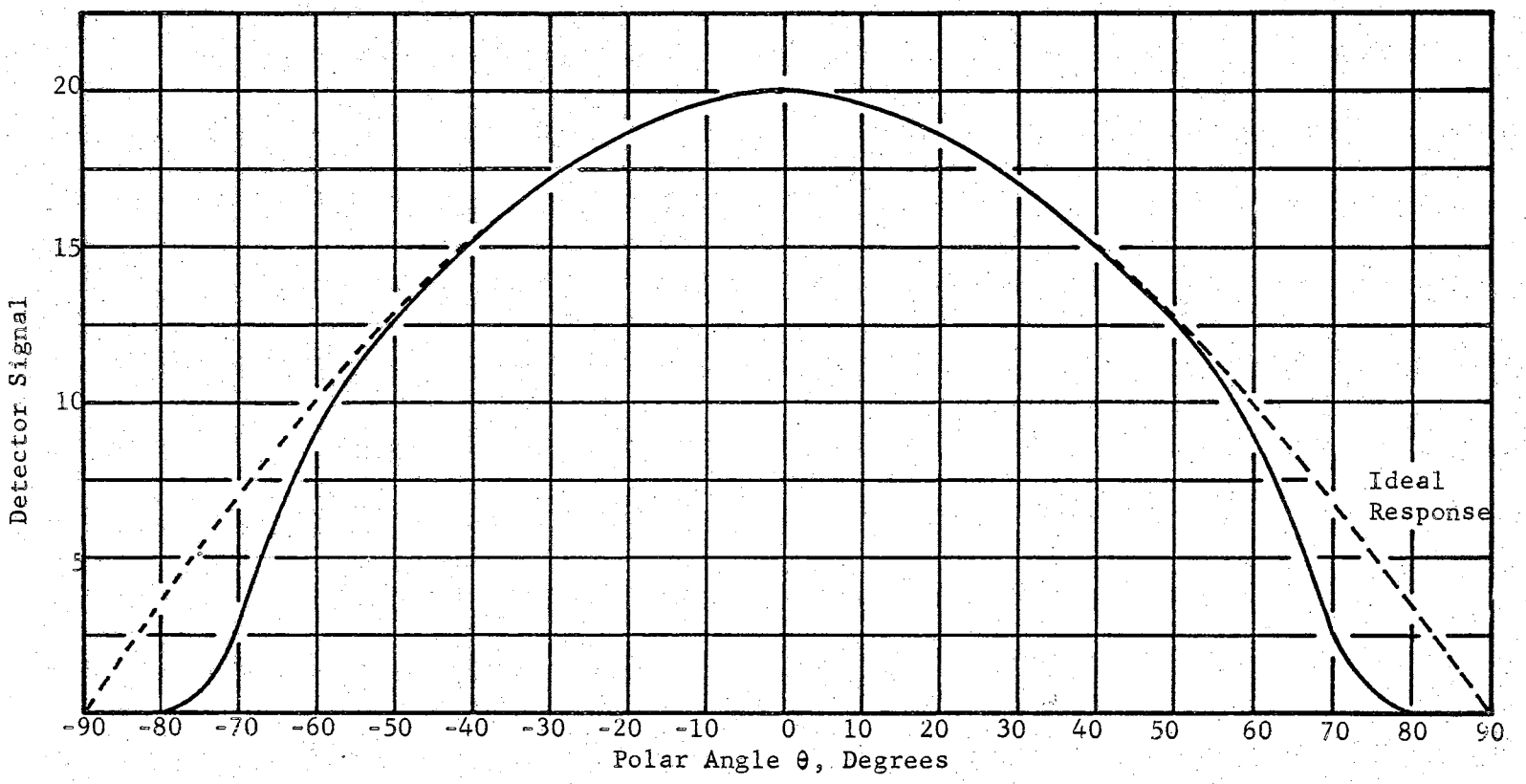

Figure 17. Test for Angular Sensitivity of Reeder Thermocouple

focal length, used to collect the diverging monochromatic beam leaving the monochromator exit slit and convert it to a collimated beam; (c) a flat mirror used to direct the collimated beam upon the entrance opening of the sphere. This optical arrangement produces, at the entrance of the sphere, an image of the source which is approximately 3/16 inch wide and 3/4 inch long.

The Energy Source

The energy source chosen to provide the long wavelength monochromatic beam was a globar mounted in a water-cooled holder. Tests were conducted to compare the ability of the globar and a carbon arc to provide a monochromatic, long wavelength beam of sufficient energy to produce a detectable signal within the sphere. At 6.6 microns, the signal produced by the globar was approximately 5 times as large as that produced by the carbon arc beam. This was attributed to the fact that the area of the globar was much greater than that of the carbon rod tip.

Because it is imperative to transfer as much energy as possible from the globar into the monochromator, the position of the globar and collecting mirror with respect to the monochromator and with respect to each other is very critical. The intensity of the globar slit image at the focal point of the mirror is a function of the solid angle intercepted by the mirror. That is, the larger the solid angle intercepted by the mirror, the greater will be the amount of energy collected by the mirror. For this reason, it would appear logical to locate the collecting mirror as near the globar as possible while still obeying the rules of image formation. However,

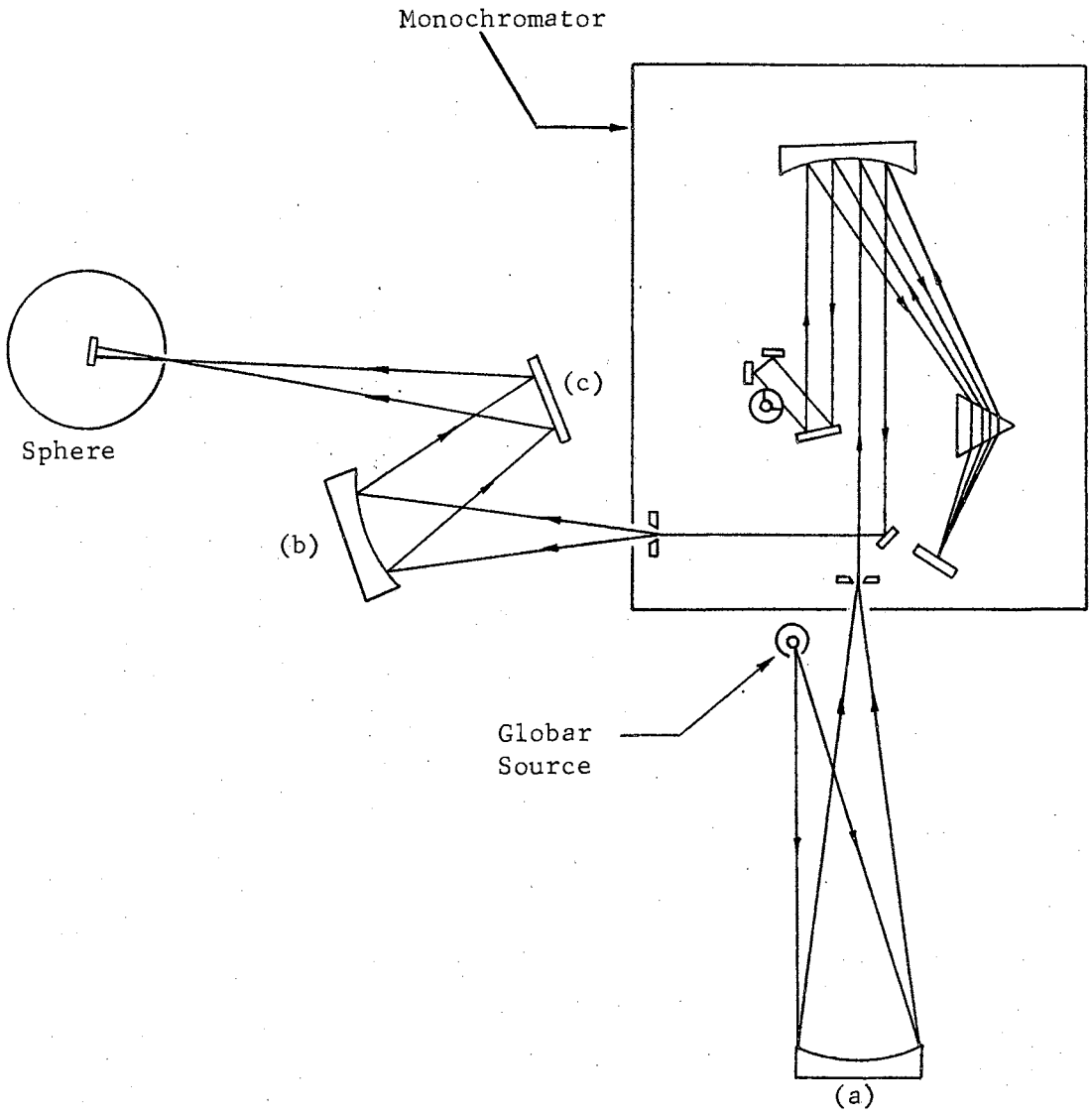

Figure 18. Schematic Diagram of Integrating Sphere Reflectometer System

spherical abberations precluded application of this logic and led to a trial and error determination of the optimum location of globar, collecting mirror, and monochromator. By using a pyroheliometer to measure the relative intensities of the images formed, it was found that the maximum intensity occurred when the mirror was approximately 15 inches from the globar and the image was approximately 19 inches from the mirror. The monochromator was then positioned such that the maximum intensity image was formed at the entrance slit of the monochromator.

Thus the sphere, detection system, and source, when suitably arranged and optically aligned, constitute an integrating sphere reflectometer.

CHAPTER V

ERROR ANALYSIS

There are several factors which may cause an integrating sphere to produce erroneous results. Several studies have been made concerning the errors involved in an integrating sphere reflectometer. Among these are works by Taylor (37), Hardy and Pineo (19), Parmer (38), Edwards, et al. (28), and Dawson, et al. (39). The latter three are particularly appropriate to this analysis since they are concerned with centered-sample spheres.

Direct Irradiation of Detector by Sample

As shown by Parmer, Edwards, and Dawson, for a sample with an unusual reflection distribution function, the error resulting from direct irradiation of the detector by the sample could be several hundred per cent for poorly constructed spheres. However, in the sphere presently being investigated, the arrangement of sample and detector precludes, for all practical purposes, any possibility of direct detector irradiation.

As stated previously, the detector was rotated 14° from a vertical plane which passed through the center of the sphere and which was parallel to the sample when the polar angle of incidence was zero. However, due to its eccentric construction, the sample holder did not hang vertically within the sphere. As shown schemat-

ically in Figure (19), the sample holder hung at an angle of approximately 5° toward the rear of the sphere. This caused the azimuthal angle of incidence to assume a value of approximately 5°. Under these conditions, the angle between the normals to the rear surface of the sample holder and the center of the detector was approximately 76°. However, the front surface of the sample was at least 1/8 inch forward of the rear surface of the sample holder. The angle between the normals to the sample surface and the center of the detector was approximately 85°. Therefore, for all samples except those with extremely unusual reflectance distributions, little if any direct irradiation would be expected to reach the detector, since the angle of reflectance would have to be very large and since the detector and the direction of incidence are on the same side of the sample normal. Therefore, no error was assumed to arise in the present sphere due to direct irradiation of the detector by the samples tested.

Directional Sensitivity of Detector

In the case that the detector is directionally sensitive, the sensitivity $K(\theta_d, \varphi_d)$ cannot be removed from the integral in Equation (10), and the signal produced by the detector will be

$$S_1 = \frac{A_d}{A_s} \int_{A_W} K(\theta_d, \phi_d) J_W \, dA_W \qquad (56)$$

In order to remove K from the integral, the functional relationship between K and θ and φ must be established, or an average value of K must be determined. For the sake of convenience, the cases of a diffuse sample and a non-diffuse sample will be

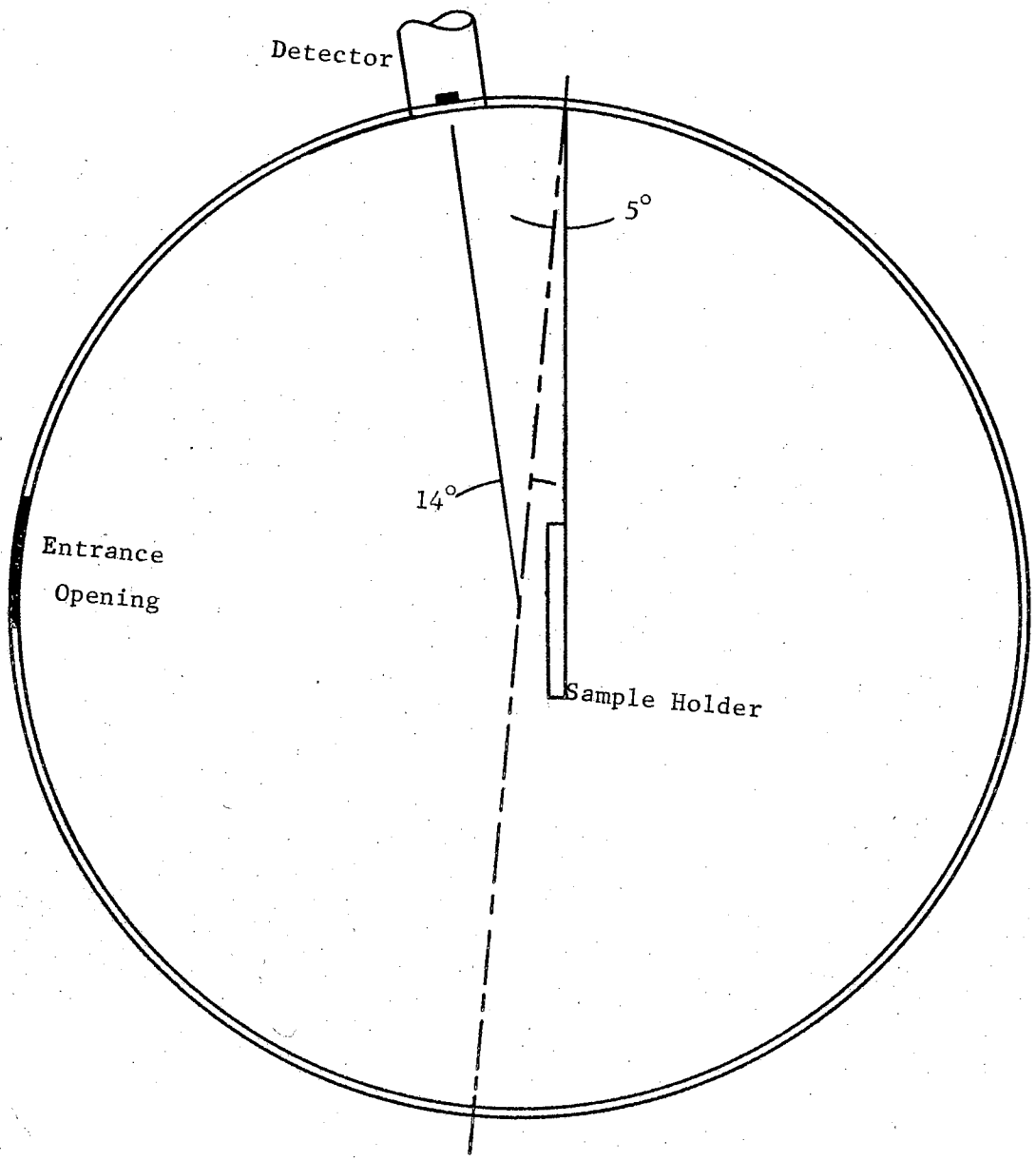

Figure 19. Position of Sample Holder With Respect to Detector

considered separetely.

If the sample is not present and the wall is irradiated directly, a fraction of the incident energy will be reflected to the detector, and the remainder will be reflected to the other sections of the wall. Of the energy reflected to the detector, some fraction K_1 will be recorded. Of the remaining energy resulting from the first reflection from the wall, some fraction K, where K is the average response of the detector, of all subsequent interreflections will be recorded by the detector. This can be illustrated by the equation given below.

$$S_1 = \frac{A_d}{A_s}\left[P\rho K_1 + P\rho K\bar{\rho} + P\rho K\bar{\rho}^2 + P\rho K\bar{\rho}^3 + \cdots\right] \tag{57}$$

$$S_1 = \frac{A_d}{A_s} P\rho\left[K_1 + K(\bar{\rho} + \bar{\rho}^2 + \bar{\rho}^3 + \cdots)\right] \tag{58}$$

$$S_1 = \frac{A_d}{A_s} P\rho\left[K_1 + K\bar{\rho}\left(\frac{1}{1-\bar{\rho}}\right)\right] \tag{59}$$

When the diffuse sample is in place, all energy which reaches the detector will be the result of interreflections, and, of each interreflection which reaches the detector, some fraction K will be recorded. Thus, a signal S_2 will be produced as shown below.

$$S_2 = \frac{A_d}{A_s}\left[P\rho\rho_s K + P\rho\rho_s K\bar{\rho} + P\rho\rho_s K\bar{\rho}^2 + \cdots\right] \tag{60}$$

$$S_2 = \frac{A_d}{A_s} P\rho\rho_s K\left[\frac{1}{1-\bar{\rho}}\right] \tag{61}$$

For the case of a diffuse sample, the reflectance will be given by the ratio of S_2 to S_1.

$$S_2/S_1 = \rho_s K\left[\frac{1}{1-\bar{\rho}}\right] \Big/ \left[K_1 + K\bar{\rho}\left(\frac{1}{1-\bar{\rho}}\right)\right] \tag{62}$$

$$S_2/S_1 = \rho_s \frac{K}{K_1 - \bar{\rho}(K_1 - K)} \tag{63}$$

where

$$\epsilon = \frac{K}{K_1 - \bar{\rho}(K_1 - K)} \tag{64}$$

is the error involved due to the angular sensitivity of the detector.

If K_1 is zero, the error relationship reduces to

$$\epsilon = 1/\bar{\rho} \tag{65}$$

K_1 can be zero if the initial incident beam is directed onto a portion of the sphere wall from which reflected energy produces no detector signal. As will be noted later, the Reeder thermocouple exhibits an angular region of zero response. Initial energy incident on the sphere wall within this angular area will produce no detector response, and K_1 will be zero.

Since K_1 will not be zero in a properly designed reflectometer, both K_1 and K must be evaluated before the magnitude of the error can be determined. Both quantities can be evaluated by comparing the performance of the detector to that of an ideal detector.

The Reeder thermocouple, as related previously, was tested for angular sensitivity by mounting it on a rotary table and rotating

it through 180° while irradiating it with a parallel beam of energy. The detector response was recorded as a function of polar angle of incidence, θ. The results are shown in Figure (17), Chapter IV. The dashed line represents the response a "perfect detector" would have shown under similar irradiation.

The integrating sphere under discussion is designed such that θ for the first reflection from the wall is 39°. K_1 represents the ratio of the real detector response to the response an ideal detector would have yielded when θ equalled 39°.

K, which was previously defined as the average response of the detector to the energy incident after the first reflection, can also be determined by comparing the real to the ideal signal. Energy reflected from the sphere wall after the first incidence will, through successive interreflections, illuminate the sphere uniformly. Therefore, the response of the detector to the energy coming from a given wall area will equal some fraction of the response an ideal detector would have yielded when irradiated by the same quantity of energy from the same given wall area. K, then is the ratio of the integral over the sphere of the energy seen by the real detector to the integral over the sphere of the energy that would be seen by an ideal detector.

The geometry of the sphere is shown in Figure (20). It is seen that $\theta_c = 2\theta_d$. K may then by expressed as:

$$K = \frac{\int_0^{\pi} S_{r/s_i} 2\pi R d\theta_c}{\int_0^{\pi} 2\pi R d\theta_c} \qquad (66)$$

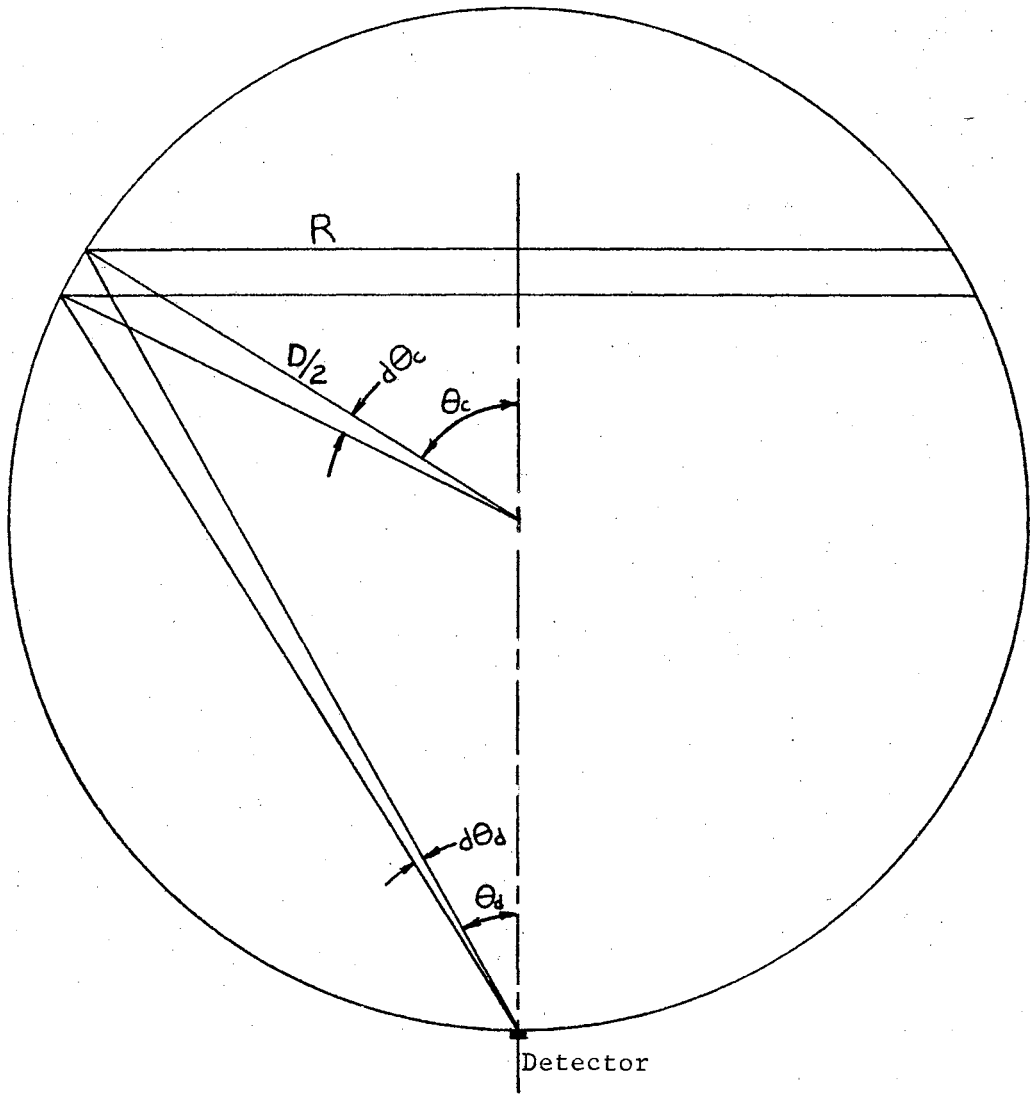

Figure 20. Detector Angular Response Geometry

where S_r is the real detector reading and S_i is the reading an ideal detector would have given. S_r was measured and S_i can be expressed as $S_{r,\theta_d=0}\cos\theta_d$. Equation (66) may be simplified as shown in the following steps.

Since
$$R = (D/2)\sin\theta_c$$
$$\theta_c = 2\theta_d$$
$$d\theta_c = 2\,d\theta_d$$

and when
$$\theta_c = 0, \quad \theta_d = 0$$
$$\theta_c = \pi, \quad \theta_d = \pi/2$$

K may be expressed as

$$K = \frac{\int_0^{\pi/2} 2\pi D\left(S_r/S_{r,\theta_d=0}\right)\frac{\sin\theta_c}{\cos\theta_d}\,d\theta_d}{\int_0^{\pi/2} 2\pi D\sin\theta_c\,d\theta_d} \tag{67}$$

But

$$\sin\theta_c = 2\sin\theta_d\cos\theta_d$$

$$K = \frac{\int_0^{\pi/2}\left(S_r/S_{r,\theta_d=0}\right)\sin\theta_d\,d\theta_d}{\int_0^{\pi/2}\sin\theta_d\cos\theta_d\,d\theta_d} \tag{68}$$

The numerator of Equation (68) was evaluated using the Trapezoidal rule and was found to be equal to 0.4240. The integral in the denominator of Equation (68) equals 0.5. K, then, was found to be

$$K = \frac{0.4240}{0.5}$$

$$K = 0.8480$$

K_1 was determined, from Figure (17), to be equal to 0.9940. The error, given by Equation (64), will then be

$$\epsilon = \left[\frac{.8480}{.9940 - \bar{\rho}(.9940 - .8480)}\right] \qquad (69)$$

If $\bar{\rho} = 0.70$,

$$\frac{S_2}{S_1} = 0.9508\,\rho_s$$

The per cent error will be

$$\frac{0.9508 - 1}{1} \times 100\% = -4.92\%$$

Equation (69) demonstrates the interesting fact that, if the average wall reflectance equals unity, the error involved in the sample reflectance will be zero, regardless of the angular sensitivity of the detector.

In the case of a non-diffuse sample, the magnitude of the error involved in the sample reading depends upon the angular distribution of the energy reflected from the sample. Due to the construction of the sphere, the detector does not "see" energy which is incident at polar angles greater than 78°. This fact introduces an error in the sample reflectance reading. Although the error is related to the angularity of the system, it should be distinguished from the error caused by the angular sensitivity of the detector. The angular sensitivity of the detector is a characteristic of the detector and does not change, regardless of the surroundings in which it is placed. If the surroundings are such that they prevent energy from reaching the detector, the error resulting should be charged to the surroundings and not to the

detector. The difference, however, is largely academic since the errors due to the angular sensitivity of the detector and to the construction of the sphere are similar in nature and are additive.

If the energy reflected from the sample is initially incident upon the sphere wall within the area of nonresponse, the first reflection from the wall produces no detector response. All subsequent interreflections to which the detector responds are reduced by the fraction $1 - A_n/A_s$ where A_n represents the area from which reflected energy produces no detector response.

The sample reading will be

$$S_2' = \frac{A_d}{A_s} P \rho_s \left[\rho Z \bar{\rho} K + \rho Z \bar{\rho}^2 K + \rho Z \bar{\rho}^3 K + \cdots \right] \tag{70}$$

where K is the average detector response and $Z = 1 - A_n/A_s$.

$$S_2' = \frac{A_d}{A_s} P \rho_s \rho Z \bar{\rho} K \left[1 + \bar{\rho} + \bar{\rho}^2 + \cdots \right] \tag{71}$$

$$S_2' = \frac{A_d}{A_s} P \rho_s \rho Z K \left(\frac{\bar{\rho}}{1 - \bar{\rho}} \right) \tag{72}$$

The error in the sample reading is

$$\epsilon = \frac{S_2' - S_2}{S_2} \times 100\% \tag{73}$$

$$\epsilon = \frac{\left(A_d/A_s\right) P \rho_s \rho Z K \left(\frac{\bar{\rho}}{1-\bar{\rho}}\right) - \left(A_d/A_s\right) P \rho_s \rho \left(\frac{1}{1-\bar{\rho}}\right) K}{\left(A_d/A_s\right) P \rho_s \rho \left(\frac{1}{1-\bar{\rho}}\right) K} \times 100\% \tag{74}$$

$$\epsilon = \left(Z \bar{\rho} - 1 \right) \times 100\% \tag{75}$$

From Figure (21), $A_n/A_s = \frac{1-\cos 2\beta}{2}$. Hence, $Z = 1-\frac{1-\cos 2\beta}{2}$. However, because the detector does not respond to energy which is incident at angles greater than 80°, Z must be reduced accordingly:

$$Z = 1-\left[\frac{1-\cos 24^\circ}{2} - \frac{1-\cos 20^\circ}{2}\right] = 0.9870$$

If $\bar{\rho} = 0.70$, the error will be, from Equation (75):

$$\epsilon = [(.987)(.7) - 1] \times 100\% \tag{76}$$

$$\epsilon = -30.91\%$$

If the initial reflection from the sample is incident on the sphere wall outside the area of nonresponse, only subsequent interreflections are affected by the reduction in signal and the sample reading will be

$$S_2'' = \frac{A_d}{A_s} P\rho_s \left[K\rho + K\rho Z\bar{\rho} + K\rho Z\bar{\rho}^2 + \cdots\right] \tag{77}$$

$$S_2'' = \frac{A_d}{A_s} P\rho_s \rho K \left[1 + \frac{Z\bar{\rho}}{1-\bar{\rho}}\right] \tag{78}$$

The error in sample reading is then

$$\epsilon = \frac{\left[1 + Z\bar{\rho}/(1-\bar{\rho}) - 1/(1-\bar{\rho})\right]}{1/(1-\bar{\rho})} \times 100\% \tag{79}$$

$$\epsilon = \bar{\rho}\,(Z-1) \times 100\% \tag{80}$$

For $\bar{\rho} = .70$,

$$\epsilon = -0.91\%$$

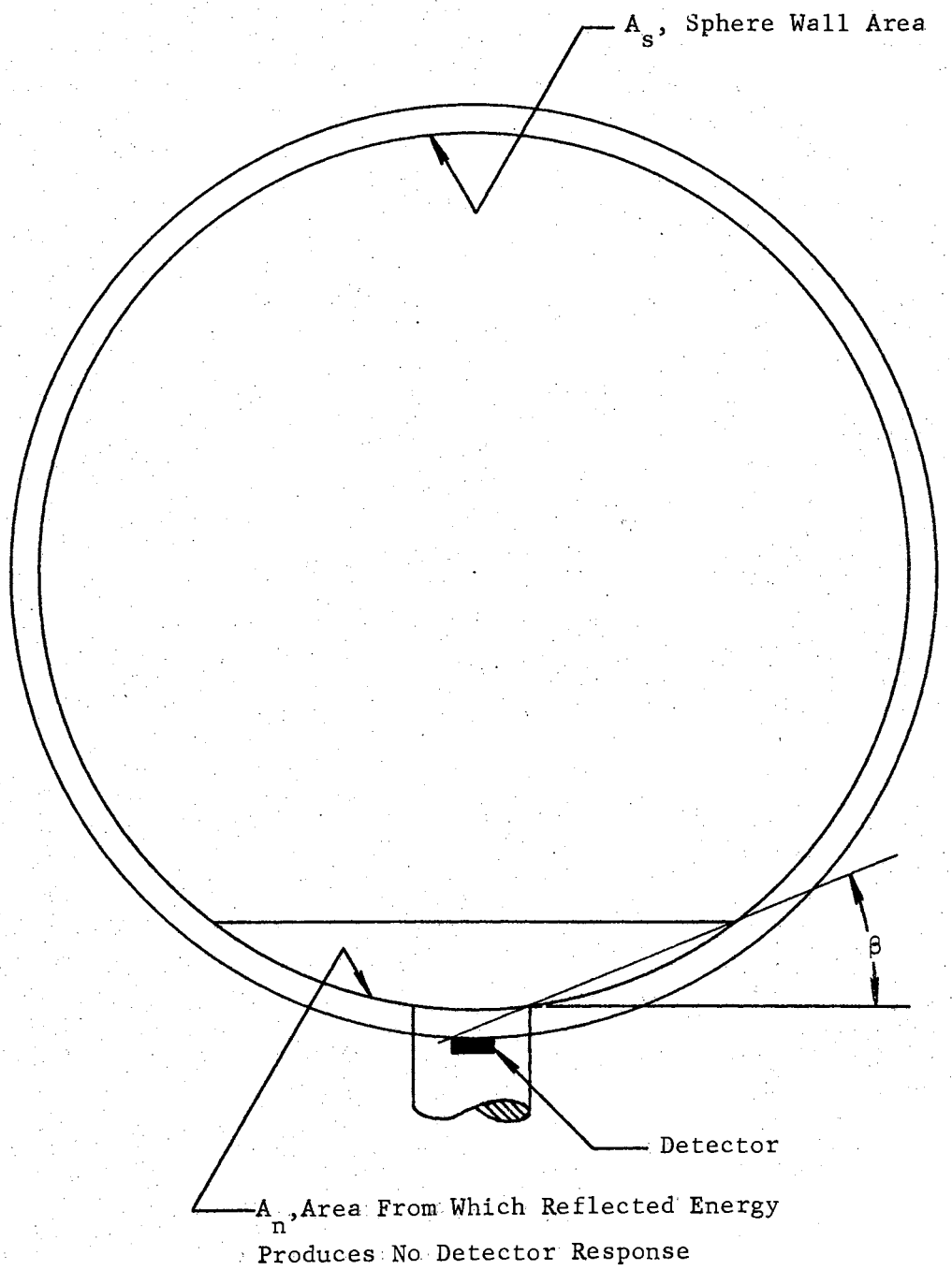

Figure 21. Detector View of Sphere Interior

Of greater interest, however, than the error involved in the sample reading is the error involved in the ratio of sample to reference reading. To determine the magnitude of the error involved in the ratio, the error involved in the reference reading must be considered since it too is subject to the effects of detector angular sensitivity.

The reference reading S_1 was given by Equation (59) as follows:

$$S_1 = \frac{A_d}{A_s} P\rho \left[K_1 + K\bar{\rho}\left(\frac{1}{1-\bar{\rho}}\right)\right]$$

The ratio of the sample to reference reading, when the initial reflection from the sample is incident in area A_n is:

$$S_2'/S_1 = \frac{A_d}{A_s} P\rho_s \rho Z K\left(\frac{\bar{\rho}}{1-\bar{\rho}}\right) \Big/ \frac{A_d}{A_s} P\rho \left[K_1 + K\left(\frac{\bar{\rho}}{1-\bar{\rho}}\right)\right] \qquad (81)$$

$$S_2'/S_1 = \rho_s K Z \left(\frac{\bar{\rho}}{1-\bar{\rho}}\right) \Big/ \left[K_1 + K\left(\frac{\bar{\rho}}{1-\bar{\rho}}\right)\right] \qquad (82)$$

The error involved is:

$$\epsilon = \frac{\rho_s \left[\frac{KZ\bar{\rho}}{K_1 - \bar{\rho}(K_1 - K)}\right] - \rho_s}{\rho_s} \times 100\% \qquad (83)$$

If $\bar{\rho} = .70$,

$$\epsilon = -34.20\%$$

When the initial reflection from the sample is not incident in area A_n,

$$S_2''/S_1 = \frac{A_d}{A_s} P\rho_s \rho K\left[1 + \frac{Z\bar{\rho}}{1-\bar{\rho}}\right] \Big/ \frac{A_d}{A_s} P\rho \left[K_1 + K\left(\frac{\bar{\rho}}{1-\bar{\rho}}\right)\right] \qquad (84)$$

$$S_2''/S_1 = \rho_s K\left[1 + \frac{Z\bar{\rho}}{(1-\bar{\rho})}\right] \Big/ \left[K_1 + K\left(\frac{\bar{\rho}}{1-\bar{\rho}}\right)\right] \tag{85}$$

$$S_2''/S_1 = \rho_s K\left[\frac{1 + \bar{\rho}(Z-1)}{K_1 - \bar{\rho}(K_1 - K)}\right] \tag{86}$$

If $\bar{\rho} = 0.70$, the error is:

$$\epsilon = \left\{(.848)\left[\frac{1 + .7(.987-1)}{.994 - .7(.994-.848)}\right] - 1\right\} \times 100\% \tag{87}$$

$$\epsilon = -5.78\%$$

Thus it is seen that a non-diffuse sample is subject to larger errors due to the angular sensitivity of the system than is a completely diffuse sample. Since all real surfaces exhibit both a diffuse and a specular component, the error involved may lie between -4.9% and -6%, for an average wall reflectance of 0.70. A completely specular sample can be rotated to prevent the reflected energy from falling initially within the area of nonresponse. Thus, if reasonable care is exercised, the maximum error due to angular sensitivity should be approximately -6% for a completely specular sample.

Nonuniformity of Sphere Wall Coating

Nonuniformity of the sphere wall coating may be in two forms. The coating may be of nonuniform thickness and it may have a nonuniform reflectance.

A nonuniform wall thickness effects the basis of the integrating sphere theory. That is, if the walls are not of the same thick-

ness at all points, the cavity is no longer a sphere and the assumption of equal configuration factors between all points is no longer valid.

In actual practice, it is almost impossible to apply a wall coating which is completely uniform and almost as difficult to measure the thickness without destroying the coating.

At all points where the thickness of the coating could be measured (detector opening, sample stop opening, and hemisphere edges), the thickness did not vary by a measurable amount. Since the coating was applied to the whole sphere at the same time and in the same manner as that at the measurable locations, it is assumed that the errors caused by nonuniform wall thickness are negligible.

Although it is not possible to determine a numerical value for the error resulting from nonuniform wall thickness, an order of magnitude may be determined in the following manner. If the equation for the detector signal is written in an expanded form,

$$S_1 = K\left[P\rho\frac{A_d}{A_s} + P\rho\frac{A_d}{A_s}\bar{\rho} + P\rho\frac{A_d}{A_s}\bar{\rho}^2 + \cdots\right] \qquad (88)$$

it will be noted that each term on the right side represents the energy reflected from the sphere wall multiplied by the configuration factor between the total wall area and the detector.

Assume now that a large sphere is composed of a large number of areas, each of which equals the area of the original sphere. Assume further that each area reflects the energy incident upon it in two components, one directed upon the detector and the other directed upon an area which has not been irradiated. The component directed upon the detector is assumed to be a fraction

of the total incident energy equal to the configuration factor between the area and the detector. It is also assumed that, no area is irradiated twice by the same beam. The signal produced when P power is introduced into the hypothetical sphere is

$$S = K\left[P\rho\frac{A_d}{A_s} + P\rho\frac{A_d}{A_s}\bar{\rho} + P\rho\frac{A_d}{A_s}\bar{\rho}^2 + \cdots\right] \tag{89}$$

which is seen to be identical to Equation (88) for an actual sphere.

Assume that one of the areas differs from all the other areas, causing the configuration factor between it and the detector to be increased by some fraction X. The resulting signal will then be

$$S = K\left[P\rho\frac{A_d}{A_s} + P\rho\frac{A_d}{A_s}\bar{\rho} + \cdots + P\rho\left(\frac{A_d}{A_s}+X\right)\bar{\rho}^n + P\rho(1-X)\frac{A_d}{A_s}\bar{\rho}^{n+1} + \cdots\right] \tag{90}$$

where the nonuniform area is irradiated on the n^{th} interreflection and where the factor (1-X) arises from the fact that, if a larger fraction of the interreflecting beam of energy reaches the detector from the nonuniform area, the energy available for reflection to the detector from the remaining areas will be less by the same fraction.

Expanding Equation (90) and collecting terms yields

$$S = KP\rho\left[\frac{A_d}{A_s} + \frac{A_d}{A_s}\bar{\rho} + \frac{A_d}{A_s}\bar{\rho}^2 + \cdots + X\bar{\rho}^n - \frac{A_d}{A_s}X\bar{\rho}^{n+1} - \cdots\right]$$

$$S = KP\rho\left[\frac{A_d}{A_s}\left(1 + \bar{\rho} + \bar{\rho}^2 + \cdots\right) + X\left(\bar{\rho}^n - \frac{A_d}{A_s}\bar{\rho}^{n+1} - \frac{A_d}{A_s}\bar{\rho}^{n+2} - \cdots\right)\right]$$

$$S = KP\rho\left\{\frac{A_d}{A_s}\left(\frac{1}{1-\bar{\rho}}\right) + X\left[\bar{\rho}^n - \frac{A_d}{A_s}\bar{\rho}^{n+1}\left(1 + \bar{\rho} + \bar{\rho}^2 + \cdots\right)\right]\right\}$$

$$S = K\left\{P_\rho \frac{A_d}{A_s}\left(\frac{1}{1-\bar{\rho}}\right) + P_\rho X \bar{\rho}^n\left[1 - \frac{A_d}{A_s}\left(\frac{\bar{\rho}}{1-\bar{\rho}}\right)\right]\right\} \tag{91}$$

If n = 0,

$$S = K\left\{P_\rho \frac{A_d}{A_s}\left(\frac{1}{1-\bar{\rho}}\right) + P_\rho X\left[1 - \frac{A_d}{A_s}\left(\frac{\bar{\rho}}{1-\bar{\rho}}\right)\right]\right\} \tag{92}$$

If n = ∞,

$$S = K\left[P_\rho \frac{A_d}{A_s}\left(\frac{1}{1-\bar{\rho}}\right)\right] \tag{93}$$

The case of n = 0 is seen to correspond to the condition in which all of the energy is reflected from the area first irradiated to the nonuniform area, and might result in a large error depending upon the magnitude of X. Since the initially irradiated area reflects diffusely, only a small fraction of the energy first reflected from the wall reaches the nonuniform area. As further interreflections occur, further small fractions of energy reach the nonuniform area. This type of reflection corresponds to the case in which n = ∞.

From Equation (91),

$$S = K P_\rho\left\{\frac{A_d}{A_s}\left(\frac{1}{1-\bar{\rho}}\right) + X\bar{\rho}^n\left[1 - \frac{A_d}{A_s}\left(\frac{\bar{\rho}}{1-\bar{\rho}}\right)\right]\right\} \tag{94}$$

Let $E = X\bar{\rho}^n\left[1 - \frac{A_d}{A_s}\left(\frac{\bar{\rho}}{1-\bar{\rho}}\right)\right]$, where E is the error caused by the nonuniform wall thickness, and assume that $\bar{\rho} = 0.90$, X = 0.10, and $A_d/A_s = 0.00391$.

$$E = .10(.90)^n\left[1 - .00391\left(\frac{.90}{1-.90}\right)\right] \tag{95}$$

$$E = .10(.90)^n[1 - .00391(9)] \tag{96}$$

$$E = .0965(.90)^n \tag{97}$$

If n = 88,

$$E = .00000965$$

In the actual case, X should be much less than .10 and n should be much greater than 88. The error resulting from a nonuniform wall thickness is then seen to be very small.

If the sphere wall coating exhibits nonuniform reflectance, the detector response will depend upon the location at which the incident energy reaches the sphere wall. In this case, the reflectance of the sphere wall to the initial irradiation will not cancel out when the ratio of detector signals is taken. Under these circumstances, the reflectance of the sample will be given by

$$\rho_S = \left(\rho_{W_1}/\rho_{W_2}\right)\left(S_2/S_1\right) \tag{98}$$

where ρ_{W_1} is the reflectance of the wall coating to the initial irradiation when the sample is not present, and ρ_{W_2} is the reflectance of the wall coating when the sample is in place. The possible per cent error will then be

$$\epsilon = \left[\left(\rho_{W_1}S_2/\rho_{W_2}S_1 - S_2/S_1\right)/\left(S_2/S_1\right)\right] \times 100\% \tag{99}$$

or

$$\epsilon = \left(\rho_{w_1}/\rho_{w_2} - 1\right) \times 100\% \qquad (100)$$

The sphere investigated in this study was tested by rotating it about a vertical line through its entrance opening. The sphere was rotated through an included angle of 70° when the entrance opening was in the vertical position, and 60° when the opening was in the horizontal position. With the opening in the vertical position, the projected area of the opening was less than the width of the irradiating beam. Under these conditions, the detector response varied as much as -3.5%, indicating that the reflectance of the sphere wall varied by this much. However, as explained in Chapter IV, the edge of the entrance opening interferred, to some extent, with the incident beam. This interference might have been the cause of the apparent variation in reflectance. The fact that no variation was noted when the opening was horizontal lends substance to this possibility, particularly in view of the fact that, at all angles, the horizontally positioned opening was wider than the incident beam. In view of the two tests, -3.5% was assumed to be the maximum variation over the entire sphere.

If the variation was -3.5% and the wall reflectance was .70, the possible error could be

$$\epsilon = \left(\frac{.70 - .035}{.70} - 1\right) \times 100\% \qquad (101)$$

or

$$\epsilon = \left(\frac{.70}{.70 - .035} - 1\right) \times 100\% \qquad (102)$$

in which case the error might be as much as + 5.26% or -5%.

Nondiffuseness of Sphere Wall Coating

Nondiffuseness of the wall coating, like the nonuniform wall thickness, effects the basic premise of equal configuration factors between all points within the sphere. If the configuration factor is not the same between all points within the sphere, the energy reaching the detector from all points will not be the same. This means that the detector will not respond equally to incident energy from all directions, which is the same type of error caused by the angular sensitivity of the detector. The errors caused by nondiffuse walls and the angular sensitivity of the detector should be of the same magnitude.

A test of wall diffuseness was described in Chapter IV, in which no specular component was noted. It is assumed, therefore, that the sphere walls are diffuse to the extent that the error attributable to wall nondiffuseness is negligible.

Nonlinearity of Detection System

Linearity of the detection system is a requisite to the validity of the assumption that

$$\rho_s = S_2/S_1 \tag{103}$$

where the detection system includes the detector, preamplifier, amplifier, and recorder. The error involved in the case of a nonlinear detection system is difficult to assess, since it affects a basic assumption.

The linearity of the detector system was checked by irradiating the sphere with a monochromatic beam of radiant energy, producing a known attenuation of the amount of energy entering the sphere, and comparing the detector signal produced by the attenuated and unattenuated beam. The test was conducted at three different wavelengths using three different slit widths for each attenuation. In this way, the response of the detector system could be checked not only with respect to varying amounts of incident energy at a given slit width, but also with respect to a given amount of incident energy with varying slit widths.

The procedure involved irradiating the sphere with a monochromatic beam, from the globar, at wavelengths of 1.6, 3.4, and 5.25 microns. At each wavelength, after the beam had been directed into the sphere and the detector response noted, a rotating blade was placed in the path of the beam from the globar to the monochromator. Four equal segments, which equalled half of the area of the blade, had been removed. Since the blade was rotating at approximately 1500 revolutions per minute, the per cent attenuation of the incident beam was equal to the per cent of the blade surface area which remained. Therefore, if the detector system was linear, a fifty per cent attenuation in the incident beam, corresponding to a blade from which fifty per cent of the surface area had been removed, should produce a signal equal to half that produced by the unattenuated signal.

After tests had been conducted for fifty per cent attenuation, two of the removed sections were covered, and the detector system was checked using an incident beam which had been attenuated by

seventy-five per cent.

Each test was conducted at slit widths of 1, 1.5, and 2 millimeters. The ratio of attenuated to unattenuated signal was calculated at each slit width, and the three values averaged to provide an average detector response ratio. The results are listed in Table I. It will be noted that the maximum deviation from complete linearity is 2.68 per cent. Since it is impossible to read less than half a subdivision on the recorder scale, a deviation of this magnitude indicates that the linearity of the detection system, at a given slit width is acceptable with no correction necessary.

The variation of detector response with slit width was measured in the same test. That is, the signal was attenuated at three different slit widths, and all signals were compared to that produced when the width of the slit was a maximum. The results of the tests and the comparisons are shown in Table I.

For the type of detection system used, the relation between slit width and signal, for a perfect detection system, is

$$S_1/S_2 = \left(w_1/w_2\right)^2 \tag{104}$$

where S denotes signal and w indicates slit width. For the Perkin and Elmer Model 99, the maximum slit width is 2 millimeters. The system was checked at slit widths of 1.0, 1.5, and 2.0 millimeters. The ratio of the signals should, then, be

$$\begin{aligned} S_1/S_2 &= 1.78 \\ S_1/S_3 &= 4.00 \\ S_2/S_3 &= 2.25 \end{aligned} \tag{105}$$

TABLE I

DETECTOR LINEARITY RESPONSE

Wave-length	Percent Attenuation	2.0 mm	1.5 mm	1.0 mm
5.25μ	0	46.38	27.00	12.50
	50	23.00	13.50	6.00
	75	11.50	6.50	3.00
3.40μ	0	75.63	44.25	21.38
	50	37.50	22.00	10.50
	75	19.00	10.50	5.50
1.60μ	0	68.88	40.00	18.63
	50	34.00	20.00	9.00
	75	17.50	10.00	5.00

The average of the signal ratios for wavelengths 1.6, 3.4, and 5.25 microns is plotted in Figure (15). The solid line indicates the linearity, with respect to slit width of a perfect detector system. Since the data is plotted on log-log paper, the slope of the two lines is the exponent involved in the relationship. For a perfect detector, the exponent is, of course, 2. From Figure (15), the slope of the curve, and hence the exponent, is determined to be 1.885. The signal ratios for the ideal and the real detector systems are related to the ratio of the slit widths as follows:

$$\begin{aligned} (S_1/S_2)_{IDEAL} &= (W_1/W_2)^2 \\ (S_1/S_2)_{REAL} &= (W_1/W_2)^{1.885} \end{aligned} \tag{106}$$

or,

$$\begin{aligned} W_1/W_2 &= (S_1/S_2)^{1/2}_{IDEAL} \\ W_1/W_2 &= (S_1/S_2)^{1/1.885}_{REAL} \end{aligned} \tag{107}$$

Since the same slit width ratio represents the same relative change in the amount of energy incident on the detector, the difference in the two quantities on the right hand side of Equations (107) represents the nonlinearity of the detection system, with respect to slit width. Therefore, since an ideal detector system would be assumed to yield a true ratio of signals,

$$(S_1/S_2)_{TRUE} = (S_1/S_2)^{2/1.885}_{REAL} \tag{108}$$

$$(S_1/S_2)_{TRUE} = (S_1/S_2)^{1.061}_{REAL} \tag{109}$$

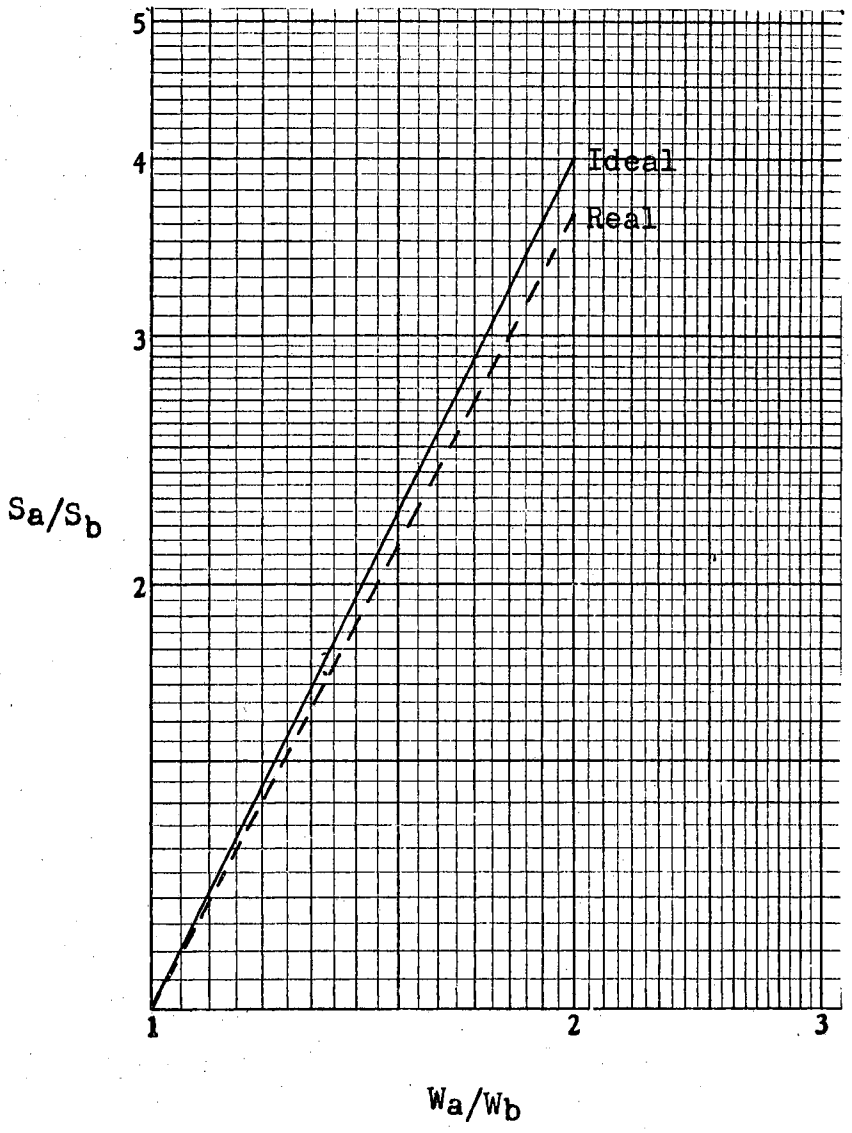

Figure 22. Signal Ratio as Function of Slit Width

or,

$$\rho_{S_{TRUE}} = \rho_{S_{INDICATED}}^{1.061} \tag{110}$$

That is, an indicated signal ratio would have to be raised to a power of 1.061 to yield a true signal ratio.

Sphere Openings

As pointed out in Chapter III, there is an efficiency associated with the sphere which is a function of the size of the sphere and its openings, and the reflectance of the sphere walls. The efficiency of the sphere depends upon whether the sample is or is not present, and the difference in efficiencies gives rise to an error in the ratio S_2/S_1.

As previously shown in the simplified theory of the integrating sphere, a sphere with the sample not present, when irradiated by a beam of monochromatic energy, will yield a signal given by Equation (14),

$$S_1 = K \frac{A_d}{A_s} \int_{A_W} J_W \, dA_W \tag{111}$$

and, according to Equation (15),

$$\int_{A_W} J_W \, dA_W = P\rho + P\rho\bar{\rho} + P\rho\bar{\rho}^2 + \cdots \tag{112}$$

Each term on the right side of Equation (112) represents a reflection from the wall. In an actual sphere, at each reflection,

a fraction of the reflected energy passes out the entrance opening. Since the sphere wall is diffuse, the fraction of reflected energy lost out the entrance opening equals the ratio of the area of the entrance opening to the area of the sphere. Equation (112) then becomes

$$\int_{A_W} J_W \, dA_W = P\rho + P\rho\bar{\rho}\left(1 - \frac{A_e}{A_s}\right) + P\rho\bar{\rho}^2\left(1 - \frac{A_e}{A_s}\right)^2 + \cdots \qquad (113)$$

The fact that the detector itself is not a perfect reflector alters, in a real sphere, the expression for the radiosity of the wall. Far from being a good reflector, most detector elements are coated with a black material to insure maximum absorption of incident energy. This being the case, each energy term in the infinite series representing the interreflections within the sphere is diminished by a factor proportional to the energy absorbed by the detector. If the detector is assumed to absorb all of the energy incident upon it, Equation (113), which expresses the radiosity of the wall, will be altered to the form shown below.

$$\int_{A_W} J_W \, dA_W = P\rho + P\rho\bar{\rho}\left(1 - \frac{A_e}{A_s} - \frac{A_d}{A_s}\right) + P\rho\bar{\rho}^2\left(1 - \frac{A_e}{A_s} - \frac{A_d}{A_s}\right)^2 + \cdots \qquad (114)$$

One other factor which must be considered is the sample holder, since it is present even when the sample is not. After the initial reflection from the sphere wall, interreflections occur between the sample holder and the wall. Each time an interreflection occurs, a fraction of the energy reflected from the wall is absorbed by the sample holder and the energy available for further reflections from the wall is diminished by a factor equal to

$$(1 - \rho_h)(A_h/A_s)$$

where ρ_h is the reflectance and A_h the area of the sample holder. Equation (114) then becomes

$$\int_{A_W} J_W \, dA_W = P\rho + P\rho\bar{\rho}\left[1 - \frac{A_e}{A_s} - \frac{A_d}{A_s} - \frac{A_h}{A_s}(1-\rho_h)\right] + P\rho\bar{\rho}^2\left[1 - \frac{A_e}{A_s} - \frac{A_d}{A_s} - \frac{A_h}{A_s}(1-\rho_h)\right]^2 + \cdots \quad (115)$$

The signal produced by the detector will then be given by

$$S_1 = K\frac{A_d}{A_s} P\rho \left\{ \frac{1}{1 - \bar{\rho}\left[1 - \frac{A_e}{A_s} - \frac{A_d}{A_s} - \frac{A_h}{A_s}(1-\rho_h)\right]} \right\} \quad (116)$$

Since K is a characteristic of the detector, it is not considered in determining the efficiency of the sphere. Since P identifies the energy introduced into the sphere, the efficiency can be considered to be given by the term

$$\eta_1 = \rho \frac{A_d}{A_s} \left\{ \frac{1}{1 - \bar{\rho}\left[1 - \frac{A_e}{A_s} - \frac{A_d}{A_s} - \frac{A_h}{A_s}(1-\rho_h)\right]} \right\} \quad (117)$$

The effect of the different parameters on the efficiency of the sphere can be determined by taking partial derivatives of η_1 with respect to the parameters and noting the resulting sign.

Letting $A_e/A_s = u$, $A_d/A_s = v$, and $A_h/A_s = y$, Equation (117) becomes

$$\eta_1 = \frac{\rho v}{1 - \bar{\rho}\left[1 - u - v - y(1-\rho_h)\right.} \quad (118)$$

and

$$\partial\eta_1/\partial\rho = \frac{v}{1 - \bar{\rho}\left[1 - u - v - y(1-\rho_h)\right.} > 0 \quad (119)$$

$$\partial \eta_1 / \partial \nu = \frac{\rho[1-\bar{\rho}(1-u-y(1-\rho_h)]}{\{1-\bar{\rho}[1-u-\nu-y(1-\rho_h)]\}^2} > 0 \qquad (120)$$

$$\partial \eta_1 / \partial \bar{\rho} = \frac{\rho\nu[1-u-\nu-y(1-\rho_h)]}{\{1-\bar{\rho}[1-u-\nu-y(1-\rho_h)]\}^2} > 0 \qquad (121)$$

$$\partial \eta_1 / \partial u = \frac{-\rho\nu\bar{\rho}}{\{1-\bar{\rho}[1-u-\nu-y(1-\rho_h)]\}^2} < 0 \qquad (122)$$

From Equation (117),

$$\partial \eta_1 / \partial A_s = \frac{-\rho A_d (1-\bar{\rho})}{\{A_s(1-\bar{\rho}) + \bar{\rho}[A_e + A_d + A_h(1-\rho_h)\}^2} < 0 \qquad (123)$$

Thus it is seen that the efficiency of the sphere increases as the initial reflectance, the average reflectance, and the detector area increase, and the sphere radius and entrance area decrease. This agrees with the results given by Jacquez and Kuppenheim (24).

When the sample is in place within the sphere, two other events occur which may effect the radiosity of the wall. First of all, part of the energy incident upon the sample may be reflected out through the entrance opening. When this occurs, the radiosity equation becomes

$$\int_{A_w} J_w dA_w = \rho\rho_s(1-F) + \rho\rho\rho_s(1-F)\bar{\rho}\left[1 - \frac{A_e}{A_s} - \frac{A_d}{A_s} - \frac{A_h}{A_s}(1-\rho_h)\right] + \rho\rho\rho_s(1-F)\bar{\rho}^2\left[1 - \frac{A_e}{A_s} - \frac{A_d}{A_s} - \frac{A_h}{A_s}(1-\rho_h)\right]^2 + \cdots \qquad (124)$$

where F is the fraction of energy reflected from the sample which is lost out the entrance opening.

The second event which occurs only when the sample is in place is interreflection between the sample and the sphere walls. As in the case of the sample holder, each time an interreflection occurs, the energy available for further reflections from the wall is diminshed by a factor equal to

$$(1-\rho_s)(A_t/A_s)$$

where A_t is the area of the sample. The expression for the wall radiosity then becomes

$$\int_{A_w} J_w \, dA_w = P\rho\rho_s(1-F)\left\{1+\bar{\rho}\left[1-\frac{A_e}{A_s}-\frac{A_d}{A_s}-\frac{A_h}{A_s}(1-\rho_h)-\frac{A_t}{A_s}(1-\rho_s)\right]\right. \qquad (125)$$
$$\left.+\bar{\rho}^2\left[1-\frac{A_e}{A_s}-\frac{A_d}{A_s}-\frac{A_h}{A_s}(1-\rho_h)-\frac{A_t}{A_s}(1-\rho_s)\right]+\cdots\right.$$

and the detector signal is expressed by

$$S_2 = K\frac{A_d}{A_s}P\rho\rho_s\left\{\frac{(1-F)}{1-\bar{\rho}\left[1-\frac{A_e}{A_s}-\frac{A_d}{A_s}-\frac{A_h}{A_s}(1-\rho_h)-\frac{A_t}{A_s}(1-\rho_s)\right]}\right\} \qquad (126)$$

The efficiency of the sphere, when the sample is in place, is given by

$$\eta_2 = \rho\frac{A_d}{A_s}(1-F)\left\{\frac{1}{1-\bar{\rho}\left[1-\frac{A_e}{A_s}-\frac{A_d}{A_s}-\frac{A_h}{A_s}(1-\rho_h)-\frac{A_t}{A_s}(1-\rho_s)\right]}\right\} \qquad (127)$$

Again letting $A_e/A_s = u$, $A_d/A_s = v$, and $A_h/A_s = y$, and letting $A_t/A_s = x$, Equation (127) becomes

$$\eta_2 = \frac{\rho v(1-F)}{1-\bar{\rho}\left[1-u-v-y(1-\rho_h)-x(1-\rho_s)\right]} \qquad (128)$$

The extreme values of F correspond to the cases of diffuse sample reflection and specular sample reflection. When the sample reflects in a diffuse manner, F equals the ratio of the area of the entrance opening to half the area of the sphere, or $2A_e/A_s$. When the sample reflects specularly, the fraction can be made equal to zero by rotating the sample slightly so that the polar angle of incidence is not zero. Hence, for diffusely reflecting samples,

$$\eta_2 = \frac{\rho v (1 - 2u)}{1 - \bar{\rho} [1 - u - v - y(1 - \rho_h) - x(1 - \rho_s)]} \tag{129}$$

and for specularly reflecting samples,

$$\eta_2 = \frac{\rho v}{1 - \bar{\rho} [1 - u - v - y(1 - \rho_h) - x(1 - \rho_s)]} \tag{130}$$

It is evident that the sphere efficiency is a maximum when measuring the reflectance of a specular surface, and a minimum when measuring a diffuse surface.

Having already determined the effect of coating reflectance and detector area on the efficiency of the sphere, the effect of sample area, entrance opening area, and sample holder reflectance will be determined in the same manner. From Equation (129),

$$\partial \eta_2 / \partial u = - \frac{\{ 2\rho v [1 - \bar{\rho}(1 - u - v - y(1 - \rho_h) - x(1 - \rho_s))] + \bar{\rho} \rho v (1 - 2u) \}}{\{1 - \bar{\rho} [1 - u - v - y(1 - \rho_h) - x(1 - \rho_s)]\}^2} \tag{131}$$

Since $\partial \eta_2 / \partial u < 0$, the efficiency of the sphere increases as the entrance area decreases.

$$\partial \eta_2 / \partial x = \frac{-\bar{\rho} \rho v (1 - 2u)(1 - \rho_s)}{\{1 - \bar{\rho} [1 - u - v - y(1 - \rho_h) - x(1 - \rho_s)]\}^2} < 0 \quad \text{for } u < 1/2 \tag{132}$$

$$\partial\eta_2/\partial\rho_h = \frac{\bar{\rho}\,y\rho v\,(1-2u)}{\left\{1-\bar{\rho}\left[1-u-v-y(1-\rho_h)-x(1-\rho_s)\right]\right\}^2} > 0 \quad \text{for } u < 1/2 \tag{133}$$

Equations (132) and (133) indicate that the efficiency of the sphere, with the sample in place, increases as the reflectance of the sample holder increases, and the area of the sample decreases.

The reflectance of the sample is given by the ratio of the signal produced when the sample is in place within the sphere to the signal produced when the sample is not in place. In terms of the previously defined equations, the reflectance ρ_s is given by

$$S_2/S_1 = \frac{K\frac{A_d}{A_s}P\rho\rho_s(1-F)\left\{\dfrac{1}{1-\bar{\rho}\left[1-\frac{A_e}{A_s}-\frac{A_d}{A_s}-\frac{A_h}{A_s}(1-\rho_h)-\frac{A_t}{A_s}(1-\rho_s)\right]}\right\}}{K\frac{A_d}{A_s}P\rho\left\{\dfrac{1}{1-\bar{\rho}\left[1-\frac{A_e}{A_s}-\frac{A_d}{A_s}-\frac{A_h}{A_s}(1-\rho_h)-\frac{A_t}{A_s}(1-\rho_s)\right]}\right\}} \tag{134}$$

$$S_2/S_1 = \rho_s(1-F)\left\{\frac{1-\bar{\rho}\left[1-\frac{A_e}{A_s}-\frac{A_d}{A_s}-\frac{A_h}{A_s}(1-\rho_h)\right]}{1-\bar{\rho}\left[1-\frac{A_e}{A_s}-\frac{A_d}{A_s}-\frac{A_h}{A_s}(1-\rho_h)-\frac{A_t}{A_s}(1-\rho_s)\right]}\right\} \tag{135}$$

where the error is given by the quantity

$$\epsilon = (1-F)\left\{\frac{1-\bar{\rho}\left[1-\frac{A_e}{A_s}-\frac{A_d}{A_s}-\frac{A_h}{A_s}(1-\rho_h)\right]}{1-\bar{\rho}\left[1-\frac{A_e}{A_s}-\frac{A_d}{A_s}-\frac{A_h}{A_s}(1-\rho_h)-\frac{A_t}{A_s}(1-\rho_s)\right]}\right\} \tag{136}$$

Assuming a value of 0.70 for ρ_s, ρ, and $\bar{\rho}$, and 0.90 for ρ_h, the error for a diffusely reflecting sample is

$$\epsilon = \left[1-2(.00265)\left\{\begin{matrix} 1-.70\left[1-.00265-.00391-.0112(1-.90)\right] \\ 1-.70\left[1-.00265-.00391-.0112(1-.90)-.0199(1-.70)\right] \end{matrix}\right\}\right. \quad (137)$$

$$\epsilon = 0.9813$$

For a specular sample, F = 0. For ρ_s = 0.95,

$$\epsilon = 0.9977 \quad (138)$$

Summary of Error Analysis

In the examples chosen for the determination of possible error magnitude, the value of 0.70 was consistently chosen for the reflectance of the sphere wall. The reason behind this choice was the fact that the uncorrected reflectance of a smooth, quenched sulfur sample varied from 0.817 to 0.612 over a wavelength range of 1.5 to 9.5 microns. Thus, 0.70 was chosen as a typical reflectance value.

With the assumed values listed previously, the maximum error predicted by the analysis was -11.79% for diffuse samples and -11.27% for specular samples. The minimum error for diffuse and specular samples was predicted to be -1.53% and -0.75%, respectively. A specular sample (freshly vacuum-coated aluminum) was tested in the sphere and the maximum variation in reflectance from reference values was -1.36%, which lies within the predicted error limits. (Positive variations were attributable to lack of recorder resolution.)

CHAPTER VI

RESULTS AND RECOMMENDATIONS

The objective of this dissertation, as previously stated, was the construction and analysis of a long wavelength integrating sphere reflectometer. Previous chapters have described the construction and analysis. This chapter presents views of the final instrument assembly, results obtained using the instrument, and recommendations for improving the instrument.

Instrument Assembly

Figure (23) shows the opened sphere, with the sample holder and detector in place. The hemisphere which accomodates the detector, and through which the incident beam enters the sphere, is rigidly attached to the channel-iron base. The other hemisphere is attached to one side of a 3 inch wide hinge, the other side of which is also rigidly fastened to the base. With this arrangement, samples can be inserted and withdrawn from the sphere without danger of disturbing the optical alignment of the sphere. The preamplifier is shown in the upper right corner of the figure.

The entire reflectometer system, with the exception of the amplifier and recorder, are shown in Figure (24). The monochromator is shown in the center of the figure, and the globar is directly in front of the monochromotor.

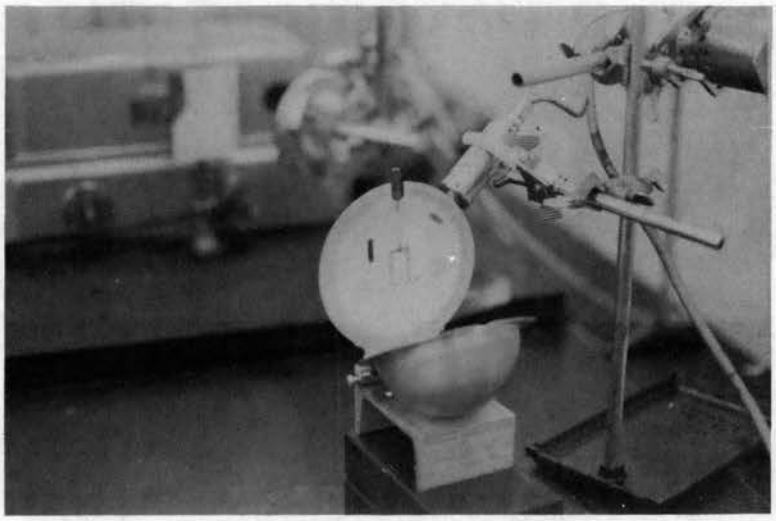

Figure 23. Integrating Sphere, Showing Sample Holder and Detector

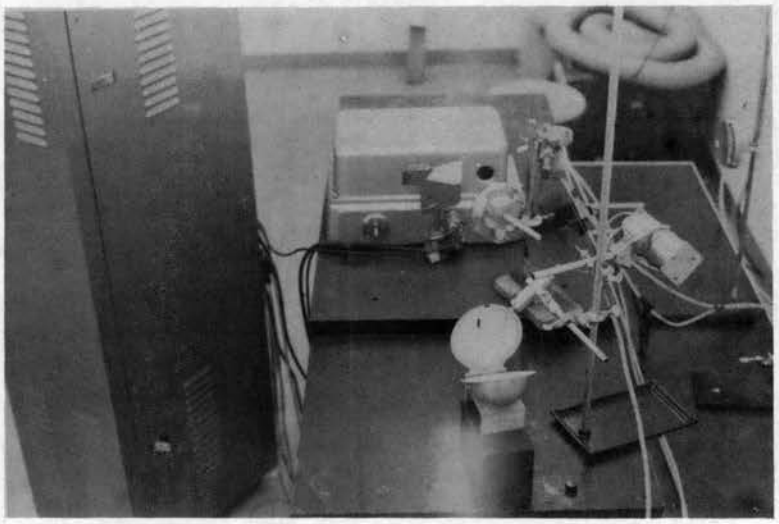

Figure 24. Reflectometer System

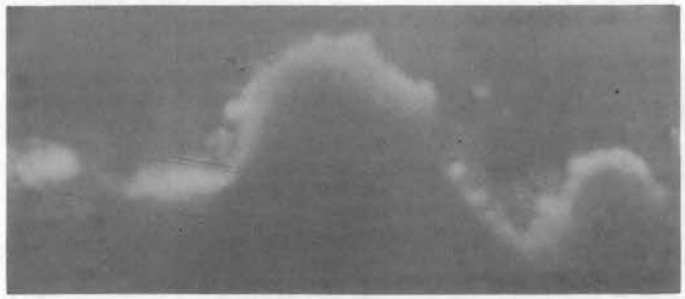

Figure 25a

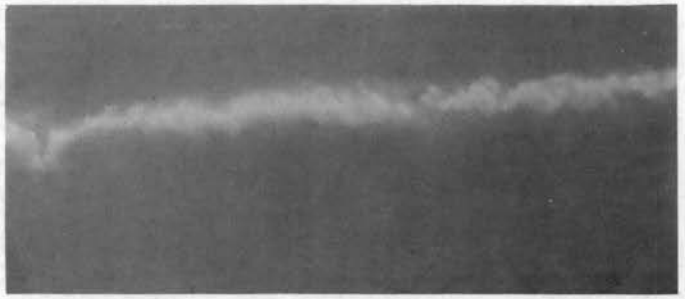

Figure 25b

Figure 25c

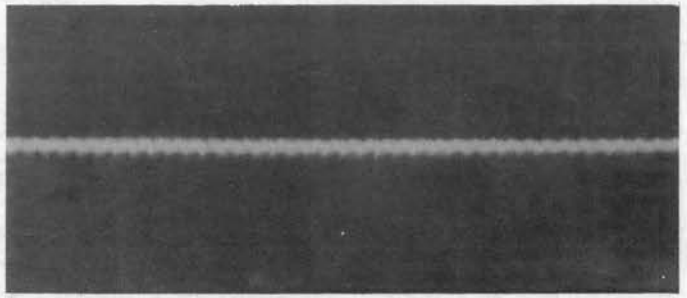

Figure 25d

Figure 25. Surface Profiles of Sphere Coatings
And Reference Sample

Reflectance of Selected Samples

The total monochromatic directional reflectance, as defined in Chapter III, was measured for five different samples. Four of the samples are commonly regarded as diffuse reflectors, one is a specular reflector. The diffusely reflecting group was composed of rough and smooth samples of quenched sulfur, smooth flowers of sulfur, and rough sodium chloride samples. The specular sample was a first surface mirror prepared by evaporating aluminum onto a glass sample blank.

The terms "rough" and "smooth", as applied to the diffusely reflecting materials, can be regarded only as qualitative in that no roughness measurements were made. The "rough" surfaces were the unaltered surfaces which resulted from the application of the material to the sample blank, the roughness being a function of the method of application. The "smooth" surfaces were the surfaces which resulted from attempts to make the initial material coating as nearly like a specular surface as possible.

Since the method of application was different for each material, it was to be expected that the roughness was different for each sample. This fact is illustrated by Figures (25a), (25b), and (25c). These figures show surface profiles obtained using a Zeiss light-section microscope with a magnification of 400, of a rough quenched sulfur (Crystex) sample, a smooth Crystex sample, and a smooth flowers of sulfur sample respectively. Figure (25d) shows, for comparison purposes, a 0.5 micron rms roughness saw-toothed sample.

Because of the difference in surface roughness, it is difficult to obtain a meaningful comparison of the reflectances of the different materials which were investigated. For the same reason, comparison of data obtained from the instrument under consideration with that presented by other investigators is of doubtful utility. Thus, the figures presented in this section concerning reflectance data for different materials by different investigators are subject to this restriction.

Figure (26) shows the uncorrected reflectance of the vacuum-coated aluminum sample. The polar angle of incidence for these values was 20° and the azimuthal angle was approximately $5.^{\circ}$. All reflectance measurements discussed in this chapter were made with the same angles of incidence. Also shown are the reflectance values, as presented by Bennett, et al.(40), of a freshly evaporated aluminum film. Because of the high degree of control exercised over the coating and measuring procedures and because of the high quality of the materials used, these values were chosen as reference values.

As seen in Figure (26), the measured monochromatic aluminum film differs from the reference values by a maximum of 1.36%, with most values differing by less than 1.0%. The measured reflectance values of 100% are attributable to the fact that it was impossible to read recorder values smaller than 5% at the longer wavelengths. In Chapter V, it was shown that the error in the measured reflectance of a specular surface could be as much as 11.27% or as little as 0.75%. Thus the reference curve serves as a rough check on the error analysis, subject to the fact that different samples, investigated under different conditions, were compared.

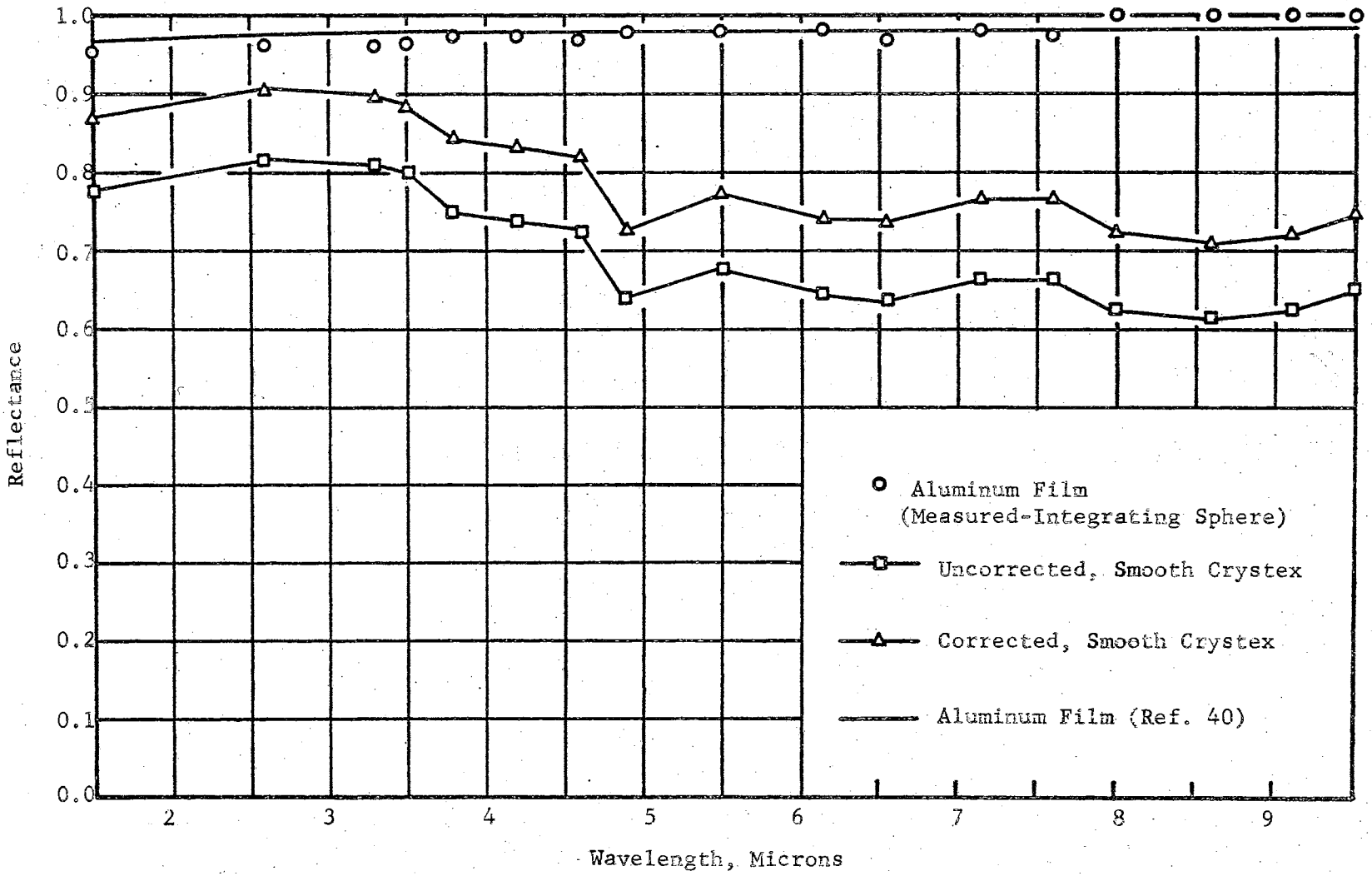

Figure 26. Spectral Reflectance of Selected Samples

Also shown in Figure (26) is the measured monochromatic reflectance of a smoothed sample of Crystex. These reflectance values were assumed equal to the reflectance of the sphere wall coating.

Figure (27) is a curve of maximum error, as a function of wall reflectance, for Crystex. This curve was derived by assuming that the reflectances of the Crystex sample and the sphere coating were equal. The sample holder was assumed to have a reflectance of 0.90 at all wavelengths. These error values were then applied to uncorrected Crystex reflectance to arrive at the corrected values shown in Figure (26).

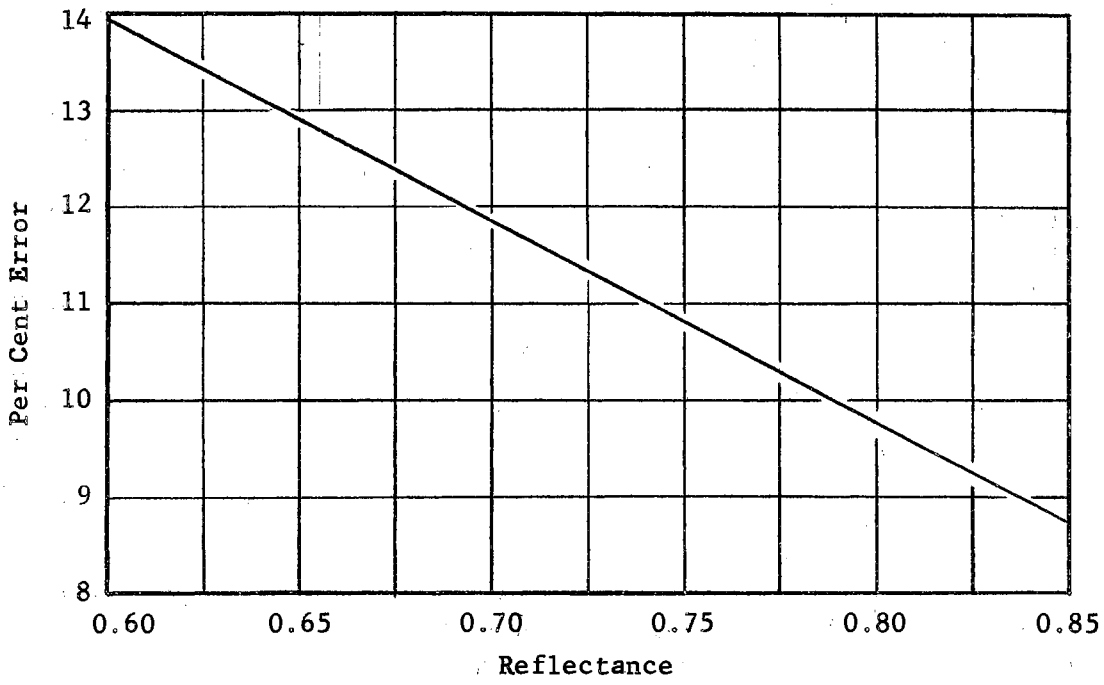

Figure 27. Error in Reflectance Measurements as a Function of Coating Reflectance

The monochromatic reflectance values of smooth Crystex, rough Crystex, and smooth flowers of sulfur samples are shown in Figure (28). These values tend to explain the findings given in Chapter IV that the average reflectance of the smooth Crystex coating was

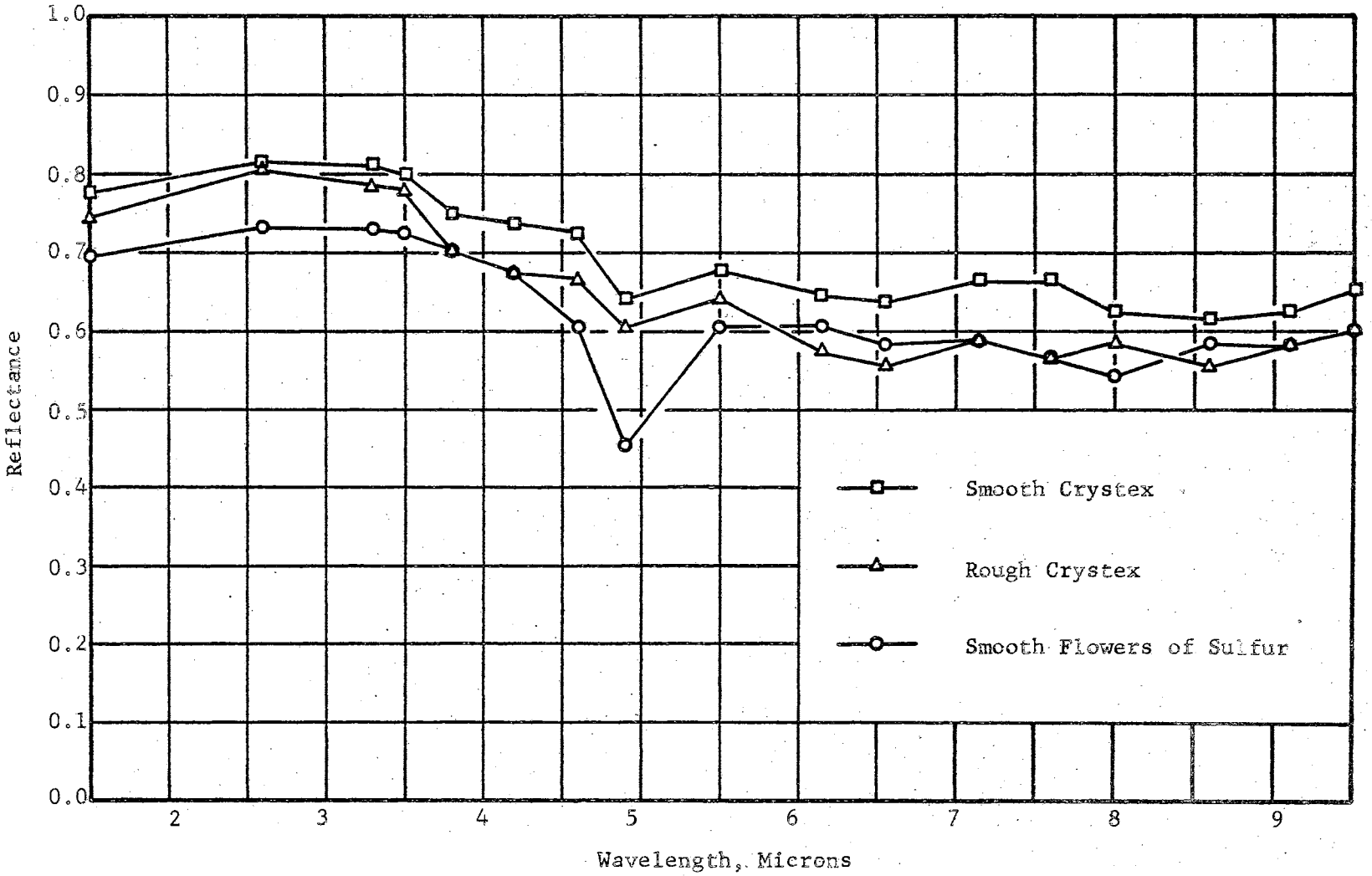

Figure 28. Spectral Reflectance of Coating Materials

greater than that of the rough Crystex coating which, in turn, was greater than that of the smooth flowers of sulfur coating.

Figure (29) shows the measured, uncorrected reflectance of smooth flowers of sulfur sample. Also shown are the uncorrected and corrected data for flowers of sulfur, as presented by Kronstein, et al. (35). The smooth sample was chosen for comparison with Kronstein's sample because the latter sample was prepared by pressing the sulfur into a boat, a process which probably produced a relatively smooth sample.

The data presented by Kronstein was obtained using a Coblenz hemisphere reflectometer. In an attempt to account for the error involved in this type of instrument, Kronstein derived correction factors for diffusely reflecting surfaces by measuring the reflectance of flowers of sulfur relative to magnesium oxide to determine the absolute reflectance of the sulfur sample. The average ratio of the calculated absolute reflectance to the measured absolute reflectance, 1.8, was assumed the appropriate correction factor and was applied to all measured values beyond the 2.45 micron limit of appreciable magnesium oxide reflectance. It was in this manner that the corrected curve data was obtained. It is interesting to note that the maximum correction factor for specular surfaces, determined by comparing the measured reflectance of a rhodium mirror to the known reflectance, was 1.07.

The results of the measurements made with the reflectometer under consideration indicate that, of the materials considered, the proper sphere coating material was chosen. They also indicate that

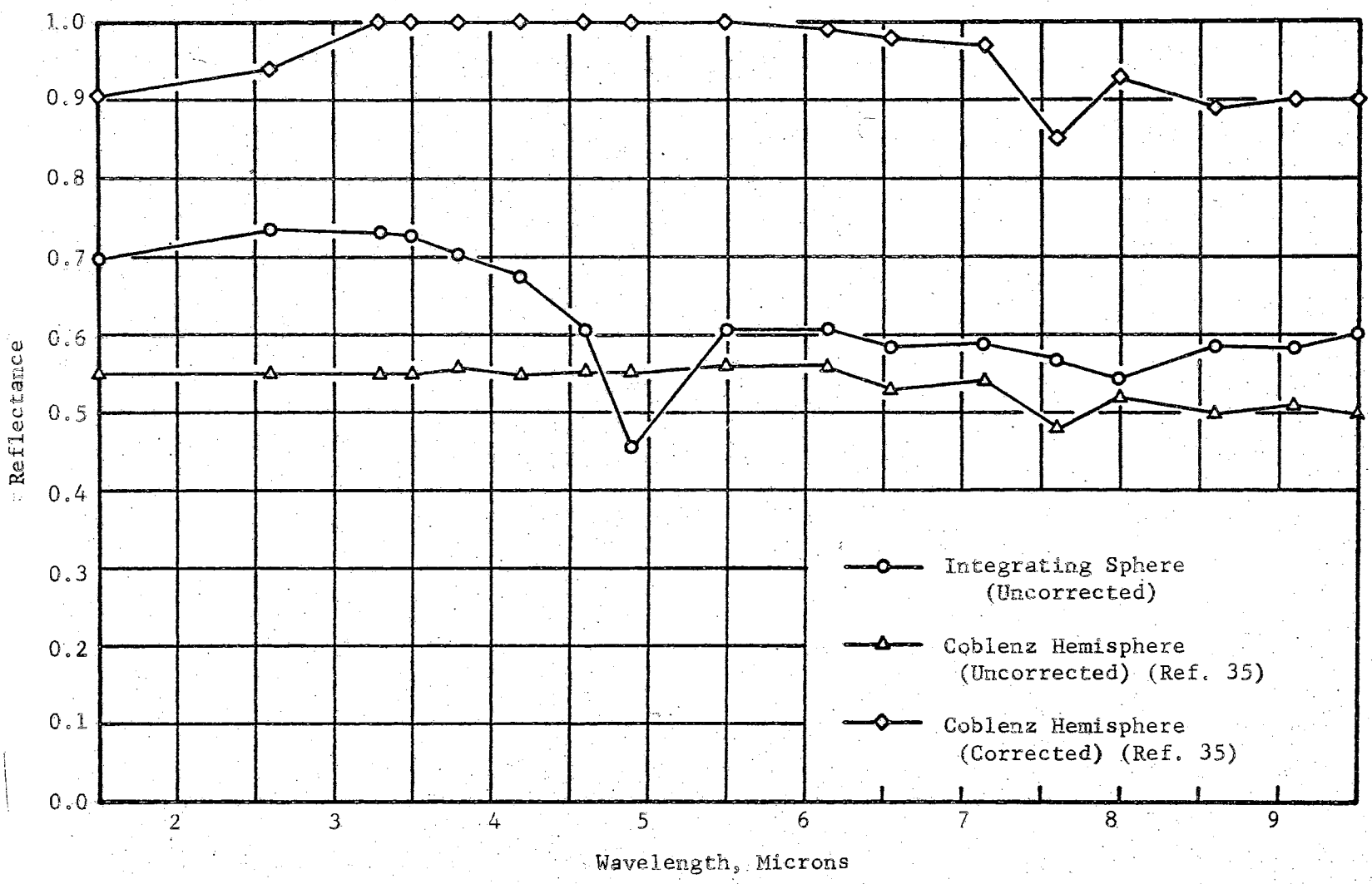

Figure 29. Spectral Reflectance of Flowers of Sulfur

total directional monochromatic reflectance values can be determined whose error may be greater than 10% or less than one per cent, the size of the error depending upon the reflectance and specularity of the sample.

Recommendations for Instrument Improvement

A reflectometer of the type being considered can be improved, in the final analysis, in only two ways. The range may be extended and the accuracy improved. However, as previously pointed out, these two parameters are intimately related and any improvements in one will often improve the other.

Because the magnitude of the error involved in the reflectance measurements is an inverse function of the sphere wall reflectance, the accuracy of the instrument under consideration could be increased by increasing the coating reflectance. It was shown qualitatively in Chapters IV and VI that the reflectance of quenched sulfur is a function of the surface roughness. For this reason, it is recommended that a procedure be developed for applying the quenched sulfur coating in a manner such that the resulting surface finish is as smooth as possible. The degree of "smoothness" is, of course, subject to the restriction that the coating reflect in a diffuse manner at all wavelengths of interest. This procedure would involve a coating technique, a smoothing procedure, a method for determining specularity, and possibly a technique for measuring the roughness of the coating.

Any increase in sphere wall reflectance will, as noted previously, increase the efficiency of the sphere. This, in turn, will increase

the range of the instrument. Thus the recommendation for the application of smooth, diffuse walls encompasses improvement in both the range and accuracy of the integrating sphere reflectometer.

A logical extension of the idea of smooth sphere walls seemed to be the utilization of specular walls. This of course violates the basic theory of the integrating sphere. It was reasoned, however, that a specular sphere wall would reflect diffusely if it was diffusely irradiated. That is, a portion of the sphere wall could be a specular reflector, without violating the basic integrating sphere premise, as long as it was diffusely, and only diffusely, irradiated.

A test was conducted to determine the effect of a high reflectance, specularly reflecting sphere coating. A smooth glass hemisphere having a diameter of 4 inches, was vacuum-coated with an aluminum film. This specular hemisphere which was fitted with detector and the entrance opening, as described in Chapter IV, was arranged such that the entering beam was always incident on the wall of the Crystex-coated hemisphere. Signals resulting from this arrangement were compared with those resulting when the aluminum-coated hemisphere was replaced by a smoothed Crystex-coated hemisphere, all other test conditions having remained the same. The results, as shown in Figure (30), indicate that the sphere wall reflectance for the diffuse-specular combination is almost twice that of the diffuse-diffuse hemisphere combination.

It appears, then, that the range of the integrating sphere reflectometer might be improved by combining a specularly reflecting hemisphere with a diffusely reflecting hemisphere. The effect

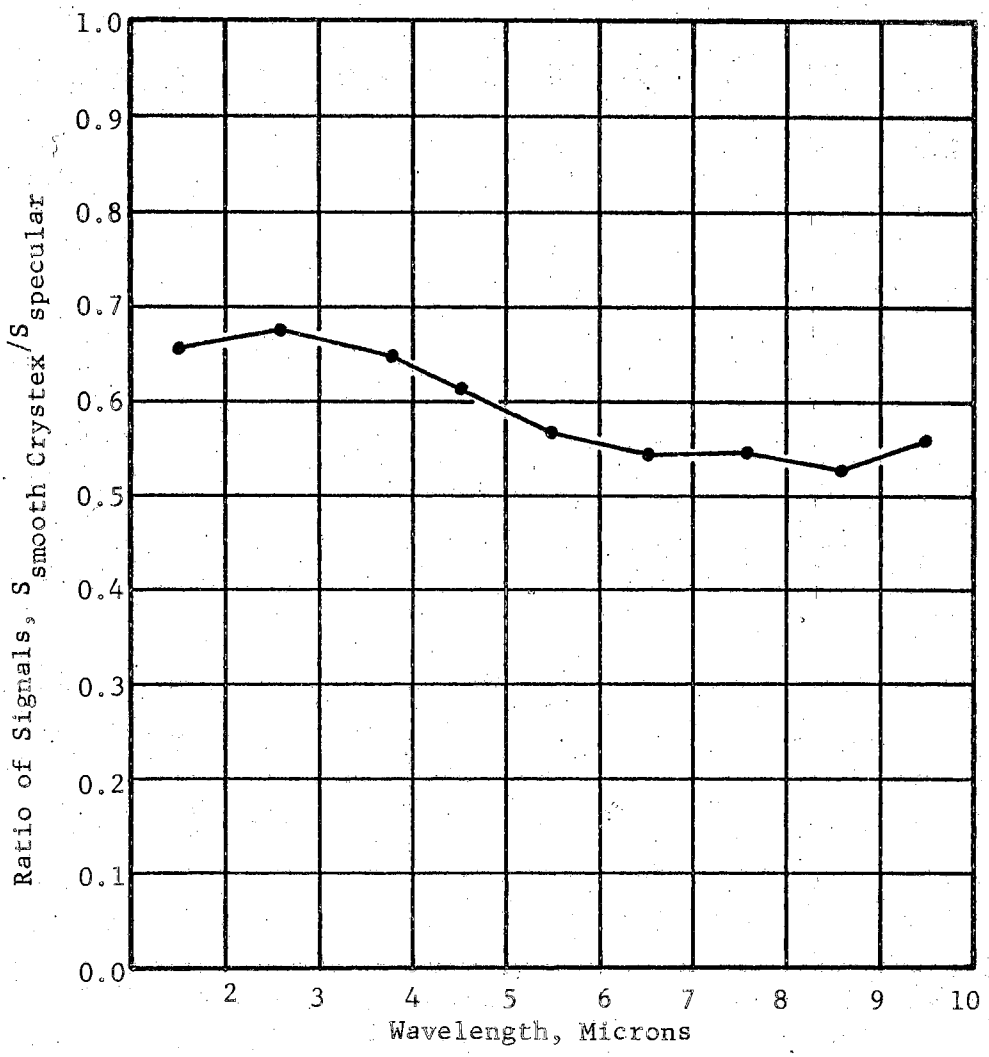

Figure 30. Comparison of Detector Signal for Diffuse Sphere and Diffuse-Specular Sphere

of the specular portion upon the accuracy of the measurements would have to be determined, although no extreme errors should occur if the specular hemisphere received only diffusely reflected energy.

As noted previously, the range of the integrating sphere reflectometer, for a given coating, geometry, and detector, is limited by the amount of energy available for detection. Conversely, for a given coating, geometry, and source, the range is limited by the sensitivity of the detector.

A higher temperature blackbody source appears to offer little hope of significantly improving the range of the instrument under consideration. The globar operates at approximately 2500°R. A carbon arc system may operate at temperatures as high as 6000°R, but the configuration of the rods causes the source area to be so small that the energy presented for detection is less than that produced by the globar. A tungsten element can be operated at higher temperatures than the globar, but must be protected by some type of envelope that reduces the intensity of the source beam.

The development of long wavelength lasers does offer some hope of range improvement. However, since the lasers developed to date are not continously emitting devices, provision of laser sources at all wavelengths of interest would be prohibitively expensive. A more logical procedure would be the selection of several long wavelengths which might be considered as "representative". A small number of lasers, each of which could be adapted to more than one wavelength, could be used to provide a monochromatic source corresponding to the "representative" wavelengths. These could be used, in conjunction with the globar, to produce continuous

reflectance measurements up to the wavelength limit imposed by the globar and selected reflectance values at longer wavelengths.

There are available at present gas-filled bolometers which are much more sensitive than the Reeder thermocouple used in this investigation. Better amplifiers are also available. The acquistion of either would undoubtedly increase the range of the instrument under consideration, the magnitude of the increase depending upon the detector or amplifier selected.

Thus, instrument improvement may be achieved by the use of smooth, diffuse sphere walls, a diffuse-specular sphere, laser sources, a better detector, and a better amplifier. The first two items involve experimental programs, while the last three involve expenditures for equipment.

SELECTED BIBLIOGRAPHY

1. Helmholz, H.L.F.V., Physiological Optics, Third Edition, 1909, Translated by J.C.P. Southall, Published by the Optical Society of America, 1924.

2. Bevans, J.T., R.V. Dunkle, and J.T. Gier, "Measurement of Absolute Spectral Reflectivity From 1.0 to 15 Microns," Journal of the Optical Society of America, Vol. 44, 1954, pp. 558-562.

3. Dunn, S.T., "Design and Analysis of an Ellipsoidal Mirror Reflectometer, Ph.D. Dissertation, Oklahoma State University, 1965.

4. Janssen, J.E., and R.H. Torburg, "Measurement of Spectral Reflectance Using an Integrating Hemisphere," Measurement of Thermal Radiation Properties of Solids, NASA SP-31, 1963, pp. 169-182.

5. Middleton, E.E.K., and C.L. Sanders, "The Absolute Spectral Reflectance of Magnesium Oxide in the Near Infrared," Journal of the Optical Society of America, Vol. 43, 1953, p. 58.

6. Agnew, J.T., and Richmond B. McQuisten, "Experiments Concerning Infrared Diffuse Reflectance Standards in the Range 0.8 to 20.0 Microns," Journal of the Optical Society of America, Vol. 43, 1953, pp. 999-1007.

7. Birkebak, R.C., J.P. Dawson, B.A. McCullough, and B.E. Wood, "Vacuum Integrating Spheres for Measuring Cryodeposit Reflectances from 0.35 to 15 Microns," AIAA Thermophysics Specialist Conference, AIAA Paper No. 65-674, 1965.

8. Sumpner, W.E., "The Diffusion of Light," Philosophical Magazine Vol. 35, 1893, pp. 81-89.

9. Ubricht, V.R., "Die Bestimmung der mittlern raumlichen Lichtintensitat durch nur eine Messung," Elektrotechnische Zeitschrift, Vol. 29, 1900, pp. 595-596.

10. Little, W.H., and C.H. Sharp, "Measurement of Reflection Factors," Transactions of the Illuminating Engineering Society, Vol. 15, 1920, pp. 802-807.

11. Rosa, E.B., and A.H. Taylor, "The Integrating Photometric Sphere; its Construction and Use," Transaction of the Engineering Society, Vol. 11, 1916, pp. 453-464.

12. Luckiesh, M., "The Measurement of Reflection and Transmission Factors," Journal of the Optical Society of America, Vol. 2, 1919, pp. 39-45.

13. Benford, F., "An Absolute Method for Determining Coefficients of Diffuse Reflection," General Electric Review, Vol. 23, 1920, pp. 72-76.

14. Taylor, A.H, "Measurement of Diffuse Reflection Factors, and a New Absolute Reflectometer," National Bureau of Standards, Scientific Papers, Vol. 17, 1920, pp. 421-436.

15. Taylor, A.H., "A Simple Portable Instrument for the Measurement of Reflection and Transmission Factors," National Bureau of Standards, Scientific Papers, Vol. 17, 1920, pp. 1-6.

16. Taylor, A.H., "The Measurement of Reflection Factors in the Ultraviolet," Journal of Optical Society of America, Vol. 21, 1931, pp. 776-784.

17. Karrer, E., "Use of the Ulbricht Sphere in Measuring Reflection and Transmission Factors," National Bureau of Standards, Scientific Papers, Vol. 17, 1922, pp. 203-225.

18. McNicholas, H.J., "Absolute Methods in Reflectometry," National Bureau of Standards Journal of Research, Vol. 1, 1928, pp. 29-73.

19. Hardy, A.C., and O.W. Pineo, "The Errors Due to the Finite Size Holes and Sample in Integrating Sphere," Journal of the Optical Society of America, Vol. 21, 1931, pp. 502-506.

20. Benford, F., "A Reflectometer for All Types of Surfaces," Journal of the Optical Society of America, Vol. 24, 1934, pp.165-174.

21. Benford, F., G.P. Lloyd, and S. Schwartz, "Coefficients of Reflection of Magnesium Oxide and Magnesium Carbonate," Journal of the Optical Society of America, Vol. 38, 1948, pp. 445-447.

22. Finkelstein, N.A., "An Integrating Sphere for Reflectance Measurements in the Ultraviolet," Journal of the Optical Society of America, Vol. 40, 1950, pp. 178-179.

23. Middleton, W.E.K., and C.L. Sanders, "The Absolute Spectral Diffuse Reflectance of Magnesium Oxide," Journal of the Optical Society of America, Vol. 41, 1951, pp. 419-424.

24. Jacques, J.A., and H.F. Kuppenheim, "Theory of the Integrating Sphere," Journal of the Optical Society of America, Vol. 45, 1955, pp. 460-470.

25. Tingwaldt, C.P., "Uber die Messung von Reflexion, Durchlassigkeit und Absorption an Prakorpen beliebiger Form in der Ulbrichtschen kugel," Optik, Vol. 9, 1952, pp. 323-332.

26. Tellex, P.A., and J.R. Waldron, "Reflectance of Magnesium Oxide," Journal of the Optical Society of America, Vol. 45, 1955, pp. 19-22.

27. Toporets, A.S., "Study of Diffuse Reflection from Powders Under Diffuse Illumination," Optics and Spectroscopy, Vol. 7, 1959, pp. 471-473.

28. Edwards, D.K., J.T. Gier, K.E. Nelson, and R.D. Roddick, "Integrating Sphere for Imperfectly Diffuse Samples," Applied Optics, Vol. 51, 1961, pp. 1279-1288.

29. Fussell, W.B., and J.J. Triolo, "Portable Integrating Sphere for Monitoring the Reflectance of Spacecraft Coatings," Symposium on Measurement of Thermal Radiation Properties of Solids, Vol. 1, 1962, pp. 1-14.

30. Brandenberg, W.M., "The Reflectivity of Solids at Grazing Angles," Measurement of Thermal Radiation Properties of Solids, Editor: J.C. Richmond, NASA Sp-31, 1963, pp. 75-82.

31. Zerlaut, G.A., and A.C. Krupnick, "An Integrating Sphere Reflectometer for the Determination of Absolute Hemispherical Spectral Reflectance," AIAA Journal, Vol. 4, 1966, pp. 1227-1232.

32. Worthing, A.G., "Temperature Radiation Emissivities and Emittances," Temperature, Its Measurement and Control in Science and Industry, Pheinhold Publishing Corporation, New York, 1941.

33. Wiebelt, J.A., Engineering Radiation Heat Transfer, Notes for Oklahoma State University, May, 1963.

34. Harrison, W.N. "Pitfalls in Thermal Emission Studies," Measurement of Thermal Radiation Properties of Solids, Editor: J.C. Richmond, NASA SP-31, 1963, pp. 3-9.

35. Kronstein, M., R.J. Kraushaar, and R.E. Deacle, "Sulfur as a Standard of Reflectance in the Infrared," Journal of the Optical Society of America, Vol. 53, 1963, pp. 458-465.

36. Kneissle, G.J., National Bureau of Standards, Personal Communication.

37. Taylor, A.H., "Errors in Reflectometry," Journal of the Optical Society of America, Vol. 25, 1953, pp. 51-56.

38. Parmer, J.F., "The Thermal Radiation Characteristics of Specular Walled Grooves in the Solar Space Environment," Ph.D. Thesis, Oklahoma State University, May, 1965.

39. Dawson, J.P., D.C. Todd, and B.E. Wood, "Deviations from Integrating Sphere Theory Caused by Centrally Located Samples," AEDC-TR-65-271, Air Force Systems Command, Arnold Air Force Station, Tennessee, April, 1966.

40. Bennett, H.E., J.M. Bennett, and E.J. Ashley, "Infrared Reflectance of Evaporated Aluminum Films," Journal of the Optical Society of America, Vol. 52, 1962, pp. 1245-1250.

41. Streiff, M.L., and C.C. Ferrisco, "Spectral Slit Width of a Small Prism Monochromator," General Dynamics Astronautics, GDA-DBE 64-054, August, 1964.

APPENDIX A

STATEMENT OF RECIPROCITY

The principle of reciprocity was formulated by Helmholz and presented in his book, Physiological Optics. He stated the principle as follows:

> Suppose light proceeds by any path whatever from a point A to another point B, undergoing any number of reflections or refractions enroute. Consider a pair of rectangular planes a_1 and a_2 whose line of intersection is along the initial path of the ray at A; and another pair of rectangular planes b_1 and b_2 intersecting along the path of the ray when it comes to B. The components of the vibrations of the other particles in these two pairs of planes may be imagined. Now suppose that a certain amount of light J leaving the point A in the given direction is polarized in the plane a_1, and that of this light the amount K arrives at the point B polarized in the plane b_1; then it can be proved that, when the light returns over the same path, and the quantity of light J polarized in the plane b_1 proceeds from the point B, the amount of this light that arrives at the point A polarized in the plane a_1 will be equal to K. (1)

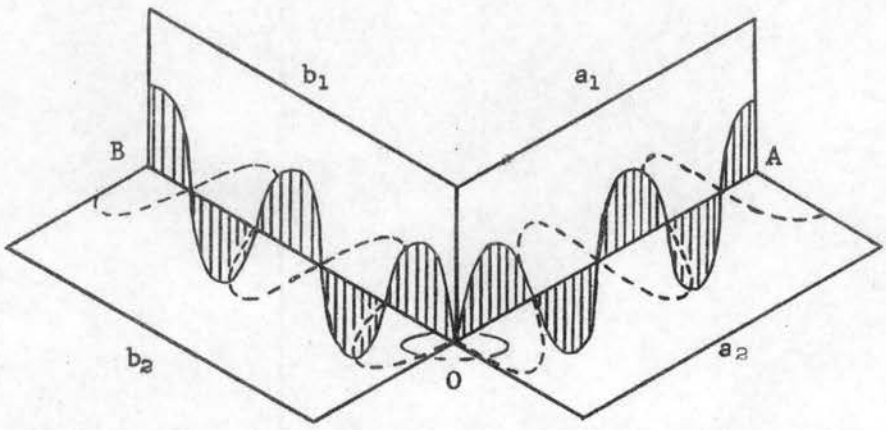

Figure A-1. Irradiation of, and Reflection from, Surface O by Monochromatic Polarized Light Ray

Southall, who translated Helmholz' work, said of Helmholz' statement:

> Apparently the above proposition is true no matter what happens to the light in the way of single or double refraction, reflection, absorption, ordinary dispersion, and diffraction, provided there is no change of its refrangibility, and provided it does not traverse any magnetic medium that affects the position of the plane of polarization, as Faraday found to be the case. (1)

McNicholas translated Helmholz' statement of the principle in the following manner:

> The loss in flux density which an infinitely narrow bundle of rays of definite wavelength and state of polarization undergoes on its path through any medium by reflection, refraction, absorption, and scattering is exactly equal to the loss in flux density suffered by a bundle of the same wavelength and polarization pursuing an exactly opposite path. (18)

McNicholas translation, as applied to reflectance studies, can be illustrated as follows: Consider surface O, Figure (A-2), from which emanate two small solid angles ω_1 and ω_2. At point A, monochromatic energy in the amount J is directed upon surface O through ω_1 and energy is reflected through ω_2 to point B where the amount of monochromatic energy is K. If the direction of the energy could be exactly reversed, and J monochromatic energy directed upon the surface from B, the amount of energy measured at A would equal K. This amounts to saying that the bundles of energy are reversible with regard to both direction and angular flux density.

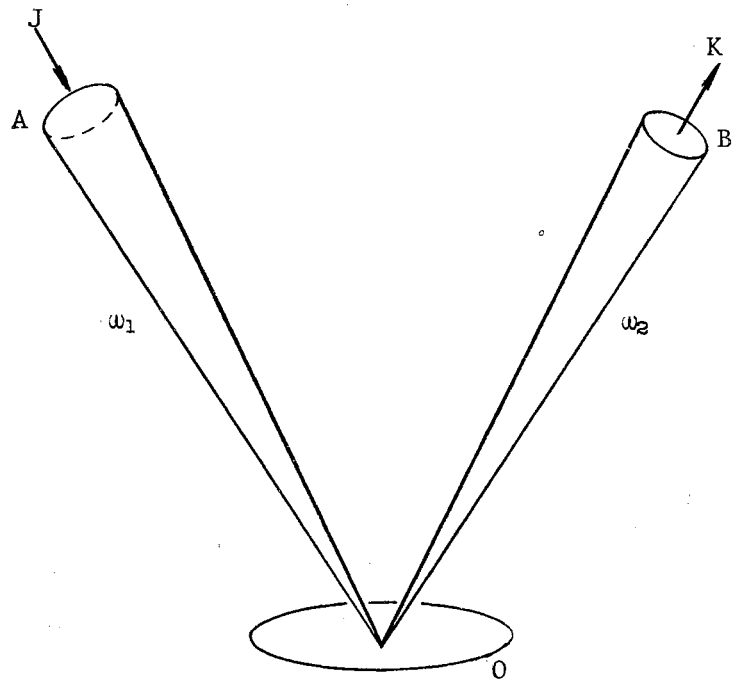

Figure A-2. Irradiation of, and Reflection from, Surface 0 Through Small Solid Angles ω_1 and ω_2

APPENDIX B

APPROXIMATION OF NUMERATOR OF EQUATION (68) BY THE TRAPEZOIDAL RULE

θ	S_r	$S_{r,\theta_d = 0}$	$\sin\theta_d$	$\frac{S_r \sin \theta_d}{S_{r,\theta_d = 0}}$
0	20.0	20.0	0.0	0.0
10	19.5	20.0	.1736	.1694
20	19.0	20.0	.3420	.3250
30	17.0	20.0	.5000	.4250
40	15.0	20.0	.6428	.4830
50	12.5	20.0	.7660	.4790
60	9.0	20.0	.8660	.3900
70	3.0	20.0	.9397	.1410
80	0.0	20.0	.9848	0.0
90	0.0	20.0	1.000	0.0
				2.4124

$$h = (10^\circ)\left(\frac{\pi}{180}\right)$$

$$\int_{\theta_d=0}^{\theta_d=\pi/2} S_r/S_{r,\theta_d=0} \sin\theta_d d\theta_d = \left(\frac{10\pi}{180}\right)(2.4124) = .4240$$

APPENDIX C

THEORETICAL CALIBRATION OF MONOCHROMATOR

Since the wavelength of the energy delivered at the exit slit of the monochromator is controlled by the wavelength drive micrometer drum setting, it is necessary to calibrate the monochromator so that the wavelength indicated by any drum setting is known. This calibration can be evaluated theoretically through the known properties of the prism and the wavelength drive mechanism.

The theoretical evaluation requires the development of an expression for the wavelength λ, as a function of the number of wavelength drive turns. This can be accomplished indirectly by relating the wavelength to the angular rotation of the Littrow mirror and by knowing the relationship of the Littrow mirror to the wavelength drive. For the Perkin-Elmer Model 99 Double Pass Monochromator, the wavelength micrometer drum, which is attached to the wavelength drive screw and which controls the rotation of the Littrow mirror, requires on turn for a Littrow mirror arc change of 1610 seconds. The indirect development mentioned above, then, can be accomplished by expressing λ as a function of θ, where θ is the angular rotation of the Littrow mirror.

This relationship may be obtained by integrating the expression, $d\lambda/d\theta = f_1(\lambda)$. The derivative may be expressed as

$$\frac{d\lambda}{d\theta} = \frac{d\lambda}{dN}\frac{dN}{d\theta} \qquad \text{(C-1)}$$

where N is the index of refraction of the prism material. However, since the inverse of each derivative on the right side of Equation (C-1) is obtainable directly, and since the end results are identical, a more convenient expression is

$$\frac{d\theta}{d\lambda} = \frac{d\theta}{dN}\frac{dN}{d\lambda} = f_2(\lambda) \qquad \text{(C-2)}$$

Then,

$$\int_{\theta_1}^{\theta_2} d\theta = \int_{\lambda_1}^{\lambda_2} f_2(\lambda)\,d\lambda \qquad \text{(C-3)}$$

Using the values of $d\theta/dN$ and $dN/d\lambda$ presented by Streiff and Ferrisco (40), $f_2(\lambda)$ was evaluated at 0.5 micron intervals from λ = 0.5 to 12.0 microns. The zero angle of rotation was chosen to correspond to a wavelength of 0.5 microns. A point by point evaluation of the two integrals, at 0.5 micron intervals, yielded Figure (C-1), which is a curve of number of wavelength drum turns, T, versus wavelength, λ. The data used in arriving at this curve is given in Table C-1.

Figure (C-2) is an expanded view of the wavelength drum turn versus wavelength curve from 0.5 to 2.0 microns. The dashed line represents the location of the Hg green line (0.5461 microns). The intersection of the green line and the curve establishes the relationship between the calibration curve and the wavelength drum setting. That is, the wavelength micrometer drum was set manually

such that the green line appeared at the exit slit when the drum setting was 2460. By correlating this point with the corresponding point on the T-λ curve, the wavelength at any other drum setting can be determined. The scale on the right side of the T-λ curve indicates micrometer drum settings.

TABLE C-I

λ	$d\theta/dN$	$dN/d\lambda$	$(d\theta/dN)(dN/d\lambda)$	T
.5	1.585	.1150	.1823	0
1.0	1.555	.0142	.0221	6.547
1.5	1.550	.0050	.00775	7.504
2.0	1.550	.0028	.00434	7.879
2.5	1.545	.0024	.00371	8.148
3.0	1.545	.0023	.00355	8.379
3.5	1.535	.0024	.00368	8.610
4.0	1.535	.0026	.00399	8.853
4.5	1.535	.0028	.00430	9.122
5.0	1.535	.0031	.00476	9.404
5.5	1.535	.0034	.00522	9.724
6.0	1.530	.0038	.00581	10.083
6.5	1.530	.0040	.00612	10.467
7.0	1.530	.0043	.00658	10.864
7.5	1.525	.0047	.00717	11.313
8.0	1.525	.0050	.00760	11.787
8.5	1.525	.0054	.00824	12.287
9.0	1.520	.0057	.00866	12.837
9.5	1.515	.0061	.00924	13.401
10.0	1.510	.0065	.00982	14.016
10.5	1.505	.0068	.01023	14.657
11.0	1.500	.0072	.01080	15.336
11.5	1.495	.0076	.01136	16.040
12.0	1.490	.0080	.01192	16.783

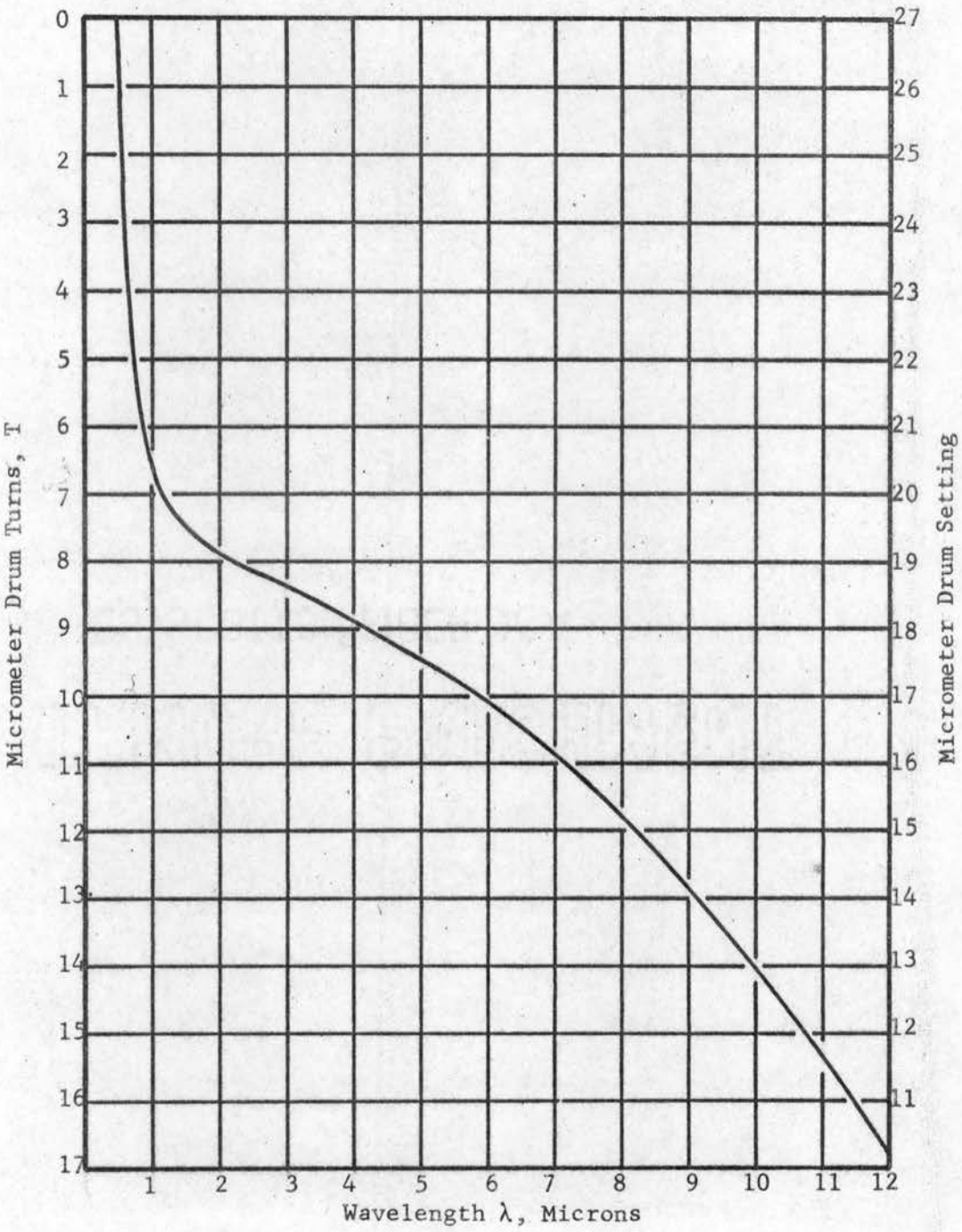

Figure C-1. Relation of Micrometer Drum Turns, T, to Wavelength, λ, for NaCl Prism

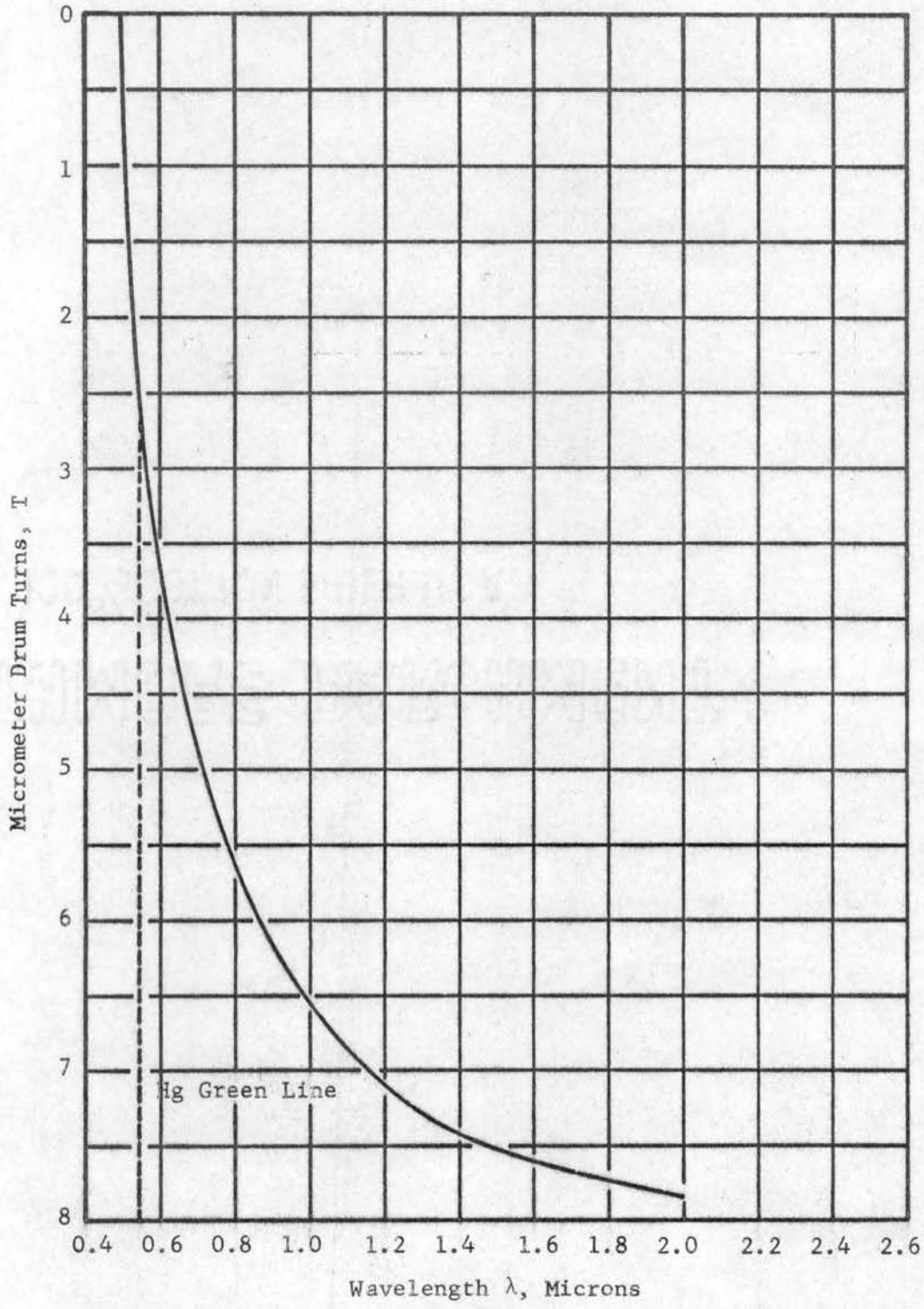

Figure C-2. Expanded λ-T Curve for NaCl Prism

APPENDIX D

EXPERIMENTAL DATA USED IN CHAPTER VI

Wave-length, microns	Monochromatic Reflectance			
	Aluminum Film	Smooth Crystex	Rough Crystex	Smooth Sulfur Flowers
1.5	.954	.777	.746	.693
2.6	.962	.817	.809	.734
3.3	.960	.811	.784	.730
3.5	.962	.800	.780	.726
3.8	.975	.750	.700	.700
4.2	.975	.738	.673	.673
4.6	.970	.726	.665	.605
4.9	.980	.641	.604	.453
5.5	.980	.678	.641	.604
6.15	.981	.643	.571	.606
6.55	.970	.638	.555	.582
7.15	.980	.666	.588	.588
7.60	.975	.666	.564	.564
8.00	1.00	.625	.584	.541
8.60	1.00	.612	.556	.584
9.10	1.00	.624	.582	.582
9.55	1.00	.650	.600	.600

TABLE D-I

Wave-length, microns	S_1 (Detector Signal for Smooth Crystex-Specular Sphere)	S_2 (Detector Signal for Smooth Crystex-Smooth Crystex Sphere)	Ratio S_2/S_1
1.5	51.00	77.75	.656
2.6	29.00	43.00	.674
3.8	41.75	64.50	.646
4.6	21.00	34.50	.609
5.5	53.25	94.00	.566
6.55	29.00	53.50	.542
7.60	15.50	28.50	.544
8.60	9.25	17.50	.529
9.50	7.0	12.50	.560

VITA

Roger Allen Williams

Candidate for the Degree of

Doctor of Philosophy

Thesis: THE CONSTRUCTION AND ANALYSIS OF A LONG WAVELENGTH INTEGRATING SPHERE REFLECTOMETER

Major Field: Mechanical Engineering

Biographical:

Personal Data: Born in Henderson, Texas, March 6, 1933, the son of Glen and Ada Williams.

Education: Attended Gaston Elementary and High School in Joinerville, Texas, and graduated in 1951; received the Bachelor of Science Degree from Texas A and M University, College Station, Texas, in 1961; received the Master of Science Degree from Oklahoma State University, Stillwater Oklahoma, in 1963; completed requirements for the Doctor of Philosophy Degree in May, 1967.

Professional Experience: Employed from June, 1964, to November, 1964 by Brown & Root Constructors, as Construction Engineer; employed from June, 1965, to August, 1966 by Research and Development Division, Texaco, Incorporated, as Research Mechanical Engineer; employed by Engineering Research at Oklahoma State University, as a Staff Assistant, from August, 1966 to February, 1967.

Organizations: Pi Tau Sigma, Tau Beta Pi, Phi Kappa Phi, American Society of Mechanical Engineers.